UILU-ENG 80-2004

CIVIL ENGINEERING STUDIES
Structural Research Series No. 474

A METHOD FOR THE ANALYSIS OF SEISMIC RELIABILITY OF LIFELINE SYSTEMS

by
J. Mohammadi
and
A. H-S. Ang

Technical Report of Research
Supported by the
National Science Foundation
under
Grant ENV 77-09090

DEPARTMENT OF CIVIL ENGINEERING
UNIVERSITY OF ILLINOIS
AT URBANA-CHAMPAIGN
FEBRUARY 1980

ACKNOWLEDGMENTS

This report is based on the doctoral dissertation of J. Mohammadi submitted to the Graduate College of the University of Illinois at Urbana-Champaign in partial fulfillment of the requirements for the Ph.D. degree. The study was directed by Dr. A. H-S. Ang, Professor of Civil Engineering as part of a research program on the evaluation of safety of structures to earthquakes and other natural hazards, and is supported by the National Science Foundation under Grant ENV 77-09090. This support is gratefully acknowledged.

Any opinions, findings, conclusions or recommendations expressed in this publication are those of the author(s) and do not necessarily reflect the views of the National Science Foundation.

TABLE OF CONTENTS

LIST OF TABLES

LIST OF FIGURES

CHAPTER 1

INTRODUCTION

1.1 Introductory Remarks

The reliability of a lifeline system against earthquake hazards, in an area of high seismic activity, is one of the most important factors that need to be considered in its design. The term "lifeline system," as used here, refers to networks of man-made or engineered systems covering vast surface areas. By this definition, oil pipelines, water distribution systems, communication, or transportation networks are all considered as lifeline systems.

In a seismically active region, the time of occurrence, location, and size as well as other characteristics of future earthquakes are not predictable. Therefore, the analysis of earthquake effects on a lifeline system requires probability consideration. More specifically, the design of a lifeline system, in an area of earthquake activity, properly requires the probabilistic assessment of the destructive potentials of future earthquakes and the risk associated with the damage that could conceivably befall the system. The damages may be either because of the fault rupture striking on one or more links of a lifeline system or the failure of the links caused by high intensity ground motions exceeding the resistance capacity of the links.

In the case of a building or nuclear power plant, the spatial dimension of the structure is negligible, and may be assumed to be a point structure. The seismic risk analysis of a point structure, therefore

may be limited to the probabilistic assessment of future ground motion intensities at the point. In other words, the probability that the maximum ground motion of a given site will exceed a specified intensity within a given time interval is considered; the results may be expressed in terms of the annual exceedance probability, or its inverse, the average return period in years. In this case the chance of a fault-rupture striking the point is extremely remote.

In contrast to a point system, the significant areal coverage or vast spatial expanse of a lifeline system requires a different approach from that of a point system. In this case, the risk associated with a fault-rupture intersecting one or more links of the system can be significant and must be considered in addition to the failure of the links caused by high seismic intensity exceeding the resistance of the links. In other words, in the case of a lifeline system, two modes of seismic hazards may be involved.

1.2 Review of Related Work

Seismic risk analysis has been mainly restricted to point systems, and it has been only in recent years that the subject is extended to lifeline systems (e.g. Campbell, et al , 1978; Duke and Moran, 1975; Shinozuka, et al , 1978; and Taleb-Agha, 1977). In one of the first studies on the reliability of lifeline systems, a system was modeled as a network of interconnected links and the probability that the network will function properly after the occurrence of an earthquake of random magnitude and location was evaluated. Later, Taleb-Agha (1977) assumed the resistance of each link as an independent random variable and extended the above model so that it can be used in networks of larger size. Recently,

Shinozuka, et al. (1978) considered the free-field strains as the resistance and developed a method for seismic risk analysis of underground pipeline systems. This model was used for the water distribution system of the city of Tokyo, Japan.

Among the recent studies, Duke and Moran (1975), and Campbell, et al (1978) discussed the problem of the seismic risk analysis of a lifeline system and gave guidelines for evaluating the reliability of lifelines against earthquakes. The importance of organizing design procedures for lifelines similar to those for buildings was stressed.

In the analysis of seismic risk, a major source of uncertainty is in the attenuation equation (Der-Kiureghian and Ang, 1977). This is particularly true for the near-source regions. The problem of the near-source regions is particularly important in the case of the seismic risk analysis of lifeline systems; because of the vast areal coverage of a lifeline system, some links may be very close to the fault-rupture of an earthquake. In such cases, because of uncertainty in the available attenuation equations for close-in regions, a suitable relation may be derived based on analytical models of wave propagation. Among the recent developments of wave propagation in half-space solids (e.g. Refs. 6, 44) is the study of Seyyedian and Robinson (1975). In this model, the three-dimensional problem of wave propagation initiated by a fault-rupture in a half-space is idealized as two two-dimensional problems, as follows: (i) a plane-strain problem; and (ii) an antiplane problem. The complete state of displacement for the close-in regions may then be obtained by properly combining the solutions to the above two problems.

The information thus obtained may be useful for establishing an intensity-distance-magnitude relationship especially applicable for the near-source regions.

1.3 Objective and Scope of Study

Tectonic earthquakes originate as ruptures along geologic faults, Housner (1975) and Newmark and Rosenblueth (1971). The length of the rupture depends on the size of a quake and may be several hundred kilometers long for a large earthquake; the destructive force during an earthquake is released along the entire length of the break.

In the case of a lifeline system located in a region of seismic activity, there is always the possibility that the rupture may strike one or more links of the system. This mode of failure could be important in the design of lifeline systems, especially in regions where earthquakes are of shallow foci. Of course, the links may also fail as a result of the effect of the destructive force released during an earthquake exceeding the resistance of the links.

The primary objective of this study is to apply the fault-rupture model of Der-Kiureghian and Ang (1977) to the seismic risk analysis of a lifeline system, and also to develop a companion model for evaluating the hazard of fault-rupture strike on a lifeline system. Because of the importance of the near-source regions in the seismic risk analysis of a lifeline system, an attenuation equation for the near-source region is also developed based on an analytical study.

In Chapter 2, the basic theory and assumptions related to the wave propagation model used in this study is described; and the variation of

intensity versus distance for different geometrical and geological parameters, associated with an earthquake source, is studied. The development of a model for the attenuation of intensity and the comparisons with existing attenuation equations are also presented in this chapter.

The basic assumptions regarding the proposed method of seismic risk analysis of lifeline systems are discussed in Chapter 3 along with the description of the three types of potential sources used in this study.

In Chapter 4, the description of a lifeline system is presented; and the possible modes of failure of a system are introduced and discussed. Also in this chapter the methods of evaluating the risk associated with the fault-rupture strike of a link and the probability of failure of a link due to ground shaking during an earthquake are presented. The probabilities associated with the failure of individual links are the basic information used to determine the failure probability of a lifeline system in either mode of failure; these are presented in Chapter 5.

Numerical examples and illustrations are presented in Chapter 6. The first example pertains to the probabilities of failure of the water distribution system of the city of Tokyo, Japan. The results are presented for the ground shaking hazards in terms of the annual probabilities of failure for different mean resistances.

In the second example problem, the safety of the network of highways around Boston, Massachusetts against fault-rupture hazard and ground shaking is analyzed.

Chapter 7 presents the summary and major conclusions of the present study.

1.4 Notation

The basic symbols used in this study are as follows:

a = maximum ground acceleration;

A = a seismically active area;

d = maximum ground displacement;

D = surface distance from a site to an earthquake source, also distance between ΔA_i and link j;

D_1, D_2 = distance terms in type 1 source;

D_x = fault displacement in dip-slip;

D_z = fault displacement in strike-slip;

E_i = occurrence of an earthquake in source i;

$E_{i,m}, E_{i,s}$ = occurrence of an earthquake in source i with magnitude m, or slip length s;

$f(m,r)$ = a function of m and r.

$f(x)$ = a function of x;

$f_X(n)$ = probability density function of X;

$F_X(n)$ = probability distribution function of X;

h = depth of an earthquake source;

ℓ = rupture length;

ℓ_j = the length of link j;

L_j = occurrence of a fault-rupture strike on link j;

m = earthquake magnitude;

M = a random variable describing earthquake magnitude;

m_o = lower-bound magnitude;

m_u = upper-bound magnitude;

$N(m)$ = number of earthquakes with magnitude m or greater;

P_F = system failure probability;

P_{F_j} = failure probability of link j;

r = distance of a point from a ruptured area;

s = rupture length;

S = a random variable describing the length of the rupture;

u_x, u_y, u_z = components of displacement at a point;

$\overline{U}$ = a vector describing the displacement at a point;

$\overline{u}_x, \overline{u}_y, \overline{u}_z$ = complex functions defining u_x, u_y and u_z;

v = maximum ground velocity;

W = fault width;

y = intensity of the ground shaking;

Y = a random variable describing y;

y_r = an intensity level for a link;

$\overline{y}_r$ = mean intensity resistance of a link;

β = regional seismicity parameter;

Ω = c.o.v. of a link resistance;

γ = angle of fault orientation, also stress drop;

λ = Lamé constant;

μ = modulus of rupture;

ν, ν_A, ν_i = earthquake occurrence rates;

σ, σ_i = standard deviations;

$\rho_{i,j}$ = correlation coefficient between two paths i and j;

$\overline{\psi}$ = a vector potential function; and,

ϕ = a scalar potential function, also standard normal distribution function.

CHAPTER 2

ATTENUATION EQUATION FOR NEAR-SOURCE REGIONS

2.1 Introductory Remarks

In the seismic risk analysis of structures and lifeline systems, a relationship between intensity and distance and magnitude is required to define the intensity at a point; i.e. a structure or any point of a lifeline system. Equations in this form, known as "attenuation equations," have been developed by several authors (e.g. Donovan, 1973, 1974; Esteva, 1970; Kanai, 1961, 1966; McGuire, 1974; and Trifunac and Brady, 1975). These are generally in the form of,

$$y = b_1 e^{b_2 m} [f(r)]^{-b_3} \qquad (2.1)$$

where y is the ground motion intensity at an observation point, m is the earthquake magnitude in the Richter scale, r is the distance (epicentral, focal, or the distance from the causative fault), b_1, b_2, and b_3 are constant parameters, and f(r) is a function of the distance r.

The existing empirical attenuation equations are mainly based on historical earthquake data; such data are almost entirely for points relatively far from the earthquake sources. For close-in (or near-source) regions there is virtually no empirical data to establish the needed intensity-distance-magnitude relation. Strictly speaking, therefore, the available attenuation equations are applicable only for sites that are far from the earthquake sources. In the case of the seismic risk of lifeline systems, the near-source regions are important because the possibility of some sections of the lifeline being close to an earthquake source exists.

In the absence of reliable data, the attenuation equation for the near-source regions may be developed using analytical results. For this purpose results of recent developments in wave propagation in half-space solids are examined, and an attenuation equation for the near-source regions established. In particular, the model and solution method presented by Seyyedian and Robinson (1975), which is based on the self-similar potentials, seems to be appropriate for the present study.

2.2 Effect of Earthquake Magnitude

The size of an earthquake is generally measured by the Richter magnitude scale. Therefore any proposed attenuation equation will be a function of the earthquake magnitude. As with other attenuation equations, the required attenuation equations will also be presented as functions of earthquake magnitude, and in the general form of Eq. 2.1. In order to include the earthquake magnitude in the attenuation equation, the relationship between the parameters of the source mechanism and the earthquake magnitude will be necessary. Many of these relationships have been derived empirically or semi-empirically relating one or more of the source parameters, such as the fault displacements or the fault width, to the earthquake magnitude. In the study by Chinnery (1969) a number of these relationships by different authors are summarized and compared with observed data for certain strike-slip fault ruptures. Also, Slemmons (1977) summarized some of the existing relationships between the earthquake magnitude and the source parameters. Such relationships can be written in a general form as

$$m = a_1 \log x + a_2 \tag{2.2}$$

where m is the earthquake magnitude, and a_1 and a_2 are constants. The parameter X can be any of the source parameters, such as the fault displacements fault width; or it can be a combination of two or more source parameters, such as LD_1^2, where L is the length of the fault-rupture and D_1 is the fault displacement, which has been used by King and Knopoff (1968); or LD_1 as used by Iida (1959). Other parameters have also been used to relate the source parameters to earthquake magnitude such as μLD_1W, known as the "seismic moment" (Refs. 23 and 24), or LD_1W (the geometrical moment), where W is the width of the rupture plane, and μ is the shear modulus.

In the current study, the results of King and Knopoff (1968) and Chinnery (1969) are examined. However, similar equations relating the earthquake magnitude to the source parameters may be used as well.

In their study, King and Knopoff (1968) defined the energy released during a shock as

$$E = \mu k\, LD_1^2\, f(\gamma) \tag{2.3}$$

and equated it to the energy in terms of m, i.e.

$$\log E_s = p + qm \tag{2.4}$$

obtaining the following relationship

$$\log[\mu k LD_1^2\, \eta\, f(\gamma)] = p + qm \tag{2.5}$$

where k is a numerical constant, μ is the shear modulus, η is a coefficient for the efficiency of the conversion of the stress energy (Eq. 2.3) to the radiated energy (Eq. 2.4), γ is the ratio of the shear stress on the

rupture surface after and before a shock (i.e. the stress drop), and p and q are constants. Assuming an appropriate function for $f(\gamma)$, King and Knopoff (1968) showed that Eq. 2.5 can be written in a general form as

$$m = a_n + b_n \log LD_1^n \qquad (2.6)$$

with n = 2 being an appropriate value for this relation. Based on observed data, Eq. 2.6 is evaluated as (for $8.5 > m > 5.5$)

$$\log LD_1^2 = 2.24m - 4.99 \qquad (2.7)$$

The above equation can be written in a simpler form in terms of the fault displacement only. This can be done by substituting the appropriate equation relating L to the earthquake magnitude, e.g. $L = \exp(1.596m - 7.56)$ which is based on world-wide data. In this form, Eq. 2.7 becomes

$$D_1 = \exp(1.78m - 12.31) \qquad (2.8)$$

where D_1 is in meters.

Other equations, relating source parameters to the earthquake magnitude are due to Chinnery (1969). Based on historical earthquake data for some strike-slip fault movements, Chinnery has proposed a number of relationships between source parameters and the earthquake magnitude. Among these, two equations which are of importance to the present study are as follows.

$$m = 1.67 \log LW - 14.51 \qquad (2.9)$$

$$m = 0.79 \log LD_1W - 4.74 \qquad (2.10)$$

These equations indicate the importance of combining different source

parameters in determining their relationships with the earthquake magnitude. Also, based on the data given by Chinnery and a statistical analysis, a particular relation between m and $D_1 W^{0.5}$ may be derived. This relationship for $m > 4$ is shown in Fig. 2.1 and indicates a linear relation between m and $\log (D_1 W^{0.5})$ as follows

$$m = 6.456 + 0.932 \log D_1 W^{0.5} \tag{2.11}$$

or alternatively

$$D_1 W^{0.5} = \exp (2.47m - 15.97) \tag{2.12}$$

where $D_1 = D_2$ is the fault displacement in meters and W is in kilometers.

2.3 Wave Propagation in Half-Space Solids

In general, the problem of motion of a point at the ground surface due to an earthquake of fault-rupture origin is a three-dimensional wave propagation problem. In order to simplify the procedure, Seyyedian and Robinson (1975) idealized the three-dimensional problem as two two-dimensional problems and solved the wave propagation equations on the basis of the method of self-similar potentials. The solution method may be summarized as follows.

The wave propagation equations of small magnitude for a homogeneous, isotropic solid can be written as

$$(\lambda + \mu) \frac{\partial \Delta}{\partial x} + \mu \nabla^2 u_x = \rho \frac{\partial^2 u_x}{\partial t^2} \tag{2.13a}$$

$$(\lambda + \mu) \frac{\partial \Delta}{\partial y} + \mu \nabla^2 u_y = \rho \frac{\partial^2 u_y}{\partial t^2} \tag{2.13b}$$

$$(\lambda + \mu)\frac{\partial \Delta}{\partial z} + \mu \nabla^2 u_z = \rho \frac{\partial^2 u_z}{\partial t^2} \qquad (2.13c)$$

where x, y and z are cartesian coordinates, ρ is the mass density of the solids, u_x, u_y, and u_z are the components of the displacement vector $\overline{U}$, t is time, and λ and μ are the Lamé constants. In Eqs. 2.13, Δ and also the operator ∇^2 are defined by the following expressions:

$$\Delta = \frac{\partial u_x}{\partial x} + \frac{\partial u_y}{\partial y} + \frac{\partial u_z}{\partial z} \qquad (2.14)$$

$$\nabla^2 = \frac{\partial^2}{\partial x^2} + \frac{\partial^2}{\partial y^2} + \frac{\partial^2}{\partial z^2} \qquad (2.15)$$

Applying Helmotz's theorem to the displacement vector $\overline{U}$,

$$\overline{U} = \text{grad } \phi + \text{curl } \overline{\psi} \qquad (2.16)$$

where ϕ is a scalar potential function, whereas ψ is a vector potential function. The problem, then, involves finding the two potential function ϕ and ψ in order to define the complete state of displacement at a given point. To do this Seyyedian and Robinson (1975) considered the following two-dimensional problems:

(i) Plain-Strain Problem -- This is the case corresponding to a dip-slip motion (see Fig. 2.2). The x and y components of the vector potential ψ for this case are zero. From Eqs. 2.13 and 2.16, it can be shown that

$$(\nabla^2 - \frac{1}{v_p^2}\frac{\partial^2}{\partial t^2})\phi = 0 \qquad (2.17a)$$

$$(\nabla^2 - \frac{1}{v_s^2}\frac{\partial^2}{\partial t^2})\psi = 0 \qquad (2.17b)$$

where $v_p = \sqrt{(\lambda + 2\mu)/\rho}$ and $v_s = \sqrt{\mu/\rho}$ are, respectively, the speeds of the P- and S-waves, and ψ_z is the z-component of ψ.

(ii) Antiplane problem -- This case corresponds to a strike-slip motion. The displacement vector consists only of component u_z (see Fig. 2.3). Combining Eqs. 2.13 and 2.16 we obtain

$$(\nabla^2 - \frac{1}{v_s^2} \frac{\partial^2}{\partial t^2}) u_z = 0 \qquad (2.18)$$

The combination of the above two problems, therefore, defines the three components of the displacement vector $\bar{U}$ at a given point. For a general case of a half-space solid, the above problems are solved in a complex domain by considering: (i) the effect of reflected waves at the free surface of the half-space; (ii) the boundary conditions at the free surface and at the rupture surface; and (iii) the possibility of the formation of a head-wave and the effect of head-wave disturbances when an S-wave reaches the free surface.

The displacement components u_x, u_y and u_z are given as the real parts of the complex functions $\bar{u}_x$, $\bar{u}_y$ and $\bar{u}_z$, which are, in turn, functions of the potential functions introduced earlier. Other assumptions and comments with regard to this model are as follows:

(i) In the above two-dimensional problems, the length of the fault-rupture is assumed to be infinite. This assumption seems to be reasonable for the near-source region, since for major earthquakes (magnitude greater than 5 or 6) and sites close to the fault, only that portion of the rupture which is in the vicinity of the site has a dominant effect on the maximum motion at the site; i.e. the contributions from the end portions of the fault-rupture may be much less significant. Thus, the rupture may be

assumed to be infinitely extended on both sides of the focus. However, for sites that are far from the earthquake source, this assumption would be inadequate, as the three-dimensional effects become more important.

(ii) The different source parameters associated with this model are as follows:

1. Parameters D_x and D_z--These are fault displacements in dip-slip and strike-slip rupture, respectively, as shown in Figs. 2.2 and 2.3.

2. Geometrical dimensions--These parameters are shown in Figs. 2.2 and 2.3 and include the focal depth h (depth of earthquake source), angle γ representing the orientaiton of the rupture surface relative to the free surface, and width of the rupture surface W.

3. Geological parameters--These parameters are the speed of the P- and S-waves which are, respectively, $v_p = \sqrt{(\lambda+2\mu)/\rho}$ and $v_s = \sqrt{\mu/\rho}$, and also the speed of rupture propagation.

2.4 Acceleration, Velocity, and Displacement in Vertical and Horizontal Motions

The term "intensity" is used as a measure of the severity and destructiveness of the ground shaking at a site. By this definition, therefore, the maximum ground acceleration (a), maximum velocity (v), maximum displacement (d), or the Modified Merecalli scale (MM) are all measures of ground motion intensity.

Seyyedian and Robinson (1975) developed their results in terms of displacements at a given point on the surface. Although an attenuation equation may be derived for maximum ground displacements, the maximum acceleration is usually used as a measure of earthquake intensity for engineering purposes. The maximum acceleration components a_x, a_y, and a_z

may be found by differentiating the respective displacement functions. Alternatively, the maximum acceleration may be found using the ratios v/a and ad/v^2, in which a, v and d are, respectively, the maximum ground acceleration, velocity and displacement. Newmark, Hall, and Mohraz (1973) obtained values of v/a and ad/v^2 for both horizontal and vertical earthquake on the basis of an extensive study of horizontal and vertical earthquake spectra. Such results may be appropriate for converting the maximum displacements to maximum acceleration at a point. In the present study the average of the values proposed in Newmark, Hall, and Mohraz (1973), reproduced in Tables 2.1 to 2.4, will be used for this purpose.

2.5 Variation of Intensity in Near-Source Regions

The analytical method of Seyyedian and Robinson (1975) yields the maximum displacements components at a point; these may be given in non-dimensional terms as d_x/D_x, d_y/D_x and d_z/D_z, where d_x, d_y and d_z are the respective maximum ground displacements in the x, y, and z directions, and D_x and D_z are, respectively, the fault displacements in dip-slip and strike-slip. The corresponding accelerations are obtained using the intensity ratios of Table 2.1 through 2.4 in terms of a_x/D_x, a_y/D_x and a_z/D_z, where a_x and a_y are the acceleration components in the vertical and horizontal directions, respectively, in a dip-slip rupture; whereas a_z is the horizontal component of acceleration in a strike-slip rupture. The variation of these accelerations with the horizontal distance D of a point from an earthquake source (epicentral distance) are examined in this section including the effects of the individual source parameters.

2.5.1 The Strike-Slip Case

The two-dimensional problem in this case is an anti-plane problem which results in the horizontal component of motion in the z direction. The maximum acceleration is given as a_z/D_z in this case, which has units of g/m.

Analytical results appear to show that intensity is not much affected by a change in the material properties of the half-space; the variation of a_z/D_z are mainly affected by the geometrical parameters such as the depth of the focus, h, the angle of fault orientation, γ, and the fault width W. The specific effects of these parameters may be described as follows.

The Fault-Width W--The variation of a_z/D_z with D highly depends on W. Typical results indicating this are shown in Figs. 2.4 and 2.5 for a variable W and constants γ and h ($\gamma = 90°$ and h = 15 and 20 kilometers). It can be seen that the dependence of a_z/D_z on W is reduced for values of W/h close to or equal to 1. This can also be seen in Fig. 2.6 where the variation of a_z/D_z against W for h = 15 kilometers and $\gamma = 90°$ is shown. An examination of the results of Figs. 2.4 through 2.6 shows that for values of $W < h$, the effect of W on the intensity may be represented as $W^{0.5}$; whereas, for $W > h$, the intensity may be represented as independent of W.

The Focal Depth h--For a variable h and constants W and γ the variation of a_z/D_z against D shows that for sites very close to an earthquake source, the intensity increases with a decrease in the focal depth h; whereas, for points with distances greater than about 10 kilometers from the source ($D > 10$ km.) the intensity decreases for a shallow source (see Figs. 2.7).

Fault Orientation γ--The variation of a_z/D_z with D is shown in Figs. 2.8 for different fault orientations γ. In particular, the effect of γ on the variation of a_z/D_z with D is shown for W = 4 and h =15 ($W < h$), and W = 20

($w > h$). It appears that with $\gamma = 90^0$ the average effect of γ would be obtained. Also for points very close to the earthquake source, the intensity becomes approximately independent of γ.

A change in any of the source parameters, therefore will alter the result for the intensity. This fact, perhaps, verifies the large scatter observed in available historical data which have been used to establish most existing attenuation equations. Thus, the effect of the source parameters is important and must be included in any proposed attenuation equation. In the present study, on the basis of above discussion, the effect of the source parameters in the proposed attenuation equation for a strike-slip case is considered.

1. The intensity depends on the fault width W especially for cases where W is smaller than h; this dependence is proportional to the square root of the fault width. For cases in which W is larger than h, the intensity tends to be independent of the fault width.

2. The focal depth, h, has a decreasing effect on the intensity at a point close to an earthquake source; and an increasing effect on the intensity at a farther site ($D > 10$ km). For cases in which h is between 10 to 20 kilometers (common values for most earthquakes in California) and for points close to the source, the intensity stays approximately constant (see Figs. 2.7).

3. The proposed attenuation equation may be obtained for a specific fault orientation; or the effect of γ can be represented in the equation by the average for all values of γ. In the current study, the case at which $\gamma = 90^0$, i.e. vertical fault, will be considered.

Based on the above discussion, the following equations are proposed for the horizontal motion in a strike-slip case.

$$a_z/D_z = 0.8\ h^{1.08}\ W^{0.50}\ (0.7\ D+h)^{-1.62} \qquad w \leq h \qquad (2.19a)$$

$$a_z/D_z = 0.8\ h^{1.58}\ (0.7D + h)^{-1.62} \qquad w > h \qquad (2.19b)$$

where a_z is the horizontal acceleration in g's, D_z is the fault displacement in a strike-slip rupture, in meters, and W, h, and D are in kilometers. Also, in terms of the focal distance, R, the following equations may be used:

$$a_z/D_z = 0.45\ h^{1.08}\ W^{0.50}\ R^{-1.523} \qquad w \leq h \qquad (2.20a)$$

$$a_z/D_z = 0.45\ h^{1.58}\ R^{-1.523} \qquad w > h \qquad (2.20b)$$

where R is in kilometers.

2.5.2 The Dip-Slip Case

This is the case corresponding to a plane-strain problem; and the results are the displacements in the x and y directions (see Fig. 2.2). The maximum acceleration components in this case are a_y/D_x and a_x/D_x. Again, in this case, the variation of a_y/D_x and a_x/D_x with epicentral distance D has been examined with regard to the effects of different source parameters. Aside from the effects of the parameters W, h and γ, the results in this case are also affected by the type of material in the half space as represented by the ratio of the speed of the P-wave to that of the S-wave; i.e. $v_p/v_s = \sqrt{(\lambda+2\mu)/\mu}$. However, this effect is not very

significant on the y-component of motion. The effects of the various parameters may be summarized as follows.

(i) Effects on Horizontal Component a_y/D_x -- Figs. 2.9 and 2.10 show the variation of a_y/D_x with epicentral distance D for different W. Constant values of h and γ were used, with h = 15 and 20 kilometers, and $\gamma = 90^0$. These results show that the effect of W is not very pronounced, especially at the close-in regions. Other parameters examined are the focal depth, h, the ratio v_p/v_s, and the angle γ. The results obtained in this case indicated that for points close to the source, the effects of the parameters h and v_p/v_s are also not very pronounced; these can be seen in Figs. 2.11 and 2.12. However, the intensity in this case depends highly on the fault orientation γ. The effect of γ can be seen in Fig. 2.13, where for the case of W=4 and h=15 kilometers the variation of a_y/D_x versus D is shown. On the basis of the results described above, a suitable attenuation equation may be obtained, using the average values obtained with W=4 to 10 and h=10 to 25 kilometers, and a specific fault orientation. Accordingly, the following equation is proposed:

$$a_y/D_x = 125\ (D + 12.5)^{-1.95} \qquad (2.21)$$

where a_y, the horizontal acceleration, is in g's, D_x in meters and D in kilometers.

(ii) Effects on Vertical Component a_x/D_x -- The results for the vertical acceleration, a_x/D_x are shown in Figs. 2.14 to 2.18. The parameter which affects a_x/D_x significantly is, again, the rupture angle γ (see Fig. 2.18). However, other parameters such as W, v_p/v_s and h

(Figs. 2.14 through 2.17) also affect the vertical acceleration; generally to a greater degree than the corresponding effects on a_y/D_x. Based on a detailed examination of the results for this case, the following are suggested:

1. The attenuation equation may be obtained by fitting a curve to that part of the results corresponding to points close to the source.

2. The effect of the rupture width, W, and the ratio of wave speeds, v_p/v_s, may be represented as $W^{0.8}$ and $(v_p/v_s)^{-1.54}$.

3. The attenuation equation ought to be given explicitly as a function of γ; because of the irregularity in the effect of γ (see Fig. 2.18), a single parameter cannot represent the effect of the fault position. Here, an attenuation equation is presented for the case of a vertically oriented rupture ($\gamma = 90^0$).

Based on the above discussion, the following attenuation equation is proposed for the vertical acceleration arising from earthquakes of dip-slip origin.

$$a_x/D_x = 17.3\ W^{0.80}\ (v_p/v_s)^{-1.540}(D+15)^{-1.80} \qquad (2.22a)$$

or alternatively

$$a_x/D_x = 17.3\ W^{0.80}\ (2+\lambda/\mu)^{-0.77}\ (D+15)^{-1.80} \qquad (2.22b)$$

where a is in g's, D in meters and W and D in kilometers.

The analytical results presented herein for both the horizontal and vertical accelerations, show that the maximum ground motion at a given epicentral distance from the source is a function of several parameters of the source. In particular, the rupture angle γ appears to have the

largest effect on the maximum motion. Consequently, unless an attenuation equation is expressed as a function of these parameters (particularly γ), it would not be surprising to see significant scatter in the observed motions around the given attenuation equations.

The attenuation equations may be presented in terms of the earthquake magnitude with the aid of Eqs. 2.8 through 2.12. After performing the necessary calculations and replacing D_1 by D_x or D_z wherever necessary, the following equations are obtained by virtue of Eq. 2.8.

(i) For strike-slip

$$a_z = 3.6\times10^{-6}\ h^{1.08}\ W^{0.50}\ e^{1.78m}\ (0.7D+h)^{-1.62} \qquad w\leq h \qquad (2.23a)$$

$$a_z = 3.6\times10^{-6}\ h^{1.58}\ e^{1.78m}\ (0.7D+h)^{-1.62} \qquad w>h \qquad (2.23b)$$

and in terms of the focal distance R,

$$a_z = 2.02\times10^{-6}\ h^{1.08}\ W^{0.50}\ e^{1.78m}\ R^{-1.523} \qquad w\leq h \qquad (2.24a)$$

$$a_z = 2.02\times10^{-6}\ h^{1.58}\ e^{1.78m}\ R^{-1.523} \qquad w>h \qquad (2.24b)$$

(ii) For Dip-slip

$$a_y = 5.59\times10^{-4}\ e^{1.78m}\ (D+12.5)^{-1.95} \qquad (2.25)$$

$$a_x = 7.80\times10^{-5}\ W^{0.8}\ (2+\lambda/\mu)^{-0.77}\ e^{1.78m}\ (D+15)^{-1.8} \qquad (2.26)$$

where D is the epicentral distance in kilometers, R is the focal distance in kilometers, and a_x, a_y and a_z are maximum accelerations in g's.

The proposed attenuation equations for the strike-slip case may also be given in a simpler form and independent of the parameter W. This can be done by applying Eq. 2.12, which relates $D_1 W^{0.5}$ to m, which yields the following equations

$$a_z = 9.26 \times 10^{-8} \, h^{1.08} \, e^{2.47m} \, (0.7D+h)^{-1.62} \qquad (2.27)$$

and in terms of R,

$$a_z = 5.21 \times 10^{-8} \, h^{1.08} \, e^{2.47m} \, R^{-1.523} \qquad (2.28)$$

Although, the magnitude-source parameters relations specified by Eqs. 2.8 through 2.12 have been used here, other appropriate equations relating m to W, D_z or D_x may be used also to develop the attenuation equations in terms of the earthquake magnitude. In this regard, if there is enough information available in a specific region, suitable attenuation equations may then be obtained based on Eqs. 2.19 through 2.22 for that region.

2.6 Comparison with Existing Attenuation Equations

A number of existing attenuation equations proposed by different authors are summarized in Table 2.5. In these equations the maximum ground acceleration is given in terms of the magnitude m and distance R. However, the distance R has different interpretations in different equations. Comparison of results from these equations with those of the present study has been made for a strike-slip motion and specific source parameters appropriate for earthquakes in the Western United States.

Based on the data given by Chinnery (1969) regarding different values of W for a number of important earthquakes in California, a W equal to 5-6 kilometers will be used with Eqs. 2.23; also a depth, h, equal to 20 kilometers will be considered. These values appear to be equivalent to California earthquakes with magnitudes $6 \rightarrow 7$ in the Richter scale. The epicentral distance is used here for the purpose of comparison. Wherever necessary, a suitable transformation was made to define the results in terms of epicentral distance. The results are then compared with those proposed in the present study as described below.

Equations 2.23 and 2.27 are shown in Fig. 2.19 along with results from the attenuation equations given in Table 2.5 for $m = 7$. As it can be seen, for sites close to an earthquake source the equation by Donovan (1974) gives lower values for maximum acceleration than the values from the present study. For sites with $D \geq 10$ kilometers, the situation is reversed. Comparing with Esteva's equation (Ref. 17), it can be seen that the maximum accelerations from the equations proposed in the current study are generally higher. With regard to the equation by McGuire (1974) a better agreement is observed; and as it can be seen in Fig. 2.19, for sites close to the source, the ground accelerations predicted by the present study are slightly higher than those obtained with McGuire's equation. Finally the attenuation equation of Trifunac and Brady (1975), with the appropriate values for the parameters in their model, is shown in Fig. 2.19. In contrast to the attenuation equations of Donovan and McGuire, results obtained with the Trifunac and Brady relation are consistently higher than those of the present study. As it can be seen, the difference becomes significant for sites that are close to the earthquake source.

In summary, according to the present study, for California earthquakes, the existing attenuation equations generally underestimate the ground accelerations for close-in or near-source regions. However, this is not always the case and a number of existing equations (e.g. that of Trifunac and Brady) would consistently predict higher ground accelerations particularly at points close to the earthquake sources.

The differences in the calculated intensities based on different attenuation equations (see Fig. 2.19) become critical in the design of important structures, such as nuclear power plant; in the sense that some of the attenuation equations may under-estimate the site intensities whereas others may tend to over-estimate the true intensity at a site.

CHAPTER 3

RELATIONSHIPS NEEDED IN SEISMIC RISK ANALYSIS

3.1 Earthquake Mechanism

Most earthquakes of significance to engineering are believed to be of tectonic origin. A tectonic earthquake is the result of the sudden release of stored energy through the rupture of the earth's crust, along lines or zones of weakness, known as "faults." The point where the rupture first occurs is the focus of the earthquake. In a strong-motion earthquake, a chain reaction would take place along the entire length or area of rupture, but at any given instant the earthquake origin would lie in a small volume of the crust (practically a point) and would travel along the fault (Ref. 39). The intensity of the earthquake shocks will attenuate with distance such that at locations far from the breaks the ground motions are not significant to engineering.

The length, s, of the rupture zone is related to the total energy released, to the type of fault, and to other geological and regional factors and may be several hundred kilometers long for a large-magnitude earthquake. Generally, a linear relationship between magnitude and the logarithm of the fault length is given to relate s to the Ricter magnitude, m. Such a relation can also be shown as

$$s = \exp(am-b); \tag{3.1}$$

where a and b are constants. For example, based on world-wide data,

Eq. 3.1 is evaluated to be

$$s = \exp(1.596m - 7.56) \tag{3.2}$$

Despite the large uncertainty in the rupture length-magnitude relationship, such relationships are useful for seismic risk analyses. It has been shown by Der-Kiureghian and Ang (1975) that the effect of this uncertainty is much less than that from the uncertainty in the attentuation equation.

Equations similar to Eq. 3.2 may also be derived based on the study of the availabel data for a specific region. Due to the smaller scatter, which is expected for data available in a specific region, the corresponding rupture length-magnitude relation, therefore, involves less uncertainty. However, such relations are not available for many regions because of the lack of adequate data.

3.2 Earthquake Magnitude and Slip Length

Based on the Richter's law of earthquake magnitude, the probability density function of magnitude, i.e. $f_M(m)$, may be derived. According to this law, in a certain zone of the crust and during a given period of time, the occurrence of earthquakes can be approximated by the relationship

$$\log N(m) = p - qm \tag{3.3}$$

where $N(m)$ is the number of occurrences with magnitude m or greater, and p and q are constants (Richter, 1958). Alternatively, Eq. 3.3 can be

written in the following form:

$$N(m) = \exp(\alpha - \beta m) \tag{3.4}$$

where $\alpha = 2.3p$ and $\beta = 2.3q$.

Considering a lower bound magnitude, m_o, and an upper bound magnitude, m_u, it can be shown that the cumulative distribution function of magnitude may be derived from Eq. 3.4 in the following form:

$$F_M(m) = \frac{1 - e^{-\beta(m-m_o)}}{1 - e^{-\beta(m_u-m_o)}} \tag{3.5}$$

The corresponding probability density function will, then, be

$$f_M(m) = \frac{\beta}{k} \exp[-\beta(m-m_o)]; \quad m_o \leq m \leq m_u \tag{3.6}$$
$$= 0 \qquad\qquad\qquad\qquad \text{elsewhere}$$

which is in the form of a shifted exponential distribution function with constant k being equal to

$$k = 1 - \exp[-\beta(m_u - m_o)]. \tag{3.7}$$

In the seismic risk analysis of lifeline systems, sometimes it is more convenient to use the probability density function of rupture length, s, instead of that of earthquake magnitude, m. The probability density function of s can be easily obtained from Eq. 3.6 by considering the re-

lationship between m and s (Eq. 3.1) and the following general equation

$$f_S(s) = f_M(g^{-1}) \left|\frac{dg^{-1}}{ds}\right| ; \qquad (3.8)$$

where $g^{-1}(s)$ is the inverse of function $s = g(m)$, i.e.

$$g^{-1}(s) = m = [\ln(s) - b]/a \qquad (3.9)$$

Substituting Eqs. 3.6 and 3.9 in Eq. 3.8 and carrying out the differentiation, the probability density function of s becomes

$$f_S(s) = c\, s^{-(\beta/a + 1)} \qquad s_o \leq s \leq s_u \qquad (3.10)$$

$$= 0 \qquad \text{elsewhere}$$

in which

$$c = \frac{\beta}{a(s_o^{-\beta/a} - s_u^{-\beta/a})} ; \qquad (3.11)$$

and

$$s_o = \exp(am_o - b); \qquad (3.12)$$

$$s_u = \exp(am_u - b); \qquad (3.13)$$

where rupture length s_o and s_u correspond to the lower-bound and upper-bound magnitudes, respectively.

In the study by Der-Kiureghian and Ang (1975,1977), the influences of parameters m_o and m_u and β on the calculated risk were examined. Among the major conclusions are the following:

(i) The parameter β, which is the slope of the magnitude-recurrence curve (Eq. 3.3), should be chosen carefully for a region, since the calculated probabilities are sensitive to this parameter.

(ii) The lower-bound magnitude m_o should be such that earthquakes of magnitudes equal to m_o and smaller do not produce damaging intensities. Generally, a value of $m_o = 4$ is appropriate.

(iii) The upper-bound magnitude m_u need not be greater than 9. Even if earthquakes of magnitude greater than 9 are possible, the contributions to the calculated risk would not be significant.

3.3 Modeling Potential Earthquake Sources

As discussed earlier, geologic faults are believed to be the main potential sources of destructive earthquakes. However, for many regions, the fault system may not be known or well surveyed. For this reason, in order to permit the modeling of all conceivable seismic sources, three types of idealized models are introduced and will be used in the evaluation of the earthquake hazards to lifeline systems. These seismic sources are designated as Types 1, 2, and 3 and defined respectively as follows:

(i) Type 1 Source--A well-defined fault or fault system. The length, direction, and position of the fault relative to the site are assumed to be known in this case. This model would be appropriate if the potential seismic activity is expected from a well-defined fault or fault system, such as the San Andreas fault in California.

(ii) Type 2 Source--Fault direction known. The exact location of a fault with respect to a site is not known, but the dominant orientation of the fault or fault system is known. This case would arise when a certain zone of the crust contains numerous active faults with a common orientation, or where the location of the fault-rupture may occur in a dominant direction.

(iii) Type 3 Source--Unknown faults. The fault location as well as their directions are unknown. This model is appropriate for modeling of those areas in which a potential zone of the crust contains numerous active faults with no dominant direction, or the locations and the orientations of the faults are completely unknown.

In order to model the fault system in a region of seismic activity, one or more of the three types of seismic source models, as described above, may be used. In the following chapters, the calculation of the risk for all three types are introduced and described. In all cases, the effect of rupture length is included in this study.

CHAPTER 4

MODELS FOR SEISMIC HAZARD ANALYSIS OF LIFELINE SYSTEMS

4.1 Introductory Remarks

A lifeline system is composed of a number of elements (e.g. pipelines, segments of a highway) linked together to carry out a certain level of service for the benefit of the public. Simple lifeline networks, as shown in Fig. 4.1, consist of several links in series or parallel, with an entry point and a final point. In a water distribution system, the entry point is usually a water supply station, whereas the final point can be any point for which water is needed. The objective in this system is to maintain the flow of water from the water supply to any given point in the system. Large lifeline systems cover vast spatial areas and are composed of links each of which may be several kilometers long. In general the objective in a lifeline system is to maintain the flow of a certain quantity, such as water in the case of a water distribution system; or the flow of traffic in the case of a transportation network, between any two points of the system.

The purpose of seismic risk analysis of a lifeline system is to evaluate the reliability of the system against earthquake hazards to carry out its objective. The results of such analysis will be useful in the design and planning of a lifeline system in a region of potential earthquake activity.

Aside from the potential for seismic damage caused by the strong shaking of the ground, a lifeline system may also be subjected to the

possibility of a fault-rupture strike on one or more links of the system. This case is particularly of concern in the regions where surface ruptures are possible.

In this chapter the methods for evaluating the probabilities of encountering either of the above two modes of earthquake hazards are presented for individual links. The respective probabilities of failure of the system involves a detailed correlation analysis which is described in the next chapter. In the evaluation of probabilities in both modes of failure, the three types of source models will be considered in order to permit modeling of all possible potential sources in the region.

4.2 Fault-Rupture Hazard

This case concerns the possibility that during an earthquake the rupture, initiating at the focus, will strike one or more links of a lifeline system and, therefore, will cause the failure of the links. This mode of failure is especially important in regions where shallow-focus earthquakes are likely to occur, such as the Western United States.

Suppose that in a region, n potential earthquake sources were identified. If the average number of earthquakes per year with magnitude greater than or equal to m_o in the i^{th} source is ν_i, the average number of earthquakes in a year for the entire region then will be

$$\nu = \sum_{i=1}^{n} \nu_i \tag{4.1}$$

Given an earthquake with origin (hypocenter) located at source i, the probability of a fault-rupture strike on a given link j is $P(L_j^i|E_i)$,

in which L_j^i = a rupture strike on link j due to an earthquake in source i, and E_i is the occurrence of an earthquake in source i. Thus the probability of a fault-rupture strike on link j due to an earthquake in the i^{th} source is $P(L_j^i) = P(L_j^i|E_i)\ P(E_i)$. Considering n potential earthquake sources in the region, the probability of a fault-rupture strike on link j becomes

$$P(L_j) = P(L_j^1 \cup L_j^2 \cup \ldots \cup L_j^n) \tag{4.2a}$$

$$= 1 - P(\bar{L}_j^1\ \bar{L}_j^2 \ldots \bar{L}_j^n)$$

where $\bar{L}_j^i$ is the event of no fault-rupture strike on link j due to an earthquake in source i. It is reasonable to assume that L_j^i are statistically independent; hence,

$$P(L_j) = 1 - P(\bar{L}_j^1)\ P(\bar{L}_j^2) \ldots P(\bar{L}_j^n) \tag{4.2b}$$

$$= 1 - \prod_{i=1}^{n} [1 - P(L_j^i\ E_i)\ P(E_i)]$$

For small probabilities, $P(L_j^i\ E_i)$ and $P(E_i)$, Eq. 4.2b can be given as,

$$P(L_j) \approx \sum_{i=1}^{n} P(L_j|E_i)\ P(E_i) \tag{4.2c}$$

where the superscript i is dropped for simplicity.

Assuming the average occurrence rate in source i relative to that over the entire region remains constant with time, the probability of occurrence of the event E_i may be expressed as,

$$P(E_i) = \frac{\nu_i}{\nu} \tag{4.3}$$

Substituting Eq. 4.3 in Eq. 4.2c,

$$P(L_j) = \sum_{i=1}^{n} P(L_j|E_i) \frac{\nu_i}{\nu}$$

$$= \frac{1}{\nu} \sum_{i=1}^{n} P(L_j|E_i) \nu_i \qquad (4.4)$$

The future occurrence of earthquakes in a region may be assumed to constitute a homogeneous Poisson process, with the average occurrence rate ν per year. During each occurrence, there is a constant probability of fault-rupture strike on link j; it follows then that the occurrence of L_j is also a Poisson process with activity rate $\nu\ P(L_j)$ or $\sum_{i=1}^{n} P(L_j|E_i)\ \nu_i$. Therefore, the probability of a fault rupture strike on link j in one year is

$$P(L_j)_{\text{one year}} = 1 - \exp\left[-\sum_{i=1}^{n} P(L_j|E_i)\nu_i\right]. \qquad (4.5)$$

For small values of this probability (cases of practical interest) the above result can be approximated by

$$P(L_j)_{\text{one year}} = \sum_{i=1}^{n} P(L_j|E_i)\ \nu_i \qquad (4.6)$$

The Poisson process, which assumes temporal and spatial independence of earthquake events, may not be consistent with the elastic rebound theory of earthquakes; and this process is unable to portray earthquakes as the release of gradually accumulated strains in the earth's crust or to describe foreshocks and aftershocks. In spite of these shortcomings, the Poisson process is an acceptable and useful occurrence model in seismic

risk analysis, especially for moderate and large earthquakes (Rosenblueth, 1973).

From the above formulations, it can be observed that the main task involves the determination of the conditional probability $P(L_j|E_i)$. This conditional probability will depend on the three idealized types of sources, described earlier.

4.3 Determination of $P(L_j|E_i)$

The term $P(L_j|E_i)$ is defined as the probability of a fault-rupture strike on link j of a lifeline system, given an occurrence of an earthquake in source i. The magnitude and location of this earthquake within source i is random. In general the following are assumed.

i. The random magnitude of a given earthquake has the density function given by Eq. 3.6. Alternatively it may be defined that the random rupture length of a given earthquake has the density function given by Eq. 3.10.

ii. The distribution of the focal location is uniform over the source.

iii. An earthquake originates as a rupture propagating symmetrically on each side of the focus along the fault. The length of the fault-rupture (slip) is related to the random magnitude through Eq. 3.1.

On the basis of above assumptions, the methods to evaluate the conditional probability $P(L_j|E_i)$ for each of the three source types are as follows.

4.3.1 Type 1 Source (Well-defined faults system)

For an earthquake with magnitude m from a Type 1 source, the conditional probability $P(L_j|E_i)$ can be written as

$$P(L_j|E_i) = \int_{\ell} P(L_j|E_{i,s})\, f_S(s)\, ds; \qquad (4.7)$$

where $E_{i,s}$ = an earthquake in source i with rupture length s in which $s = \exp(am-b)$; and ℓ indicates the length of the fault.

Denoting D_1 and D_2, respectively, as distances from the intersection point to link j with the fault to the nearest and farthest ends of the fault, as shown in Fig. 4.2, and considering that the rupture is extended by s/2 at each side of the focus, the conditional probability $P(L_j|E_{i,s})$ can be obtained in terms of s, ℓ and D_1. It is observed that:

If $D_2 \leq \ell$, with uniform probability distribution along the fault, we have

$$P(L_j|E_{i,s}) = \begin{cases} s/\ell; & \text{if } s/2 \leq D \leq D \qquad (4.8a) \\ (s/2+D_1)/\ell; & \text{if } D \leq s/2 < D \qquad (4.8b) \\ 0.; & \text{otherwise} \qquad (4.8c) \end{cases}$$

Using the results of Eqs. 4.8 in Eq. 4.7 and carrying out the integration, the conditional probability $P(L_j|E_i)$ becomes

$$P(L_j|E_i) = \int_{s_0}^{2D_1} \frac{s}{\ell} f_S(s)ds + \int_{2D_1}^{s_2} \frac{s+2D_1}{2\ell} f_S(s)\, ds; \qquad (4.9)$$

or

$$P(L_j|E_i) = \frac{c}{2\ell(1-\beta/a)}\left[(2D_1)^{1-\beta/a} + s_2^{1-\beta/a} - 2s_0^{1-\beta/a}\right]$$

$$- \frac{cD_1 a}{\ell\beta}\left[s_2^{-\beta/a} - (2D_1)^{-\beta/a}\right]; \qquad (4.10a)$$

where s_2 = the smaller of $2D_2$ and s_u.

Similarly if $D_2 > \ell$,

$$P(L_j|E_{i,s}) = \begin{cases} (s/2-D_1)/\ell; & \text{if } D_1 \leq s/2 \leq D_2 \qquad (4.11a) \\ 0; & \text{otherwise.} \qquad (4.11b) \end{cases}$$

Substituting Eqs. 4.11 in 4.7 and performing the integration, the conditional probability $P(L_j|E_i)$ becomes

$$P(L_j|E_i) = \frac{c}{2\ell(1-\beta/a)}\left[s_2^{1-\beta/a} - (2D_1)^{1-\beta/a}\right]$$

$$+ \frac{cD_1 a}{\ell\beta}\left[s_2^{-\beta/a} - (2D_1)^{-\beta/a}\right] . \qquad (4.10b)$$

For certain exceptional cases s_o may become larger than $2D_1$, in which case $2D_1$ in Eq. 4.10a should be replaced by s_o and therefore, Eq. 4.10a becomes

$$P(L_j|E_i) = \frac{c}{2\ell(1-\beta/a)}\left[s_2^{1-\beta/a} - s_o^{1-\beta/a}\right]$$

$$- \frac{cD_1 a}{\ell\beta}\left[s_2^{-\beta/a} - s_o^{-\beta/a}\right] \qquad (4.10c)$$

4.3.2 Type 2 Source (Dominant fault direction known)

Consider a seismically active zone of the earth's crust as shown in Fig. 4.3 denoted by A. The dominant direction of the faults is denoted by ox making an angle α with respect to link j. In this case, reference to Fig. 4.3 will show that a fault-rupture strike will occur only if an earthquake of magnitude m occurs within the shaded area, A_1, shown in Fig. 4.3.

By dividing the shaded area, A_1, into smaller areas ΔA_i with coordinates x and y with respect to axes ox and oy, each ΔA_i can be considered as a single source with occurrence rate ν_i which can be defined in either of the following ways.

(i) Assume uniform activity rate over A; then

$$\nu_i = \frac{\Delta A_i}{A} \nu A \tag{4.12}$$

where ν_A is the activity rate for area A.

(ii) From statistical data, i.e. the average number of earthquake occurrences within ΔA_i per year, ν_i may be obtained directly.

For an earthquake of magnitude m in the ith source (ΔA_i), the rupture will extend s/2 at each side of the focus parallel to ox direction. Denoting D as the distance from ΔA_i with the link j, in this case the rupture will strike link j only if s/2 is greater than D. Therefore, the conditional probability $P(L_j|E_i)$ in this case

$$P(L_j|E_i) = P(s/2>D) = P(M>m_1) = 1-F_M(m_1) \tag{4.13}$$

where,

$$m_1 = [\ln(2D) + b]/a \ ; \tag{4.14}$$

and

$$D = |x - y \tan(\alpha)| \ ; \tag{4.15}$$

4.3.3 Type 3 Source (Unknown faults)

For a type 3 source, an earthquake may occur anywhere in an area, and the fault-rupture may propagate in any direction with equal probability; i.e. uniformly distributed in $(0,2\pi)$.

The seismically active area, A, is again divided into smaller areas ΔA_i each of which considered as a single potential source with an occurrence rate equal to ν_i. Also in this case, if the seismic activity appears to be uniform over an area A, the occurrence rate ν_i for the ith source within the area can be obtained from Eq. 4.12; whereas if the seismicity in the region is not uniform, ν_i can be obtained directly from statistical data.

As shown in Fig. 4.4, for an earthquake of magnitude m originating in ΔA_i, the possible positions of a fault-rupture will form a circular area with diameter s. The rupture will strike the link j when the circle intersects the link. From the total probability theorem, the conditional probability $P(L_j|E_i)$ can be shown to be,

$$P(L_j|E_i) = \int_{m_o}^{m_u} P(L_j|E_{i,m}) \, f_M(m) dm \ ; \tag{4.16}$$

where $E_{i,m}$ = the occurrence of an earthquake in source i with magnitude m. Denoting θ as the agnle of intersection of the circle with diameter s and link j, it appears that

$$P(L_j|E_{i,m}) = \frac{\theta}{\pi} \quad . \tag{4.17}$$

Therefore, Eq. 4.16 becomes

$$P(L_j|E_i) = \int_{m_o}^{m_u} \frac{\theta}{\pi} f_M(m)dm \; ; \tag{4.18a}$$

The value of θ in Eq. 4.18 depends on the distance D and the length of the rupture s; the different cases and corresponding values of θ are summarized in Table 4.1.

Note that θ is a function of s and, therefore, a function of m. Substituting θ's from Table 4.1 in Eq. 4.18a we obtain

$$P(L_j|E_i) = \frac{1}{\pi} \left[2 \int_{m_1}^{m_2} \left(\cos^{-1} \frac{2|y|}{s}\right) f_M(m)dm + \int_{m_2}^{m_3} \left(\cos^{-1} \frac{2|y|}{s} + \tan^{-1} \frac{x}{|y|}\right) f_M(m) + \int_{m_3}^{m_u} \tan^{-1} \frac{\ell_j - x}{|y|} + \tan^{-1} \frac{x}{|y|}\right) f_M(m)dm \; ; \tag{4.18b}$$

where x and y are the coordinates of small area ΔA_i, $s = \exp(am-b)$, and ℓ_j is the length of link j.

The magnitudes m_1, m_2 and m_3 are found from the governing conditions, given in Table 4.1 as follows:

m_1 is the larger of m_1' and m_o, where m' is found from the condition D = s/2, or equivalently

$$m_1' \quad [\ln(2D) + b]/a \; ; \tag{4.19}$$

where D = the closest distance between link j and ΔA_i.

m_2 is found from the condition D' = s/2 or

$$m_2 = [\ln(2D') + b]/a \; ; \tag{4.20}$$

where D' = distance from ΔA_i to the nearest end of the link.

m_3 is found from the condition D" = s/2 or

$$m_3 = [\ln(2D'') + b]/a \; ; \tag{4.21}$$

where D" = distance from ΔA_i to the farthest end of the link.

Once m_1, m_2 and m_3 are found from Eqs. 4.19 to 4.21, $P(L_j|E_i)$ can be evaluated numerically from Eq. 4.18b.

The following modification may be necessary for certain exceptional cases:

For sources that are far from the link, m may be larger than m_u. In such cases $P(L_j|E_i) = 0$; whereas for sources that are very close to link j, D may be equal to zero and, therefore, $P(L_j|E_i) = 1$.

The choice of the dimensions of ΔA_i should depend on the distance from the link. On the basis of a number of example problems analyzed, it appears that for sources with distances up to 20 kilometers from the link, ΔA_i = 1.5 to 2 sq. kilometers is adequate and for farther sources ΔA_i may be increased gradually.

4.4 Hazard from Severe Ground Shaking

This mode concerns the maximum ground motion intensity exceeing the resistance capacity of one or more links in a lifeline system. If a common material and the same fabrication process are used in construction a lifeline system, it is reasonable to assume that the resistances along a link are perfectly correlated, even though the correlation between any two links may be weak. On this basis, the location of potential failure of a link may be assumed to be at the point of maximum ground motion along the link. If there are n potential earthquake sources in a region, then the probability that the maximum ground motion will exceed some specified intensity y_r at any point along a link,

$$P(Y>y_r) = \sum_{i=1}^{n} P(Y>y_r|E_i)\, P(E_i) \; ; \qquad (4.22)$$

where Y is the maximum intensity (from n potential sources) at a point along the link j; and E_i is the occurrence of an earthquake in source i. Using Eq. 4.3, Eq. 4.22 becomes (Der-Kiureghian and Ang, 1977)

$$P(Y>y_r) = \frac{1}{\nu} \sum_{i=1}^{n} P(Y>y_r\, E_i)\, \nu_i \; . \qquad (4.23)$$

Again, assuming a homogeneous Poisson process, with activity rate ν_i, for the occurrence of future earthquakes, Eq. 4.23 becomes

$$P(Y>y_r)_{\text{one year}} = 1-\exp\left[1- \sum_{i=1}^{n} P(Y>y_r|E_i)\nu_i\right] \; ; \qquad (4.24a)$$

and for small probabilities

$$P(Y>y_r)_{\text{one year}} \simeq \sum_{i=1}^{n} P(Y>y_r|E_i)\,\nu_i \ . \qquad (4.24b)$$

The main problem, therefore, involves the determination of the conditional probability $P(Y>y_r|E_i)$. From the total probability theorem, this can be evaluated as

$$P(Y>y_r|E_i) = \int_{m_o}^{m_u} P(Y>y_r|E_{i,m})\, f_M(m)dm \ ; \qquad (4.25)$$

where $E_{i,m}$ = the occurrence of an earthquake with magnitude m somewhere in source i.

Eq. 4.25 must be evaluated for all potential sources in the region. In this case, also, three types of source models are necessary in order to permit the modeling of all conceivable seismic sources. These have been developed by Der-Kiureghian and Ang (1977), and may be used to evaluate the hazard to the present mode of failure of a lifeline system.

Essentially, the three types of source models of Der-Kiureghian and Ang (1977) are similar to those described earlier for fault-rupture hazard; namely:

Type 1 source model--appropriate for modeling potential sources originating from well-defined faults;

Type 2 source model--appropriate for earthquake sources originating in areas where the fault locations are not known, but the dominant orientation of the fault system is known; and

Type 3 source model--appropriate for modeling regions or areas in which the fault system is not known.

4.5 Critical Section of a Link

As indicated earlier, under quite reasonable assumptions, the safety of a lifeline system to the hazard of high-intensity motions may be confined to the consideration of the critical section of each link, where the probability of exceedance is the highest along the link. The location of the critical section along a given link, however, may not be determined a priori. In general, the probability of exceedance for several points along a link may have to be calculated, considering the effects from all n potential earthquake sources in the region. The point corresponding to the highest probability, under the assumptions indicated earlier, determines the critical section along the link.

The number of points for which the probabilities of exceedance may have to be calculated along link j will depend on the length of the link and its location relative to the potential sources in the region. On the basis of a number of example problems analyzed, it appears that for most cases, the critical section is located at either ends of a link; however, this is not always the case, especially for links that are quite long (e.g. > 20 kilometers).

CHAPTER 5

SEISMIC SAFETY EVALUATION OF LIFELINE SYSTEMS

5.1 Probability of Failure of a Link

The methods introduced and presented in the previous chapter provides information about the probability of a fault-rupture strike on a link and the probability that the ground motion intensity will exceed the resistance capacity of a link in a lifeline system. This information is needed to evaluate the probability of failure of a given link as described below.

In the case of fault-rupture strike, the occurrence of such an event for a given link would be tantamount to the complete failure of the link. Therefore, the occurrence of a fault-rupture strike, as described in Chapter 4, is also the probability of failure of the link.

For the severe ground motion hazard, the resistance of a link relative to the maximum motion-induced force or strain must be considered in evaluating its probability of failure. More precisely, in this case, convolution of the probabilities associated with all possible values of resistance and maximum ground moiton will be necessary. The annual probabilities of exceeding given levels of ground moiton intensities may be obtained by using the method given in Chapter 4. Such probabilities for different intensities may be portrayed graphically as shown in Fig. 5.1, whereas the probability distribution of the resistance of a link may be described with the probability density function (PDF) of Fig. 5.2. The annual probability of a link failure (caused by high ground moiton), there-

fore, may be calculated from

$$P_{F_j} = \int_0^\infty [1 - F_Y(y_r)] \cdot f_R(y_r)dy_r; \qquad (5.1)$$

where P_{F_j} = the annual failure probability of a link, such as j; y_r is an intensity level of ground shaking corresponding to the resistance capacity of link j, and $1-F_Y(y_r)$ is the exceedance probability of ground motion intensity as given by the curve of Fig. 5.1.

An alternative but equivalent expression for the failure probability of link j is

$$P_{F_j} = \int_0^\infty F_R(y)\ f_Y(y)dy; \qquad (5.2)$$

where $F_R(r)$ = the probability distribution function of intensity resistance, and $f_Y(y)$ = the probability density function of ground motion intensity. However, for the present study, Eq. 5.1 is preferred over Eq. 5.2 as the ordinates of the curve in Fig. 5.1 gives directly $[1-F_Y(y_r)]$.

Numerically, Eq. 5.1 can be evaluated as

$$P_{F_j} = \sum_{\text{all } y_r\text{'s}} [1 - F_Y(y_r)] \cdot \Delta F_R(y_r); \qquad (5.3)$$

where $\Delta F_R(y_r) = F_R(y_r + \frac{\Delta y_r}{2}) - F_R(y_r - \frac{\Delta y_r}{2})$ is the probability that the resistance will be in a small interval Δy_r, as presented by the incremental area shown in Fig. 5.2.

The probability distribution for the resistance R may be predicted to be lognormal (Newmark, 1974). Therefore,

$$F_R(y_r) = \phi\left(\frac{\ell_n\, y_r/\bar{y}_r}{\zeta}\right) ; \qquad (5.4)$$

in which $\phi(x)$ is the standard normal probability, and ,

$$\zeta = \sqrt{\ln(1+\Omega^2)} ; \qquad (5.5)$$

where $\bar{y}_r$ is the mean intensity resistance; and Ω is the coefficient of variation representing the uncertainty in the resistance of link j.

The coefficient of variation, Ω, represents the degree of uncertainty underlying the prediction of the resistance of link j. This must include all the uncertainties underlying the predicted or estimated resistance for the link. Therefore, the determination of the various sources of uncertainty associated with the prediction of the resistance is, perhaps, the most important task in the evaluation of the safety of a lifeline system. Available data, of course, must be used in assessing Ω. However, since available data may not be sufficient to provide completely objective bases for assessing the underlying degree of uncertainty, this may be augmented with engineering judgments. The necessary judgments, however, may have to be expressed in probability terms in order to derive the appropriate coefficient of variation (Ang and Newmark, 1977).

5.2 System Failure Probability

The failure probabilities described above applies to individual links, where $F_R(y_r)$ is evaluated for suitable increment of y_r. The failure probability (in either mode of failure) of individual links comprise the information necessary to determine the respective probability of failure of a complete lifeline system.

In a simple lifeline system of links in series, the failure of any link in the system will cause the complete failure of the entire system. The problem becomes much more complicated in the case of a real lifeline system. In this case the failure of any possible path between the entry point and the final point must be considered, taking into account the effect of possible correlations between the different paths.

5.2.1 Topological Transformation of a Lifeline System

For the purpose of evaluatingits failure probability, a lifeline system may be modeled topologically as a network of parallel "paths" each of which is composed of several links in a series (Shinozuka et al, 1978). In this form, the network shows all possible paths to the final point from the entry point in the lifeline system (see Fig. 5.3).

Assume that a lifeline system, after transformation, is composed of N parallel paths; and the ith path is n_i links in series. If the failure of a link in a path, such as π_j, is assumed to be satistically independent from the failure of other links in the same path, the probability of failure of path π_i in the system will, then be

$$P_{F_i} = 1 - \prod_{j=1}^{n_i} (1-P_{F_j}) \; ; \qquad (5.6)$$

where n_i is the number of links (in series) in path Π_i; P_{F_j} = the probability of the jth link in path π_i in either mode of failure; and P_{F_i} is the probability of failure of path π_i (in any of the two modes of failure).

5.2.2 The Method of PNET

The failure probability of a complete lifeline system is much more complicated in the sense that some paths have links in common and, for this reason, are partially correlated, even though the failures of the links, as indicated earlier, may be uncorrelated. Such correlations between the path could be significant in the evaluation of the failure probability of the entire system. In order to include the effects of such correlations, the method of PNET (Ang, Abdelnour and Chaker, 1975) is appropriate. The probabilistic network evaluation technique (PNET) has been previously developed for the analysis of activity networks (Ref. 3). The technique is applicable also for the approximate analysis of safety of lifeline systems.

The correlation between paths can be calculated by assigning a standard deviation to each link. Such standard deviation is only for the purpose of determining the correlation coefficient, ρ_{ij}, between any two paths π_i and π_j. This correlation can be shown to be

$$\rho_{ij} = \frac{\sum_{k\varepsilon(\pi_i\ \pi_j)} \sigma_k^2}{\sigma_i \sigma_j} \qquad (5.7)$$

where σ_k = the standard deviation of those links that are common to paths π_i and π_j; and σ_i and σ_j are, respectively, standard deviations of paths π_i and π_j. If standard deviations for all links are equal (e.g. σ for each link), and assuming statistical independence, the standard deviation of a path, such as π_i, is

(5.8)

where n_i = the number of links in path π_i. If there are n_k links in common to paths π_i and π_j, Eq. 5.7 becomes

$$\rho_{ij} = \frac{n_k}{\sqrt{n_i \, n_j}} \tag{5.9}$$

The PNET method, applied to the system failure probability of a complete lifeline system, is based on the premise that those paths that are highly correlated (e.g. with $\rho_{ij} > \rho_o$) may be assumed to be perfectly correlated; whereas, those with low correlations (i.e. $\rho_{ij} \leq \rho_o$) may be assumed to be statistically independent (Ang, et al, 1975). On this basis, the paths can be divided into several groups in accordance with their mutual correlations as evaluated in Eq. 5.9, such that within each group the paths are mutually highly correlated. Therefore, the paths within each group can be "represented" by the single path having the highest probability of failure in the group, i.e. $\max(P_{F_i})$; whereas, the "representative" paths between the different groups may be assumed to be statistically independent. Then the failure probability of the complete system, P_F, is approximated as

$$P_F = \prod_r P_{F_r} \tag{5.10}$$

where, r stands for the representative paths.

The demarcating correlation ρ_o, which defines the transition between high and low correlations, has been previously taken as 0.5 in the analysis

of activity networks (Ang et al, 1975). For the purpose of the present study, the same value, i.e. $\rho_o = 0.5$, appears to be also appropriate and will be used.

In order to examine the adequacy of the method of PNET, evaluating the probability of failure of lifeline systems, a number of example problems were analyzed also with Monte Carlo simulations. All possible combinations of links, in a lifeline system, which cause the failure of the entire system were considered. Using the failure probabilities of individual links, the probability of failure of the entire system was obtained by the method of Monte Carlo. In both modes of failure, the adequacy of the PNET was confirmed.

CHAPTER 6

NUMERICAL ILLUSTRATIONS

6.1 Introductory Remarks

In order to demonstrate the applicability of the methods developed and introduced in the previous chapters, the seismic safety analyses of two different lifeline systems were performed. The first one is for the water distribution system in the city of Tokyo, Japan. The seismic hazard of this system to ground motion intensities has been examined previously by Shinozuka, et al (1978). The second analysis is for the highway network around Boston, Massachusetts. For this latter network, the seismic hazard to ground shaking has been analyzed as an example problem in Ref. 49. In order to compare the results of the present study with those of Refs. 47 and 49, where appropriate, the same parameters in Ref. 47 and 49 will be used with the present study.

6.2 Seismic Safety Analysis of Water Distribution System in Tokyo, Japan

The water for the city of Tokyo is supplied through a network of pipelines from three supply stations A, B and C as shown in Fig. 6.1. The system consists of twenty three links and fourteen nodes including the three supply stations A, B and C. For the prupose of the present analysis, the pipelines are idealized to consist of straight segments (dash lines) as shown in Fig. 6.1. In this idealized form, the network is composed of thirty two links and twenty two nodes. In this problem the reliability of the system to maintain the water flow from each of the three supply stations to point 9 against ground shaking is studied.

6.2.1 Seismic Parameters and Sources for Tokyo Bay Area

The epicenter map of the Tokyo bay area is shown in Fig. 6.2. Records of past earthquakes within 300 kilometers from Tokyo and with magnitudes of 4 and greater are given in Refs. 28 and 47. An area with a 300-kilometer radius from Tokyo is considered for the analysis. Also, based on the data available for this area, the entire region may be modeled as Type 3 sources.

The magnitude-recurrence curve is shown in Fig. 6.3; on this basis, an occurrence rate equal to 3.6×10^{-4} per year per square kilometer and a slope $\beta = 1.94$ are obtained. Furthermore, for the Tokyo bay region $m_o = 4.0$, and $m_u = 8.0$ appear to be reasonable. Also, in the absence of information that may be more appropriate for the Tokyo bay area, the values $a = 1.576$, and $b = 7.560$, which are values based on world-wide data, will be used in the rupture length-magnitude relation.

The entire area is divided into five annular areas with a common center at point 9; these annular areas are as follows.

Annular Area	Radius (km)
1	10.
2	40.
3	90.
4	160.
5	250.

In this example problem, an attenuation equation in the form of $y = b_1(R+b_4)^{-b_3} \exp(b_2 m)$ is used with $b_1 = 1.1$, $b_2 = 0.5$, $b_3 = 1.32$, and $b_4 = 25$. However, any other attenuation equation that may be appropriate for the Tokyo bay region may be used instead.

Finally, an average depth, h, equal to 25 kilometers is assumed for the entire area. The assumed average depth is only for the purpose of illustration of the methods given herein; and in areas such as Tokyo, where earthquakes of deep-focus are likely to occur, the average depth may have to be revised based on information regarding the history of the important earthquakes in the region.

6.2.2 Failure Probabilities of Links Due to Severe Ground Motions

It is assumed that the intensity resistance of each link follows a log-normal density function with a mean $\overline{y}_r$ and a coefficnet of variation Ω. In this example problem, different mean resistances ranging from 0.15g to 0.6g are considered. Furthremore, a coefficient of variation equal to 20% is assumed. The assumed coefficient of variation is, again, for the purpose of illustration and for a better estimation of the risk the coefficient of variation must be evaluated based on available data and engineering judgments in probability terms (Ang and Newmark, 1977).

Based on above assumptions, the risk, i.e. probability of failure due to the ground shaking, is calculated for all links indicated in Fig. 6.1.

6.2.3 System Failure Probability

The risk associated with the failure of individual links in the second mode of failure is the basic information necessary for the calculation of the system failure probability. As shown in Fig. 6.4, the system is modeled topologically as networks of parallel paths with links in series. The failure probability of paths 1 to 14 (numbered from top to bottom) are calculated; the results are given in Table 6.1. Applying the method of PNET, the effect of correlations between paths can be included in the calculation of the failure probability of the complete lifeline system.

The paths in each of the networks A-to-9 and B-to-9 are arranged in order of decreasing failure probabilities. The correlation coefficient between path 2 (with largest failure probability in the network A-to-9) and other paths, i.e. paths 1, 3 and 4, are $\rho_{2,1} = .29$, $\rho_{2,3} = .33$, and $\rho_{2,4} = 0$. Similarly for the remaining paths the correlation coefficient are $\rho_{1,3} = .29$ and $\rho_{1,4} = .57$. Only path 4 ($\rho_{1,4}$ larger than 0.5) can be represented by path 1; and, therefore, the representative paths in the network A-to-9 are paths 1, 2 and 3. The network failure probability for the case $\bar{y}_r = 0.15g$, then, can be approximated as

$$P_F \text{ (A-to-9)} = 3.33 \times 10^{-3}$$

Similarly, for the network B-to-9, the paths are arranged in order of decreasing probabilities; the correlation coefficients in this case are: $\rho_{5,6} = .67$, $\rho_{5,7} = .8$, $\rho_{5,10} = \rho_{5,8} = .63$, $\rho_{5,9} = .47$, $\rho_{5,13} = .43$, $\rho_{5,12} = .41$, and $\rho_{5,11} = .35$. It appears that paths 6, 7, 10, and 8 are represented by path 5. Similarly, $\rho_{9,13} = .33$, $\rho_{9,11} = .45$, $\rho_{9,12} = .0$, and $\rho_{13,11} = .61$, $\rho_{13,12} = .24$. Therefore, the failure probability of the network B-to-9 is represented by the failure probabilities of paths 5, 12, 13, and 9, i.e. for the case $\bar{y}_r = 0.15$ g,

$$P_F\text{(B-to-9)} = 1.21 \times 10^{-3}$$

The similar procedure is repeated for other mean resistances. The final results--the probabilities of failure given in Table 6.2 and portrayed graphically in Figs. 6.5 and 6.6.

6.3 Seismic Safety Analysis of the Network of Boston Highways

Major highways around Boston and vicinities are shown schematically in Fig. 6.7; the highways are idealized as straight lines (dash lines in Fig. 6.7). The network in this idealized form is composed of 22 links and 18 nodes. It is assumed in Ref. 49 that the safety of the network against earthquake hazards to maintain the traffic flow from point 1 to point 5 (Fig. 6.7) is the major concern.

6.3.1 Seismic Parameters and Sources in the Boston Area

The map of important earthquakes in the region is given in Ref. 49 and reproduced in Fig. 6.8. The entire area is divided into 8 different sources; the parameters related to each source are given in Table 6.3. Furthermore, all sources in the area are modeled as type 3 sources. Also, the seismic parameter $\beta = 1.65$ is proposed in Ref. 49 and will be used here for the entire region.

The same attenuation equation, used in Ref. 49, i.e. $a = 1.183[\exp(1.15m)]/D$, will be used here. Also, in the absence of information which may be more appropriate for the Boston area, the values $a = 1.576$ and $b = 7.560$ are used with Eq. 3.1.

6.3.2 Failure Probability of the Network of Boston Highways

The failure probability of the network due to the hazards of fault-rupture strikes and severe ground motions are considered in this problem. In Ref. 49 the failure probability of the network to ground shaking is calculated for a resistance capacity of 75 cm/sec^2 (e.g. 0.076g); the same value will be used here as the mean resistance for the links. Furthermore, Ω is assumed to be 30%.

The failure probabilities of individual links are then obtained and given in Table 6.4. The method of PNET is, again, applied to the problem in order to include the effect of correlations between different paths. A total of 14 different parallel paths can be observed in the network between nodes 5 and 1, as given in Table 6.5 along with the failure probabilities of the respective paths. In both modes of failure the method of PNET indicates that paths 1 and 7 are the representative ones. On this basis the probability of a fault-rupture strike on the network is

$$P_F(5\text{-to-}1) = 2.16 \times 10^{-7}$$

and the probability of failure of the network due to the severe ground shaking is

$$P_F(5\text{-to-}1) = 2.9901 \times 10^{-4}$$

The corresponding failure probability calculated in Ref. 49 was $P_F = 1.853 \times 10^{-4}$.

CHAPTER 7

SUMMARY AND CONCLUSIONS

7.1 Summary

7.1.1 Attenuation of Earthquake Ground Motions

The attenuation of the maximum ground moiton intensity with distance is examined, with emphasis on the motions in the near-source regions. The study is based on the analytical calculations of wave propagations in a semi-infinite elastic half-space subjected to a plane of rupture at a given depth. The effects of earthquake source parameters on the maximum ground motion intensity is studied; results of this parametric study are reported and correlated with available empirical data. Specific attenuation relations are then developed, with emphasis on such relations for the near-source regions. The proposed attenuation equations are compared with some of the empirical data for the far-field regions and are invariably given as functions of magnitude and distance.

The results of this study should be particularly useful for the near-source regions as there is little or no data to develop reliable empirical attenuation equations for such regions.

7.1.2 Seismic Reliability Analysis of Lifeline Systems

Methods for assessing the seismic safety of a lifeline system are developed and introduced based on the following assumptions:

1- Earthquakes originate as ruptures along geologic faults.

2- The rupture length is a funciton of earthquake magnitude.

3- The relative frequency of earthquake magnitudes in a region of interest follows the Richter's law of magnitudes.

4- The occurrence of future earthquakes constitute a Poisson process.

Two types of hazards from earthquakes are considered; namely, the hazard of fault-rupture strike on one or more links of a lifeline system and the hazard of damage caused by strong ground shaking during an earthquake. The calculated probability of a fault-rupture strike on a link is also the failure probability of the link; whereas for the case of hazard of severe ground shaking the convolution of the probabilities associated with all possible values of resistance and the maximum ground motion will be necessary in order to calculate the failure probability of a given link.

In order to find its failure probability, a lifeline system is transformed topologically into a network of parallel "paths" each of which composed of several links in series. The failure probabilities of individual links, in either mode of failure, are used for the purpose of defining the failure probability of the entire system. Through the application of the method of PNET, the effects of correlations between different paths, because of having links in common, are considered in evaluating the failure probability of the system.

Specific application of the methods presented herein are demonstrated for the seismic risk analyses of the water distribution system of the city of Tokyo, Japan, and for the network of Boston metropolitan highways.

7.2 Principal Results and Conclusions

With regard to the study of the ground motion intensity in near-source regions and the attenuation equations, the following conclusions can be made:

1- The intensity depends on various geological and seismological parameters of the source mechanism such as the depth of the focus, the width

of the fault, the fault displacement, and the orientation of the fault with respect to the free surface. In the case of the vertical motion, the intensity also depends on the type of material in the half-space; whereas for the horizontal motions, this dependence appears to be weak and can be neglected for engineering purposes.

The effect of earthquake magnitude can be included in the proposed equations by considering the relations between the source parameters and earthquakes magnitudes in the Richter scale. These relations are based on empirical data and relate the magnitude of an earthquake to the area (or width) of the rupture plane. For points which are located in the vicinity of an earthquake source, the intensity tends to be rather independent of earthquake magnitude.

2- Wide variation in the attenuation of ground motion with distance and magnitude can be expected, because the attenuation of motions depends also on the parameters of the source mechanism as mentioned earlier.

On the basis of the seismic risk analysis of lifeline systems, the following observations may be made:

1- The method, presented herein, for evaluating seismic safety of lifeline systems in two modes, is useful and necessary for a risk-based approach to the design of lifelines against earthquake hazards.

2 - In evaluating the seismic reliability of the entire lifeline system, the correlations between different paths is important and must be considered. The method of PNET has been used for this purpose in the present study.

REFERENCES

1. Ang, A. H-S., "Probability Concepts in Earthquake Engineering," in Applied Mechanics in Earthquake Engineering, Ed. W.D. Iwan, ASME, AMD-Volume 8, 1974, pp. 225-259.

2. Ang, A. H-S., "Structural Risk Analysis and Reliability-Based Design," Journal of Structural Division, ASCE, Volume 99, ST9, September 1973, pp. 1891-1910.

3. Ang, A. H-S., Abdelnour, J., and Chaker, A.A., "Analysis of Activity Networks under Uncertainty," Journal of Engineering Mechanics Division, ASCE, Vol. 101, EM4, August 1975, pp. 373-387.

4. Ang, A. H-S., and Newmark, N.M., "A Probabilistic Seismic Safety Assessment of the Diablo Canyon Nuclear Power Plant," N.M. Newmark Consulting Engineers Services, Urbana, Illinois, Report to the U.S. Nuclear Regulatory Commission, November 1977.

5. Ang, A. H-S., and Tang, W.H., Probability Concepts in Engineering Planning and Design, Vol. 1-Basic Principles, John Wiley and Sons, New York, 1975.

6. Archuleta, R.J., and Frazier, G.A., "Three-Dimensional Numerical Simulations of Dynamic Faulting in a Half-Space," Bulletin of the Seismological Society of America, Vol. 68, No. 3, pp. 541-572, June 1978.

7. Blume, J.A., "Earthquake Ground Motion and Engineering Procedures of Important Installations near Active Faults," Third World Conference on Earthquake Engineering, New Zealand, Vol. IV., pp. 53-67, 1965.

8. Brune, J.N., and Allen, R.C., "A Low-Stress-Drop, Low-Magnitude Earthquake with Surface Faulting, the Imperial, California Earthquake of March 4, 1966," Bulletin of the Seismological Society of America, Vol. 57, No. 3, pp. 501-514, June 1967.

9. Campbell, K.W., Eguchi, R.T., and Duke, C.M., "Reliability in Lifeline Earthquake Engineering," Preprint 3427, paper presented at the ASCE Convention and Exposition, Chicago, October 1978.

10. Chinnery, M.A., "Earthquake Magnitude and Source Parameters," Bulletin of the Seismological Society of America, Vol. 59, No. 5, pp. 1969-1982, October 1969.

11. Cornell, C.A., "Engineering Seismic Risk Analysis," Bulletin of the Seismological Society of America, Vol. 58, No. 5, pp. 1583-1606, October 1968.

12. Der-Kiureghian, A., and Ang, A. H-S., "A Line-Source Model for Seismic Risk Analysis," University of Illinois at Urbana-Champaign, Civil Engineering Studies, SRS No. 419, October 1975.

13. Der-Kiureghian, A., and Ang, A. H-S., "A Fault-Rupture Model for Seismic Risk Analysis," Bulletin of the Seismological Society of America, Vol. 67, No. 4, pp. 1173-1194, August 1977.

14. Donovan, N.C., "A Statistical Evaluation of Strong Motion Data," Proceedings 5th World Conference on Earthquake Engineering, Rome, 1974.

15. Donovan, N.C., "Earthquake Hazards for Buildings," pp. 82-111 in Building Practices for Disaster Mitigation, U.S. Department of Commerce, Report NBS BSS No. 46, 1973.

16. Duke, C.M., and Moran, D.F., "Guidelines for Evaluation of Lifeline Earthquake Engineering," Proceedings of U.S. National Conference on Earthquake Engineering, Ann Arbor, Michigan, 1975.

17. Esteva, L., "Seismic Risk and Seismic Design Decisions," pp. 142-182 in Seismic Design for Nuclear Power Plants, R.J. Hansen, Editor, MIT Press, Cambridge, Massachusetts, 1970.

18. Esteva, L., "Seismicity Prediction: A Bayesian Approach," Proceedings 4th World Conference on Earthquake Engineering, Santiago, Chile, 1969.

19. Esteva, L., and Rosenblueth, E., "Spectra of Earthquakes at Moderate and Large Distances," Soc. Mex. de Ing. Sismica, Mexico 11, 1-18, 1964.

20. Evernden, J.F., "Seismic Intensity, "Size" of Earthquake and Related Parameters," Bulletin of the Seismological Society of America, Vol. 65, No. 5, pp. 1287-1313, October 1975.

21. Evernden, J.F., Hibbard, R.R., and Schneider, J.F., "Interpretation of Seismic Intensity Data," Bulletin of the Seismological Society of America, Vol. 63, No. 2, pp. 399-422, April 1973.

22. Gutenberg, B., and Richter, C., Seismicity of the Earth, 2nd Edition, Princeton University Press, Princeton, New Jersey, 1954.

23. Hanks, T.C., "Observations and Estimation of Long-Period Strong Ground Motion in the Los Angeles Basin," International Journal of Earthquake Engineering and Structural Dynamics, 4, pp. 473-488, 1976.

24. Hanks, T.C., Hileman, J.A., and Thatcher, W., "Seismic Moments of the Larger Earthquakes of the Southern California Region," Geological Society of America, Bulletin 86, pp. 1131-1139, 1975.

25. Housner, G.W., "Measures of Severity of Earthquake Ground Shaking," Proceedings of U.S. National Conference on Earthquake Engineering, Ann Arbor, Michigan, 1975.

26. Iida, K., "Earthquake Energy and Earthquake Fault," Nagoya University, Journal of Earth Science, Vol. 7, No. 2, pp. 98-107, 1959.

27. Johnson, J.J., and Robinson, A.R., "Wave Propagation in a Half Space due to an Interior Point Load Parallel to the Surface," University of Illinois at Urbana-Champaign, Civil Engineering Studies, SRS, No. 388, July 1972.

28. Japan Road Association, "Research on Earthquake Protection of Petroleum Pipelines," Tokyo, Japan.

29. Kagan, Y., and Knopoff, L., "Earthquake Risk Prediction as a Stochastic Process," Physics of the Earth and Planetory Interiors, 14 (1977), pp. 97-108.

30. Kanai, K., "An Empirical Formula for the Spectrum of Strong Earthquake Motions," Bulletin, Earthquake Research Institute, 39, pp. 85-95, 1961.

31. Kanai, K., "Improved Empirical Formula for the Characteristics of Strong Earthquake Motions," Proceedings Japan Earthquake Engineering Symposium, Tokyo, Japan, pp. 1-4, October 1966.

32. King, Y., and Knopoff, L., "Stress Drop in Earthquakes," Bulletin of Seismological Society of America, Vol. 58, No. 1, pp. 249-257, February 1968.

33. Lin, Y.K., Probabilistic Theory of Structural Dynamics, R.E. Krieger Publishing Co., Huntington, New York, 1976.

34. McGuire, R.K., "Seismic Structural Response Risk Analysis, Incorporating Peak Response Regressions on Earthquake Magnitude and Distance," MIT Department of Civil Engineering, Research Report R74-51, 1974.

35. Milne, W.G., "Measures of Severity of the Earthquake Ground Shaking," Proceedings of U.S. National Conference on Earthquake Engineering, Ann Arbor, Michigan, 1975.

36. Newmark, N.M., "Comments on Conservatism in Earthquake Resistant Design," Report to U.S. Nuclear Regulatory Commission, September 1974.

37. Newmark, N.M., Hall, W.J., and Mohraz, B., "A Study of Vertical and Horizontal Earthquake Spectra," Directorate of Licensing U.S. Atomic Energy Commission, Report WASH-1255, April 1973.

38. Newmark, N.M., and Hall, W.J., "Pipeline Design to Resist Large Fault Displacement," Proceedings U.S. National Conference on Earthquake Engineering, Ann Arbor, Michigan, 1975.

39. Newmark, N.M., and Rosenblueth, E., Fundamentals of Earthquake Engineering, Prentice-Hall, Inc., Englewood Cliffs, New Jersey, 1971.

40. Richter, C.F., Elementry Seismology, W.H. Freeman and Co., San Francisco, California, 1958.

41. Rosenblueth, E., "Analysis of Risk," Proceedings 5th World Conference on Earthquake Engineering, Rome, Italy, 1973.

42. Schnabel, P.B., and Seed, H.B., "Acceleration in Rock for Earthquakes in the Western United States," Bulletin of the Seismological Society of America, Vol. 63, No. 2, 1973.

43. Seed, H.B., Idriss, I.M., and Kiefer, F.W., "Characteristics of Rock Motion During Earthquakes," Journal of Soil Mechanics and Foundations Division, ASCE, Vol. 95, pp. 1199-1218.

44. Seyyedian-Choobi, M., and Robinson, A.R., "Motion on the Surface of a Layered Elastic Half Space Produced by a Buried Dislocation Pulse," University of Illinois at Urbana-Champaign, Civil Engineering Studies, SRS, No. 421, November 1975.

45. Shinozuka, M., Takeda, S., and Ishikawa, H., "Some Aspects of Seismic Risk Analysis of Underground Lifeline Systems," Columbia University, Department of Civil Engineering and Engineering Mechanics, Technical Report, No. NSF-PFR-78-15049-CU-1, August 1978.

46. Shinozuka, M., Takeda, S., and Ishikawa, H., "Seismic Risk Analysis of Underground Lifeline Systems with the Aid of Damage Probability Matrix," Columbia University, Department of Civil Engineering and Engineering Mechanics, Technical Report, No. NSF-PFR-78-15049-CU-2, September 1978.

47. Shinozuka, M., Takeda, S., and Kawakami, H., "Risk Analysis of Underground Lifeline Network Systems," Proceedings of U.S.-Southeast Asia Symposium on Earthquake Engineering for Natural Hazards Protection, Ed. by A. H-S. Ang, 1978.

48. Slemmons, D.B., "State-of-the-Art for Assessing Earthquake Hazards in the United States," Report 6, Faults and Earthquake Magnitude, Mackay School of Mines, University of Nevada, Reno Nevada, May 1977.

49. Taleb-Agha, G., "Seismic Risk Analysis of Lifeline Networks," Bulletin of the Seismological Society of America, Vol. 67, No. 6, pp. 1625-1645, December 1977.

50. Trifunac, M.D., and Brady, A.G., "On the Correlation of Peak Accelerations of Strong Motion with Earthquake Magnitude, Epicentral Distance and Site Conditions, Proceedings of U.S. National Conference on Earthquake Engineering, Ann Arbor, Michigan, 1975.

51. Weidlinger, P., and Nelson, I., "Seismic Analysis of Pipeline with Interference Response Spectra," Weidlinger Associates, Consulting Engineers, Grant Report, No. 7, June 1978.

52. Whitman, R.V., Cornell, C.A., and Taleb-Agha, G., "Analysis of Earthquake Risk for Lifeline Systems," Proceedings of the U.S. National Conference on Earthquake Engineering, Ann Arbor, Michigan, 1975.

TABLE 2.1 SUMMARY OF VERTICAL TO HORIZONTAL ACCELERATION RATIOS (REF. 37)

Site	No. of records	Average $\frac{\text{a - vertical}}{\text{a - horizontal}}$
alluvium & rock	28	0.53
alluvium	22	0.53
rock	6	0.54
alluvium & rock $a_h > 0.1g$, $a_v > 0.05g$	15	0.65
alluvium, $a_h > 0.1g$, $a_v > 0.05g$	9	0.72
alluvium & rock, $a_h < 0.1g$, $a_v < 0.05g$	13*	0.40

* Actually alluvium values only since all rock components had peak ground accelerations > 0.1g (horizontal) and 0.05g (vertical) (Ref. 37).

TABLE 2.2 SUMMARY OF VERTICAL TO HORIZONTAL v/a RATIOS (REF. 37)

Site	No. of records	Average $\frac{\text{v/a - vertical}}{\text{v/a - horizontal}}$
alluvium & rock	28	0.92
alluvium	22	0.92
rock	6	0.91
alluvium & rock, $a_h > 0.1g$, $a_v > 0.05g$	15	0.85
alluvium alone, $a_h > 0.1g$, $a_v > 0.05g$'	9	0.81
alluvium & rock, $a_h < 0.1g$, $a_v < 0.05g$	13*	0.99

* Actually alluvium values only since all rock components had peak ground accelerations > 0.1g (horizontal) and 0.05g (vertical) (Ref. 37).

TABLE 2.3 SUMMARY OF AVERAGE ad/v^2 VALUES (REF. 37)

Site	Direction	No. of Records	ad/v^2
alluvium & rock	horizontal	28	5.6
alluvium	horizontal	22	5.7
rock	horizontal	6	5.4
alluvium & rock, a > 0.1g	horizontal	20	5.7
alluvium, a > 0.1g	horizontal	14	5.9
rock, a > 0.1g (same as above)	horizontal	6	5.4
alluvium, a < 0.1g	horizontal	8	5.3
alluvium & rock*	vertical	14	10.7
alluvium & rock	vertical	13	9.1
alluvium*	vertical	11	10.0
alluvium	vertical	10	7.9
rock	vertical	3	13.0
alluvium & rock, a > 0.05g	vertical	8	12.4
alluvium, a > 0.05g	vertical	5	12.0
alluvium, a > 0.05g*	vertical	4	7.3
rock, a > 0.05g (same as above)	vertical	3	13.0
alluvium, a < 0.05g	vertical	6	8.4

* Not including the one extreme value, El Centro, 5-18-40, 2037 PST, vertical component $ad/v^2 = 30.58$ (Ref. 37)

TABLE 2.4 SUMMARY OF AVERAGE v/a (REF. 37)

Site	Direction	No. of Records	v/a (in/sec/g)
alluvium & rock	horizontal	28	45
alluvium & rock*	horizontal	28	48
alluvium	horizontal	22	52
rock	horizontal	6	22
rock*	horizontal	4	28
alluvium & rock, a > 0.1g	horizontal	20	39
alluvium & rock, a > 0.1g*	horizontal	18	42
alluvium, a > 0.1g	horizontal	14	47
alluvium, a < 0.1g	horizontal	8	60
alluvium & rock	vertical	14	37
alluvium & rock*	vertical	13	40
alluvium	vertical	11	43
rock	vertical	3	18
rock*	vertical	2	24
alluvium & rock, a > 0.05g	vertical	8	30
alluvium & rock a > 0.05g *	vertical	7	33
alluvium, a > 0.05g	vertical	5	37
alluvium, a < 0.05g	vertical	5	47

* Not including the extreme ratios, San Francisco Golden Gate Park, 3-22-57, 1144 PST. (Ref. 37)

TABLE 2.5 GROUND MOTION ATTENUATION EQUATIONS

No.	Ref.	Author	Equation
1	15	Donovan	$a = 1.35e^{0.58m} (R + 25)^{-1.52}$
2	14	Donovan	$a = 1.10e^{0.50m} (R + 25)^{-1.32}$
3	17	Esteva	$a = 1.26e^{0.8m} (R + 25)^{-2.0}$
4	34	McGuire	$a = 0.48e^{0.64m} (R + 25)^{-1.301}$
5	50	Trifunac & Brady	$\log a_{max} = m + \log A_0(R) + a,P + bm + c + ds + ev + fm^2$

a, a_{max} = maximum ground acceleration, g

m = magnitude

R = distance, km.

$A_0(R)$ = a function of distance

a_1, b, c, d, e, f = constants

P = confidence level

s = a factor related to the type of material

v = a factor indicating vertical or horizontal motion

TABLE 4.1 VALUES OF θ FOR TYPE 3 SOURCE

Case	Governing Inequality	θ
1	$D > s/2$	0.
2	$D'' > D' > s/2$	$2\cos^{-1}\frac{2\lvert y\rvert}{s}$
3	$D'' > s/2 > D'$	$\cos^{-1}\frac{2\lvert y\rvert}{s} + \tan^{-1}\frac{x}{\lvert y\rvert}$
4	$s/2 > D'' > D'$	$\tan^{-1}\frac{\ell_j - x}{\lvert y\rvert} + \tan^{-1}\frac{xx}{\lvert y\rvert}$

In table 5.1, x and y are coordinates of ΔA; and ℓ_j is the length of link j; and,

D' = distance from ΔA; to the nearest end of the link;

D'' = distance from ΔA; to the farthest end of the link.

TABLE 6.1 ANNUAL PROBABILITY OF FAILURE IN A PATH (TOKYO)

	Mean Link Resist. in g's						
Path	.150	.225	.300	.375	.450	.525	.600
1	.160	3.79×10^{-2}	1.17×10^{-2}	3.93×10^{-3}	1.4×10^{-3}	5.15×10^{-4}	1.95×10^{-4}
2	.160	3.79×10^{-2}	1.17×10^{-2}	3.93×10^{-3}	1.4×10^{-3}	5.15×10^{-4}	1.95×10^{-4}
3	.130	3.04×10^{-2}	9.32×10^{-3}	3.14×10^{-3}	1.12×10^{-3}	4.12×10^{-4}	1.56×10^{-4}
4	.130	3.04×10^{-2}	9.32×10^{-3}	3.14×10^{-3}	1.12×10^{-3}	4.12×10^{-4}	1.56×10
5	.295	7.43×10^{-2}	2.33×10^{-2}	7.86×10^{-3}	2.81×10^{-3}	1.03×10^{-3}	3.89×10^{-4}
6	.245	5.99×10^{-2}	1.86×10^{-2}	6.29×10^{-3}	2.25×10^{-3}	8.24×10^{-4}	3.11×10^{-4}
7	.245	5.99×10^{-2}	1.86×10^{-2}	6.29×10^{-3}	2.25×10^{-3}	8.24×10^{-4}	3.11×10^{-4}
8	.160	3.79×10^{-2}	1.17×10^{-2}	3.93×10^{-3}	1.4×10^{-3}	5.15×10^{-4}	1.95×10^{-4}
9	.220	5.26×10^{-2}	1.63×10^{-2}	5.5×10^{-3}	1.97×10^{-3}	7.21×10^{-4}	2.72×10^{-4}
10	.220	5.26×10^{-2}	1.63×10^{-2}	5.5×10^{-3}	1.97×10^{-3}	7.21×10^{-4}	$2.7x \times 10^{-4}$
11	.160	3.79×10^{-2}	1.17×10^{-2}	3.93×10^{-3}	1.40×10^{-3}	5.15×10^{-4}	1.95×10^{-4}
12	.099	2.29×10^{-2}	6.99×10^{-3}	2.36×10^{-3}	8.43×10^{-4}	3.09×10^{-4}	1.17×10^{-4}
13	.189	4.53×10^{-2}	1.40×10^{-2}	4.72×10^{-3}	1.69×10^{-3}	6.18×10^{-4}	2.33×10^{-4}
14	.130	3.04×10^{-2}	9.32×10^{-3}	3.14×10^{-3}	1.12×10^{-3}	4.12×10^{-4}	1.56×10^{-4}

TABLE 6.2 ANNUAL PROBABILITY OF FAILURE OF SUPPLY NETWORK (TOKYO)

	Mean Link Resist. in g's						
	.150	.225	.300	.375	.450	.525	.600
A→9	3.33×10^{-3}	4.37×10^{-5}	1.28×10^{-6}	4.85×10^{-8}	-	-	-
B→9	1.21×10^{-3}	4.05×10^{-6}	3.72×10^{-8}	-	-	-	-
C→9	.130	3.04×10^{-2}	9.32×10^{-3}	3.14×10^{-3}	1.12×10^{-3}	4.12×10^{-4}	1.56×10^{-4}

TABLE 6.3 IDEALIZATION OF SOURCES FOR BOSTON AREA

Number	Type	Occurrence Rate	M_u	M_o
1	3	0.024	6.1	4.3
2	3	0.008	6.8	4.3
3	3	0.004	5.5	4.3
4	3	0.028	5.9	4.3
5	3	0.020	5.2	3.7
6	3	0.0125	5.5	4.3
7	3	0.032	5.5	4.3
8	3	0.0375	5.9	4.3

TABLE 6.4 ANNUAL FAILURE PROBABILITY OF LINK

Link	Fault-Rupture Strike	Ground Shaking, $\bar{y}_r$ = 0.076g
1	0.000012	0.000678
2	0.000015	0.001226
3	0.000024	0.000660
4	0.000013	0.001226
5	0.000086	0.001572
6	0.000083	0.004469
7	0.000094	0.004469
8	0.000055	0.000465
9	0.000123	0.001252
10	0.000185	0.001957
11	0.000096	0.001957
12	0.000084	0.001961
13	0.000117	0.000315
14	0.000029	0.000531
15	0.000077	0.000994
16	0.000069	0.000995
17	0.000043	0.002226
18	0.000043	0.000678
19	0.000118	0.000680
20	0.000017	0.004469
21	0.000029	0.000405
22	0.000087	0.000405

TABLE 6.5 EQUIVALENT PARALLEL PATHS FOR BOSTON HIGHWAYS

Path	No. of Links	Links	Annual Fail. Prob.	
			Rupture Strike	Ground Shaking
1	12	15-21-13-11-10-9-8-7-20-18-2-5	0.00103	0.02094
2	12	15-21-13-10-9-16-17-19-18-20-6	0.00091	0.02024
3	10	15-22-14-9-8-7-20-18-2-5	0.00068	0.01598
4	9	15-21-13-11-10-9-5-7-6	0.00065	0.01581
5	10	15-22-14-9-16-17-19-18-20-6	0.00065	0.01538
6	9	3-4-2-19-17-16-8-7-6	0.00045	0.01519
7	6	3-4-2-18-20-6	0.00021	0.01428
8	7	1-19-17-16-8-7-6	0.00021	0.01275
9	11	15-21-13-11-10-9-16-17-19-2-5	0.00086	0.01187
10	4	1-18-20-6	0.00016	0.01185
11	7	15-22-14-9-8-7-6	0.00055	0.01095
12	9	15-22-14-9-16-17-19-2-5	0.00065	0.00701
13	3	1-2-5	0.00011	0.00490
14	3	3-4-5	0.00012	0.00350

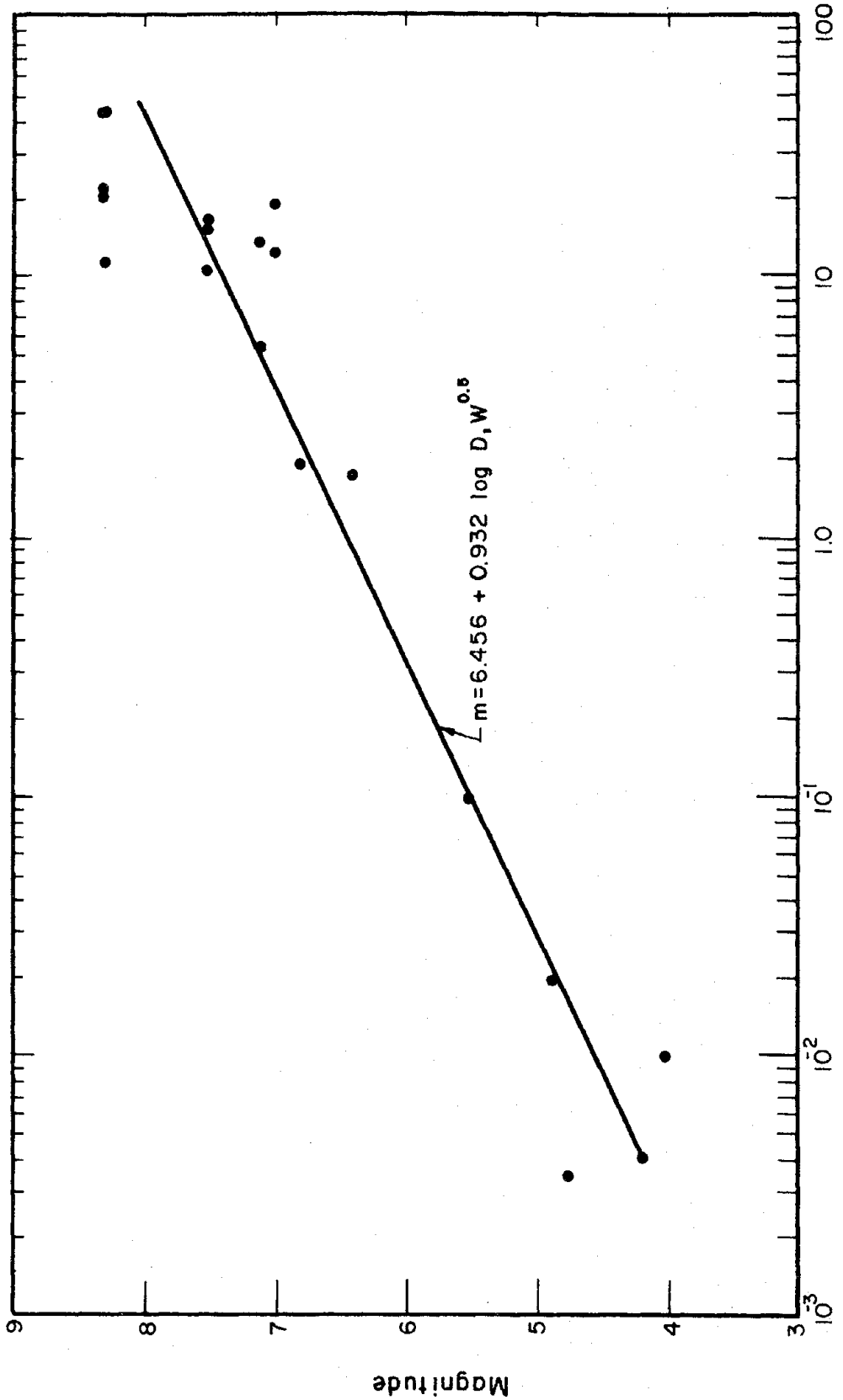

FIG. 2.1 MAGNITUDE VERSUS $D_1\sqrt{W}$ FOR $M \geq 4$ (DATA FROM REF. 10)

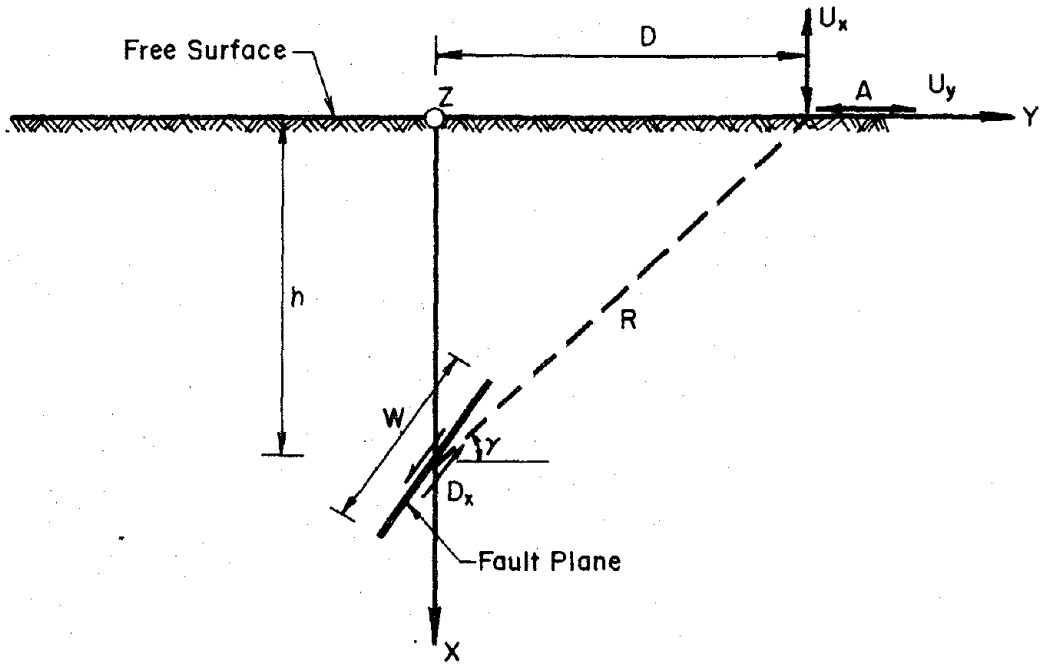

FIG. 2.2 TWO-DIMENSIONAL FAULT MODEL (DIP-SLIP)

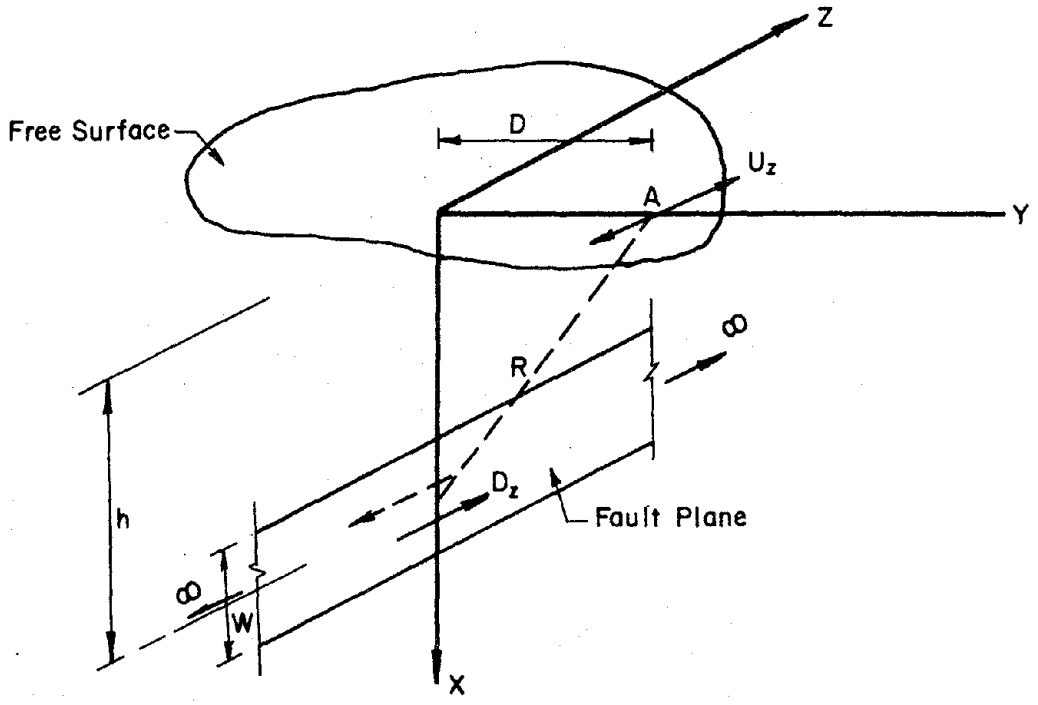

FIG. 2.3 TWO-DIMENSIONAL FAULT-MODEL (STRIKE-SLIP)

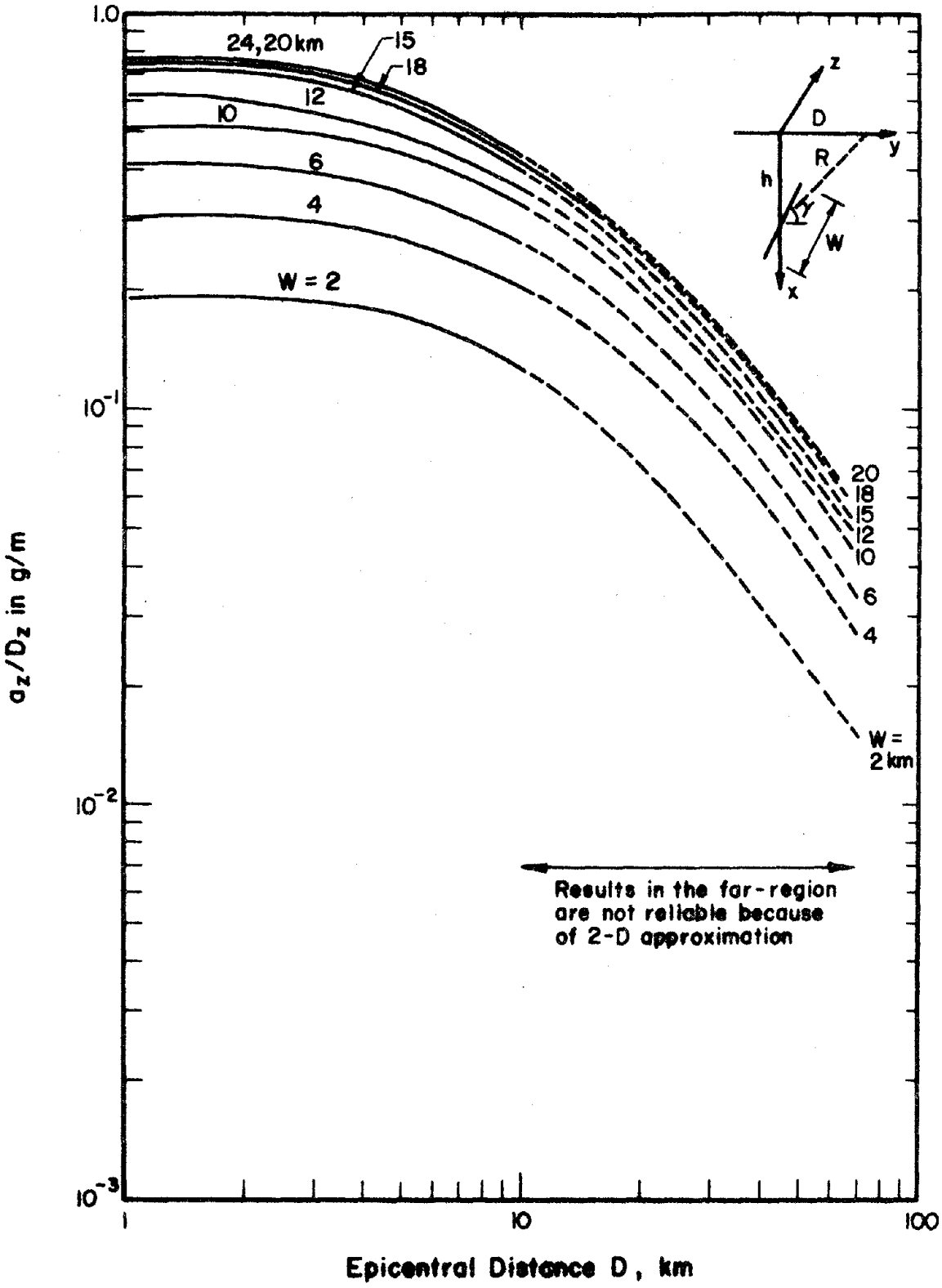

FIG. 2.4 VARIATION OF a_z/D_z WITH D FOR DIFFERENT W (h = 15 km, $\gamma = 90^0$)

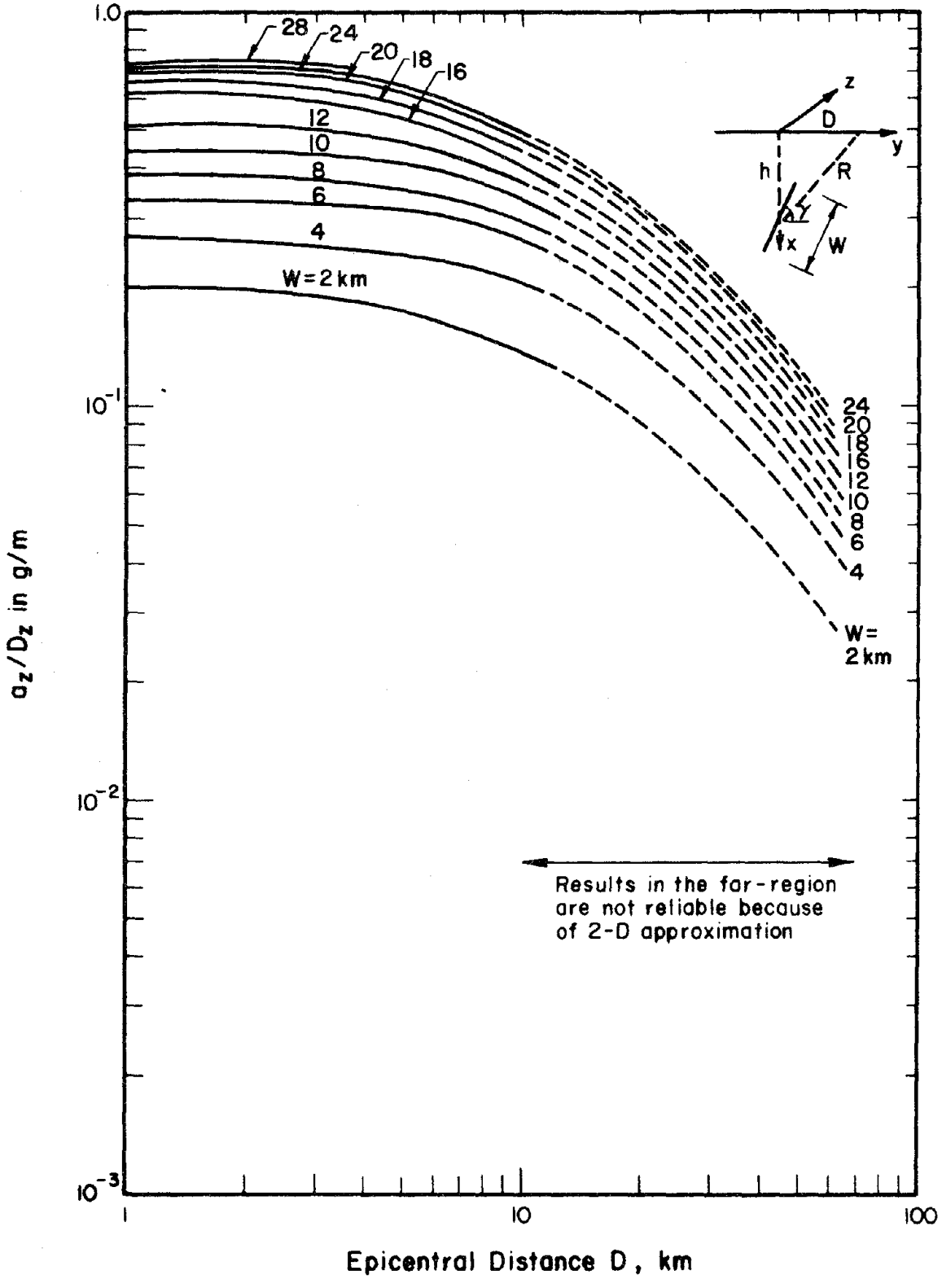

FIG. 2.5 VARIATION OF a_z/D_z WITH D FOR DIFFERENT W (h = 20 km, $\gamma = 90^0$)

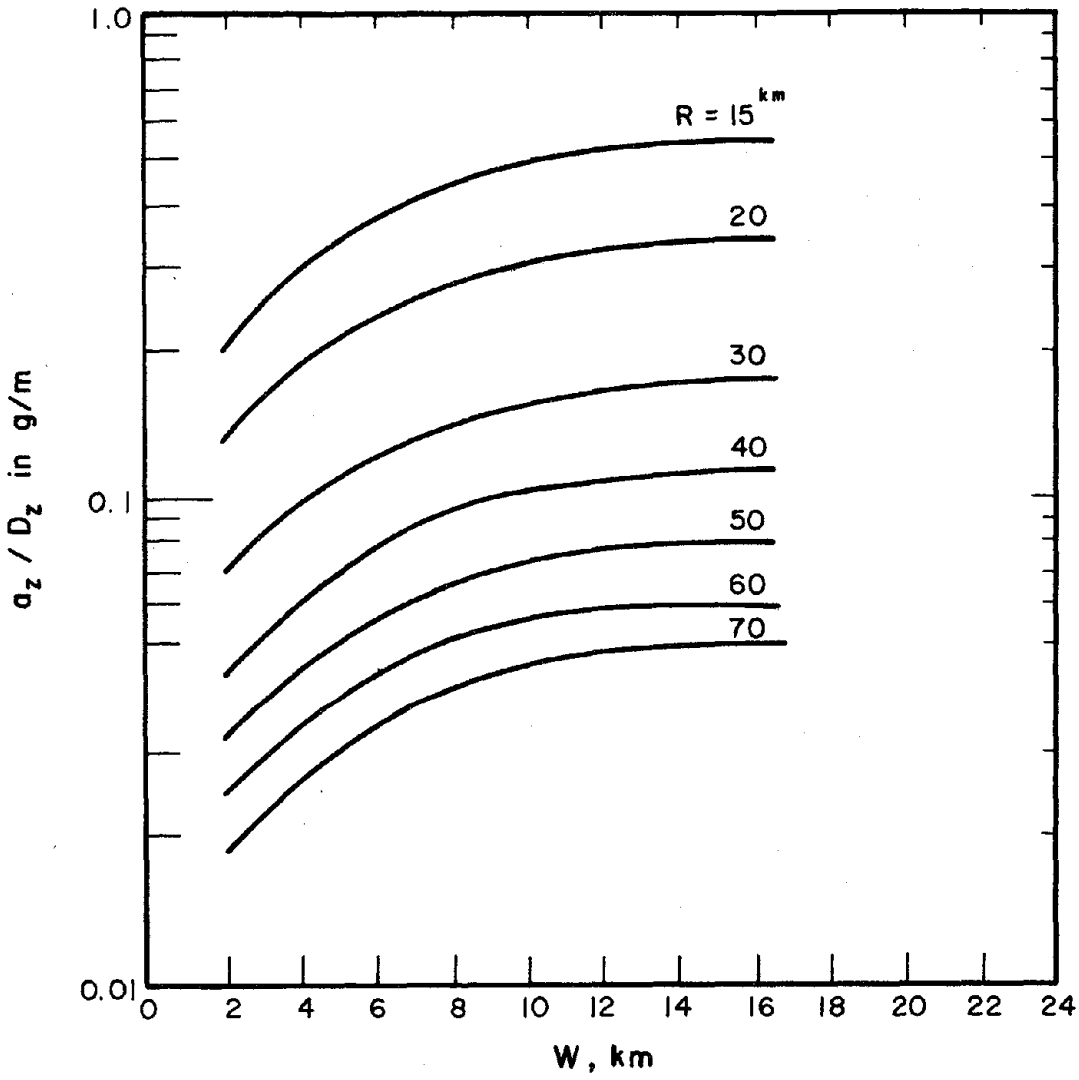

FIG. 2.6 VARIATION OF a_z/D_z WITH W FOR h = 15 AND $\gamma = 90^0$

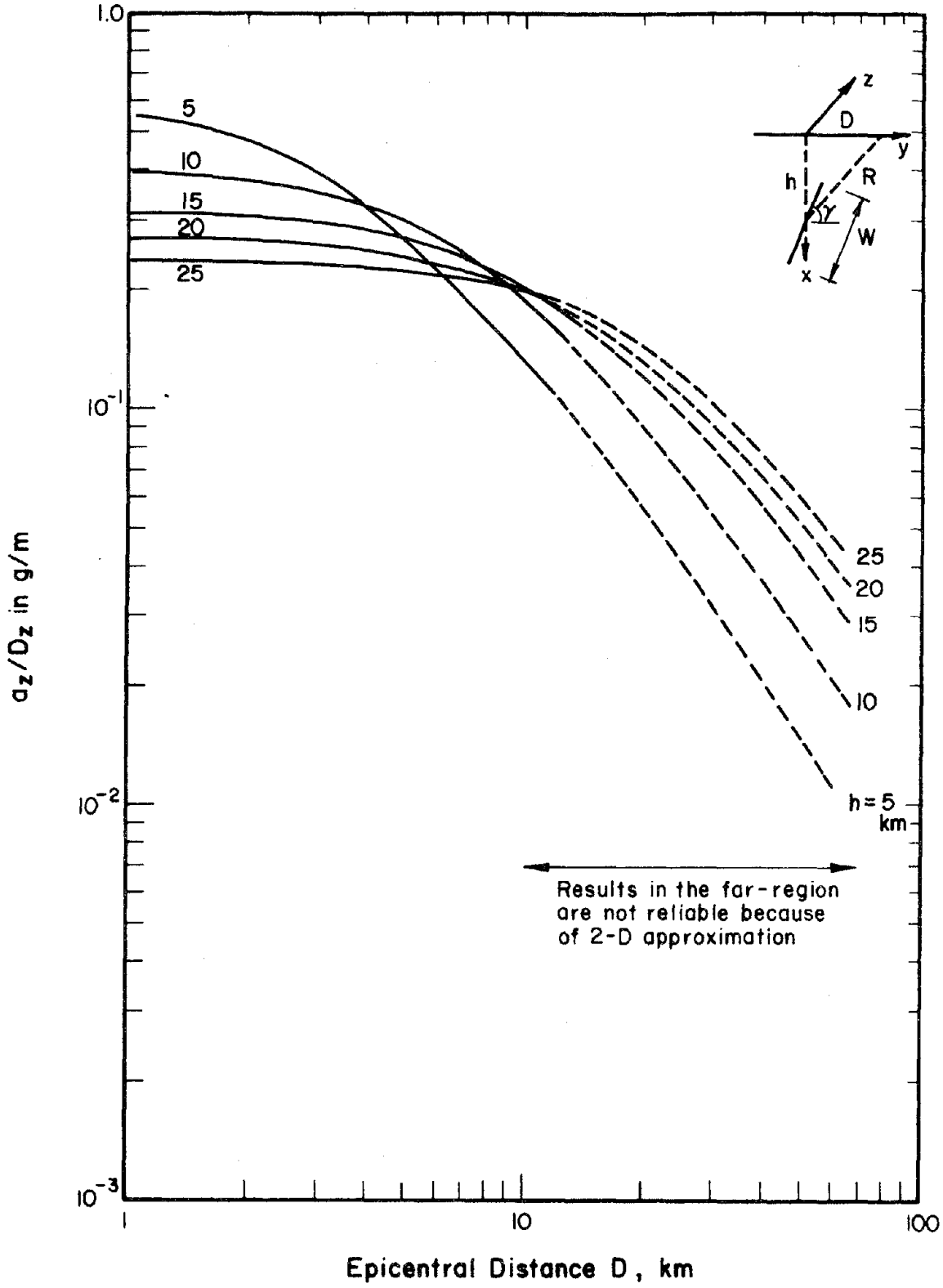

FIG. 2.7a VARIATION OF a_z/D_z WITH D FOR DIFFERENT h
($\gamma = 90^0$, W = 4 km)

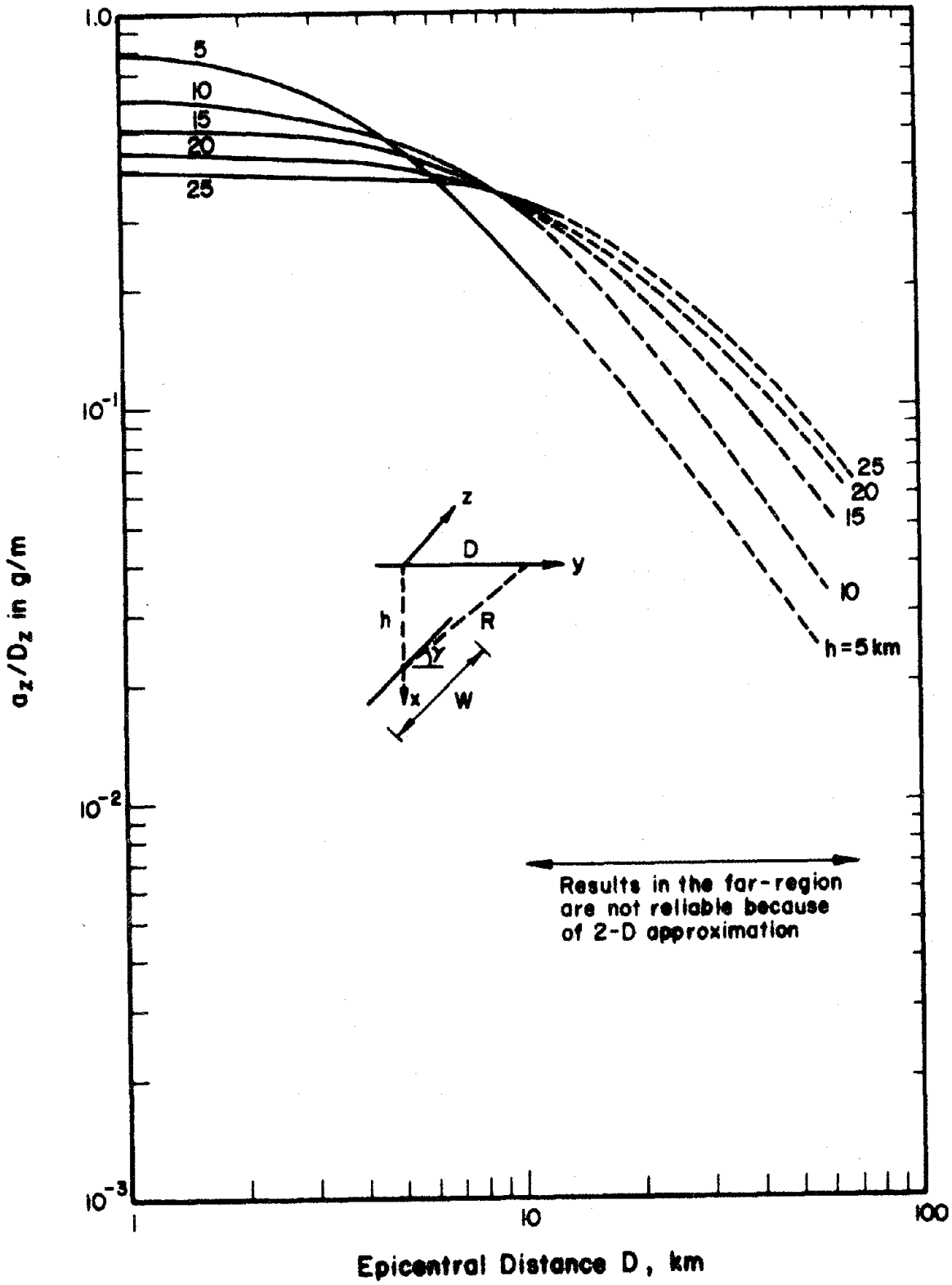

FIG. 2.7b VARIATION OF a_z/D_z WITH D FOR DIFFERENT h
($\gamma = 90^{o}$, W = 10 km)

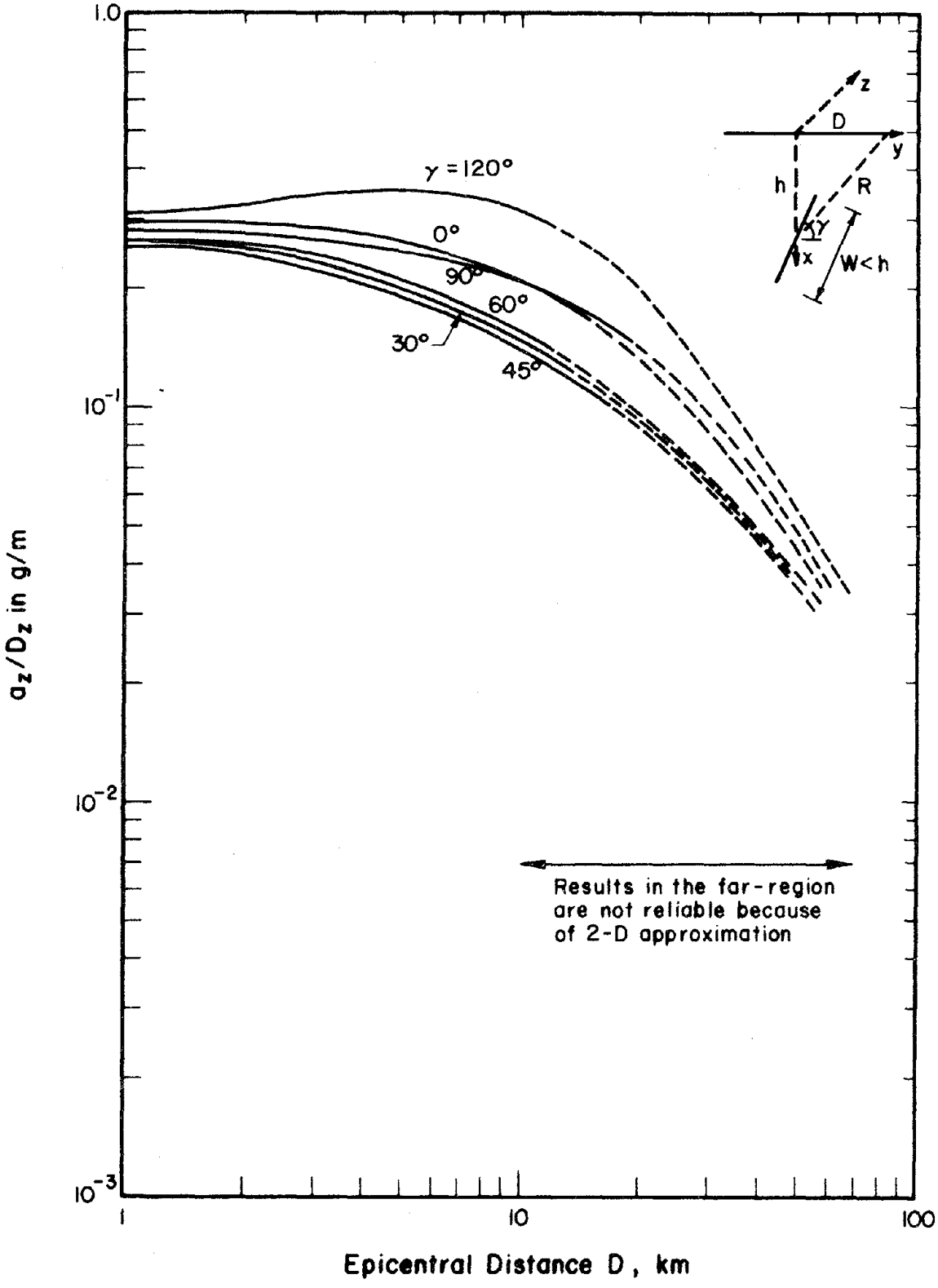

FIG. 2.8a VARIATION OF a_z/D_z WITH D FOR DIFFERENT γ
(h = 15, W = 4 km)

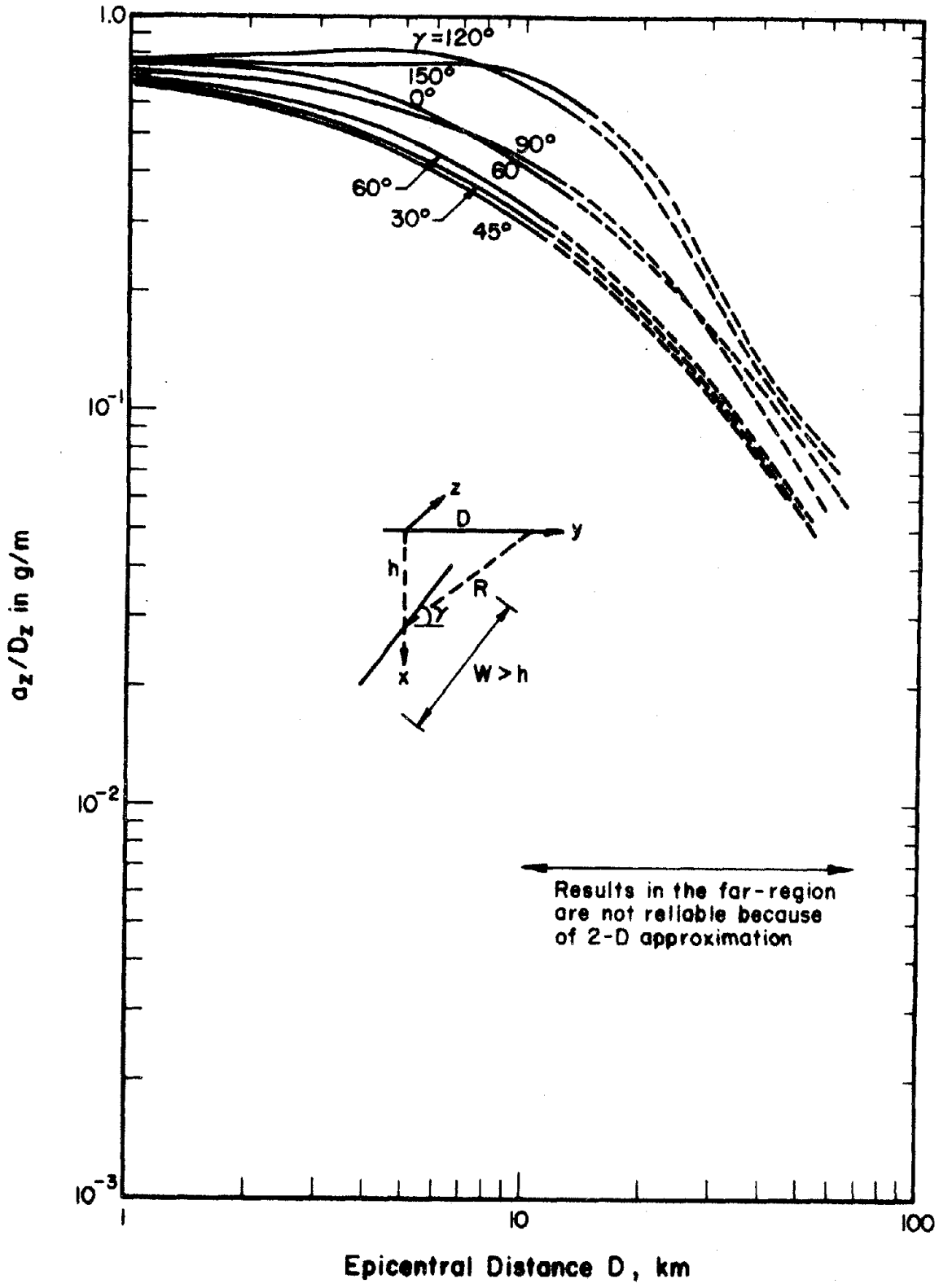

FIG. 2.8b VARIATION OF a_z/D_z WITH D FOR DIFFERENT γ
(h = 15, W = 20 km)

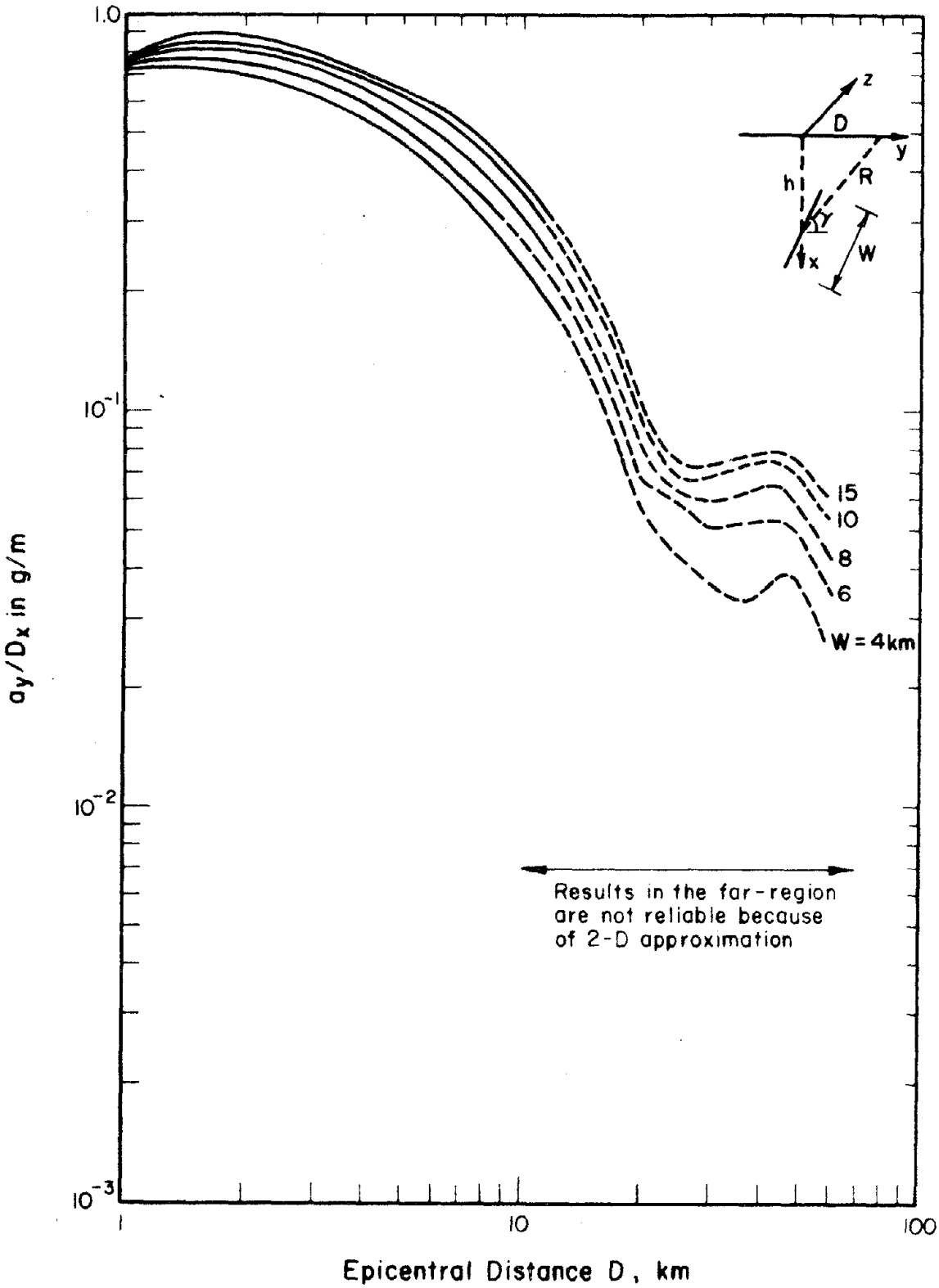

FIG. 2.9 VARIATION OF a_y/D_x WITH D FOR DIFFERENT W
($h = 15$, $\gamma = 90^0$, $v_p/v_s = 1.75$)

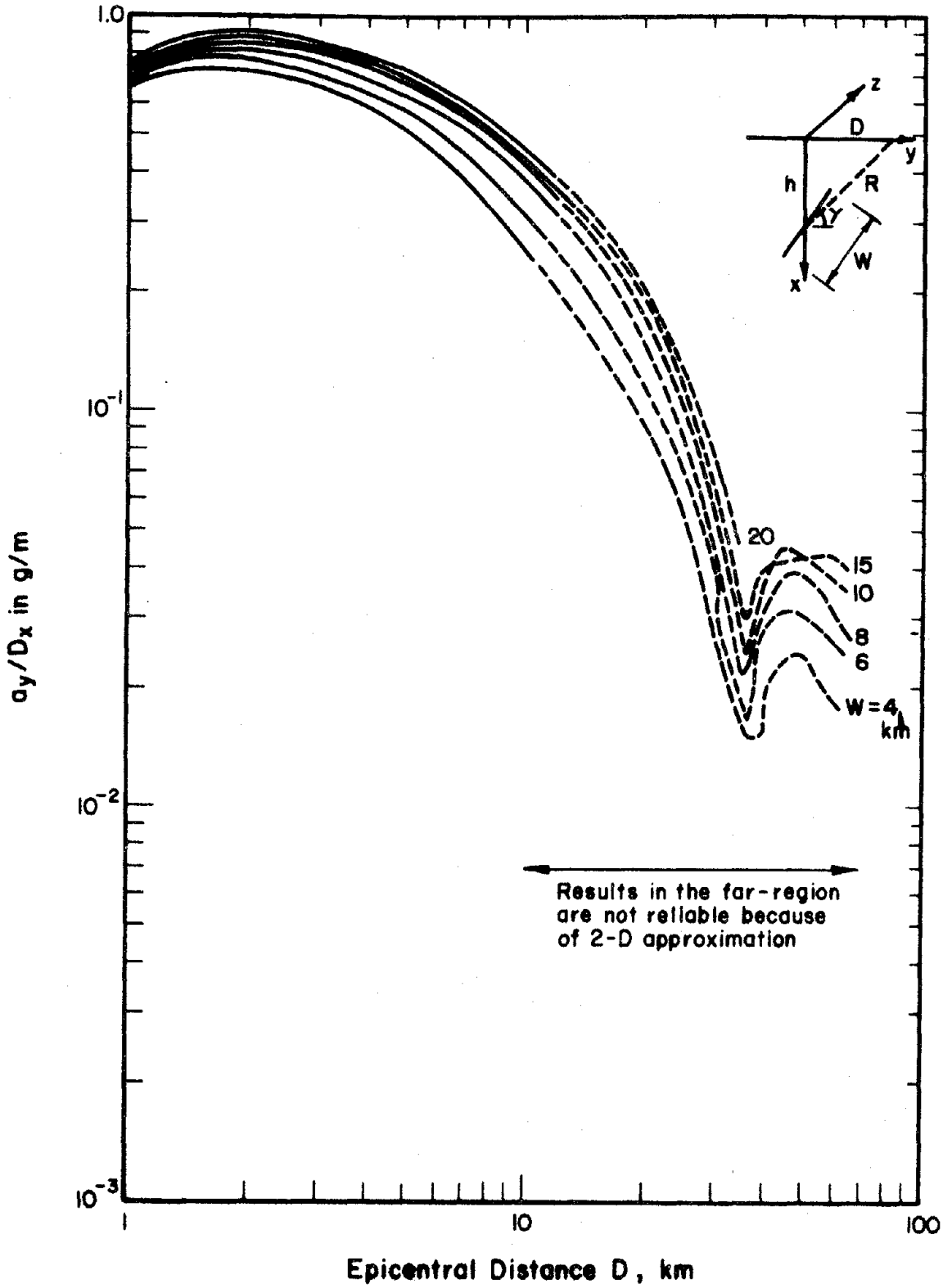

FIG. 2.10 VARIATION OF a_y/D_x WITH D FOR DIFFERENT W
(h = 20 km, $\gamma = 90^0$, $v_p/v_s = 1.75$)

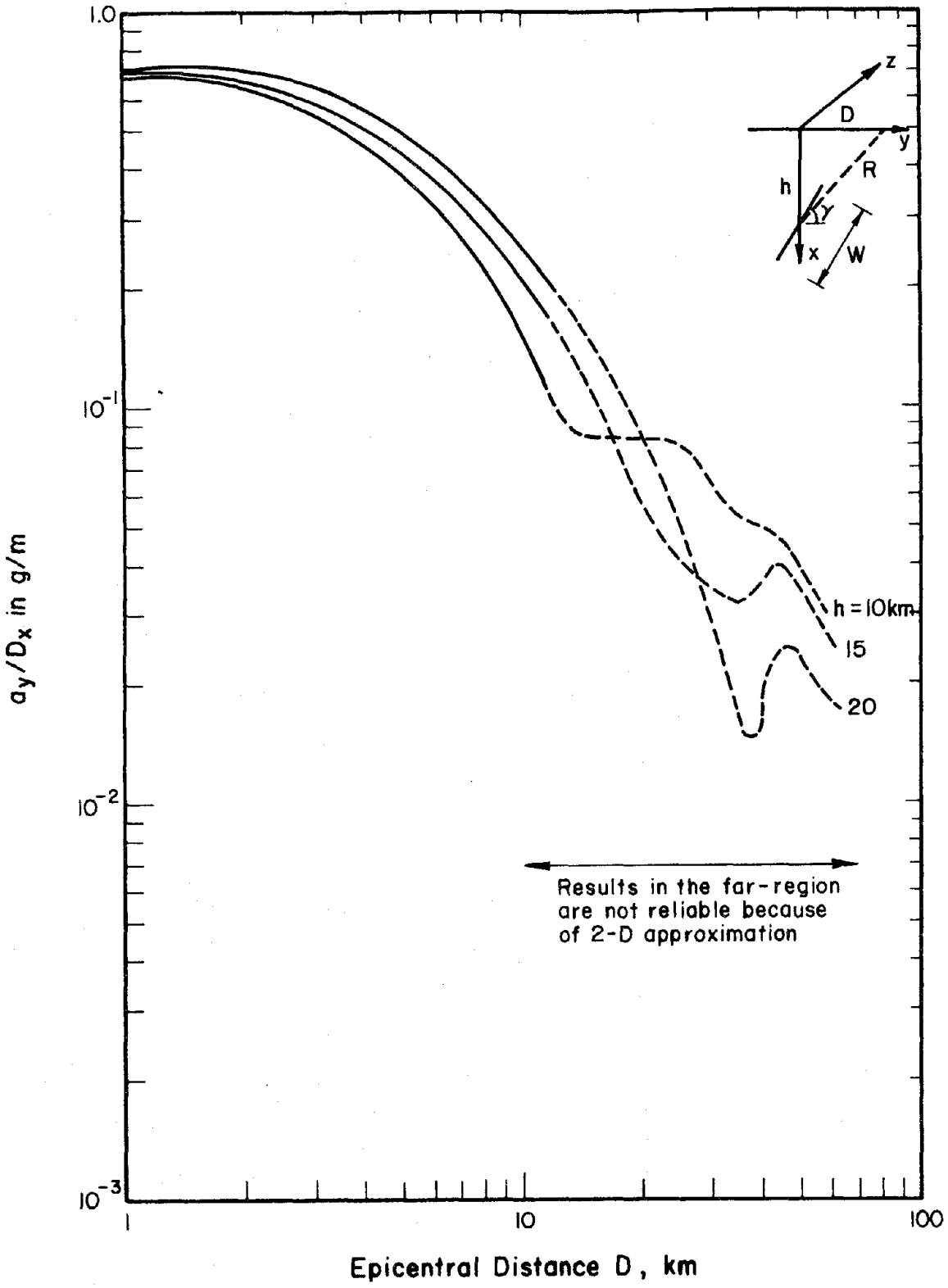

FIG. 2.11 VARIATION OF a_y/D_x WITH D FOR DIFFERENT h
($W = 4$ km, $\gamma = 90^{o}$, $v_p/v_s = 1.75$)

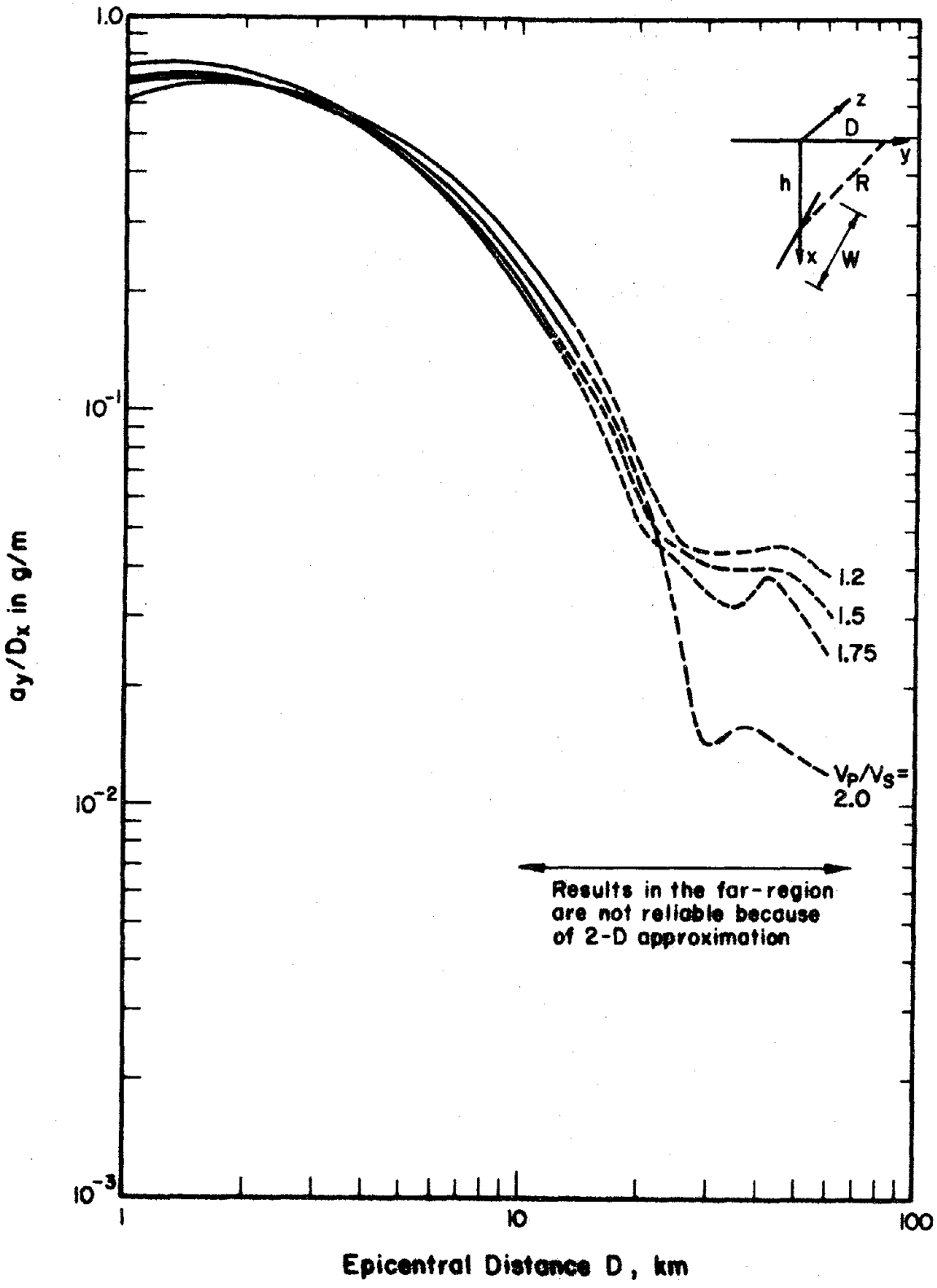

FIG. 2.12 VARIATION OF a_y/D_x WITH D FOR DIFFERENT v_P/v_S (h = 15, W = 4 km, $\gamma = 90^o$)

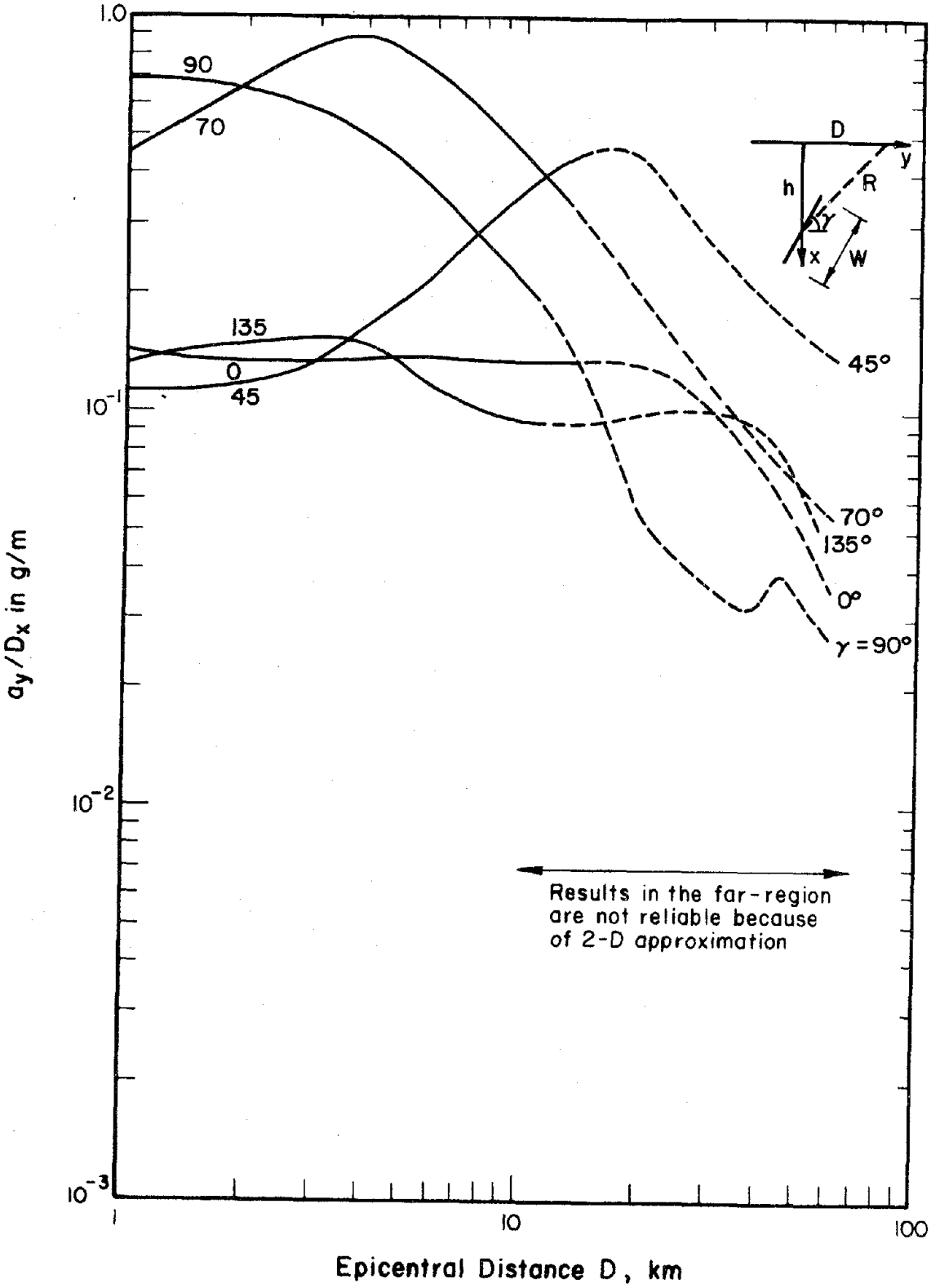

FIG. 2.13 VARIATION OF a_y/D_x WITH D FOR DIFFERENT γ
(h = 15, W = 4 km, v_P/v_S = 1.75)

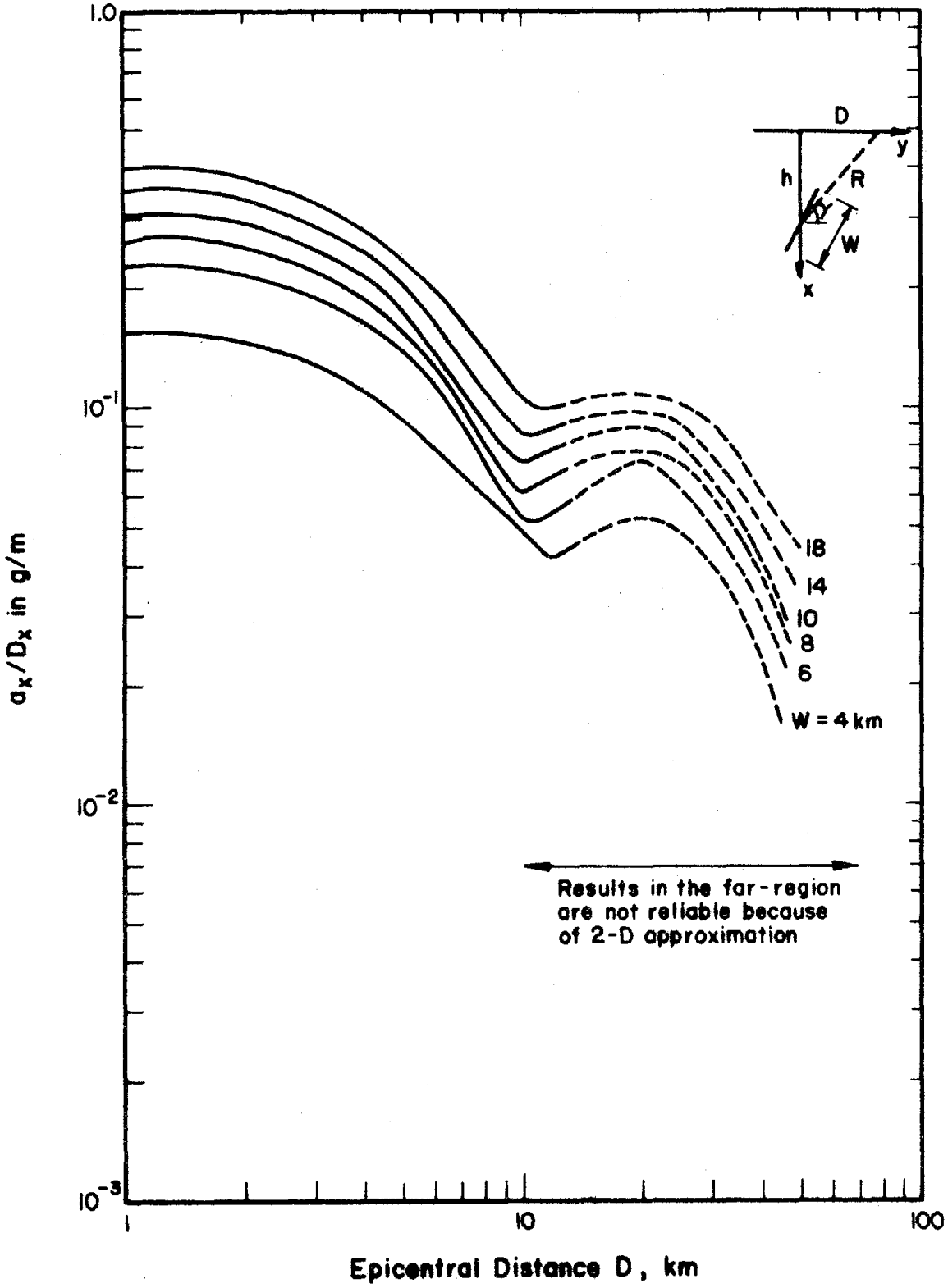

FIG. 2.14 VARIATION OF a_x/D_x WITH D FOR DIFFERENT W
(h = 15 km, $\gamma = 90^o$, v_P/v_S = 1.75)

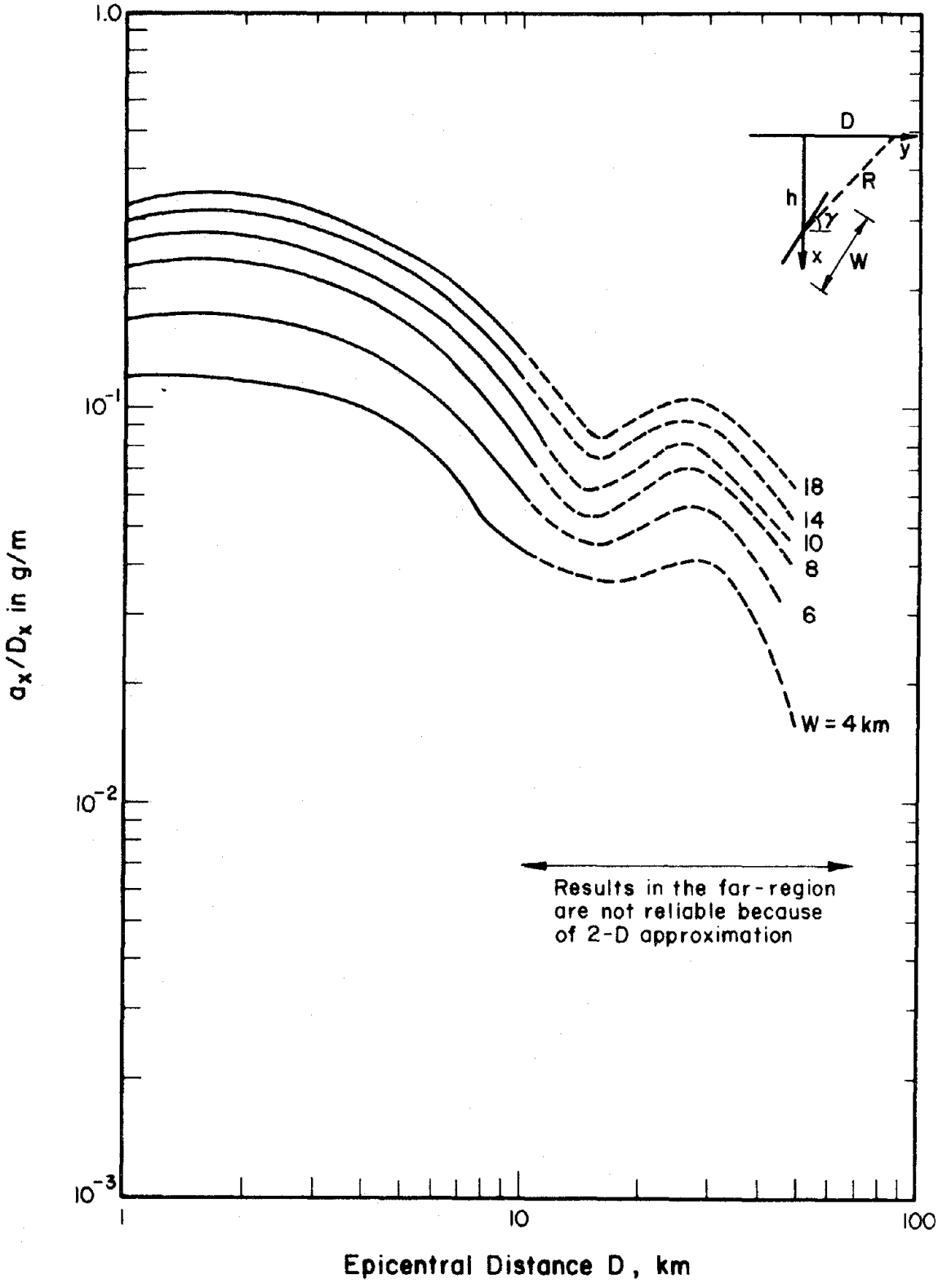

FIG. 2.15 VARIATION OF a_x/D_x WITH D FOR DIFFERENT W
(h = 20 km, $\gamma = 90^0$, $v_P/v_S = 1.75$)

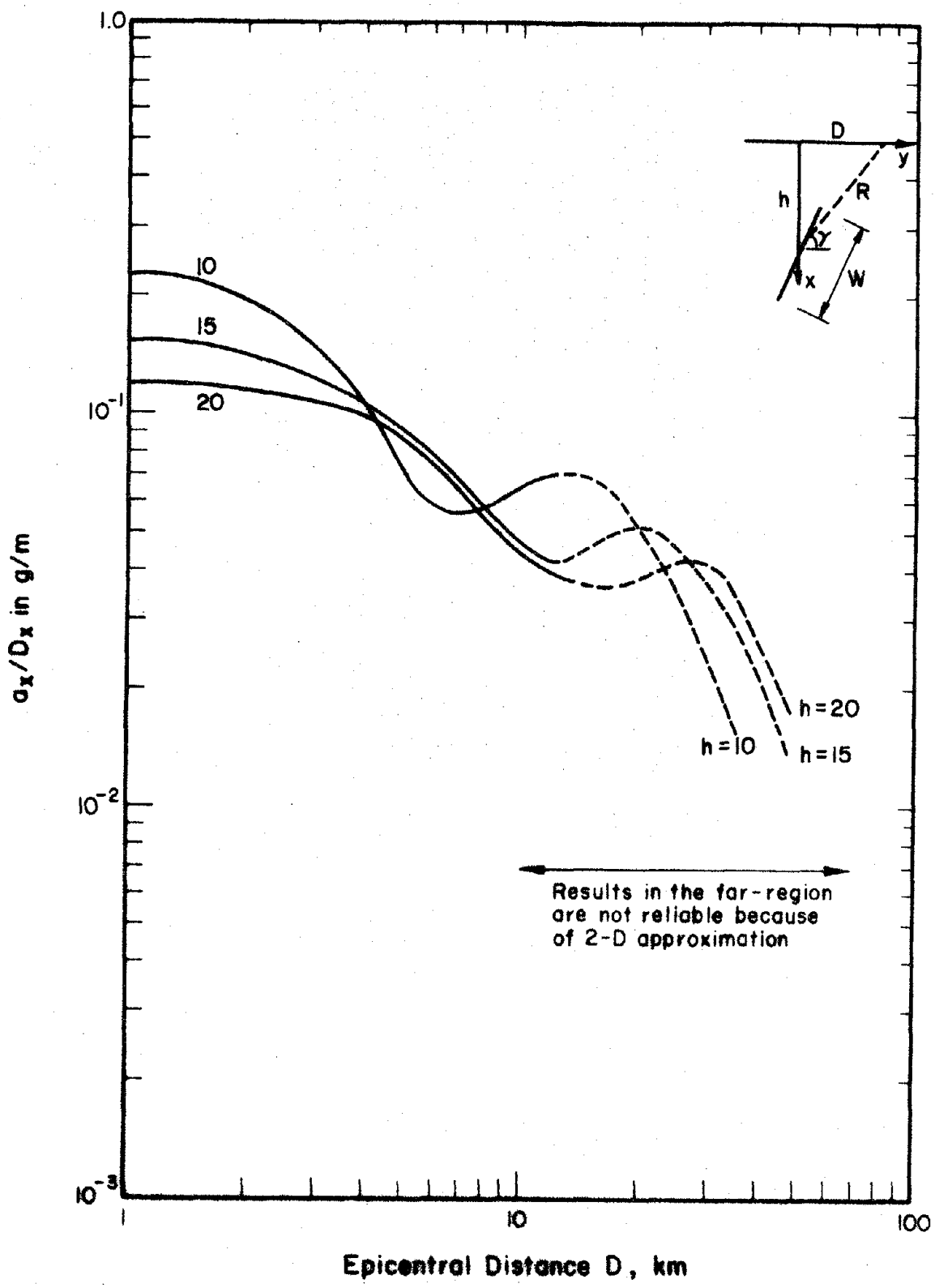

FIG. 2.16 VARIATION OF a_x/D_x WITH D FOR DIFFERENT h
(W = 4 km, $\gamma = 90^0$, $v_p/v_s = 1.75$)

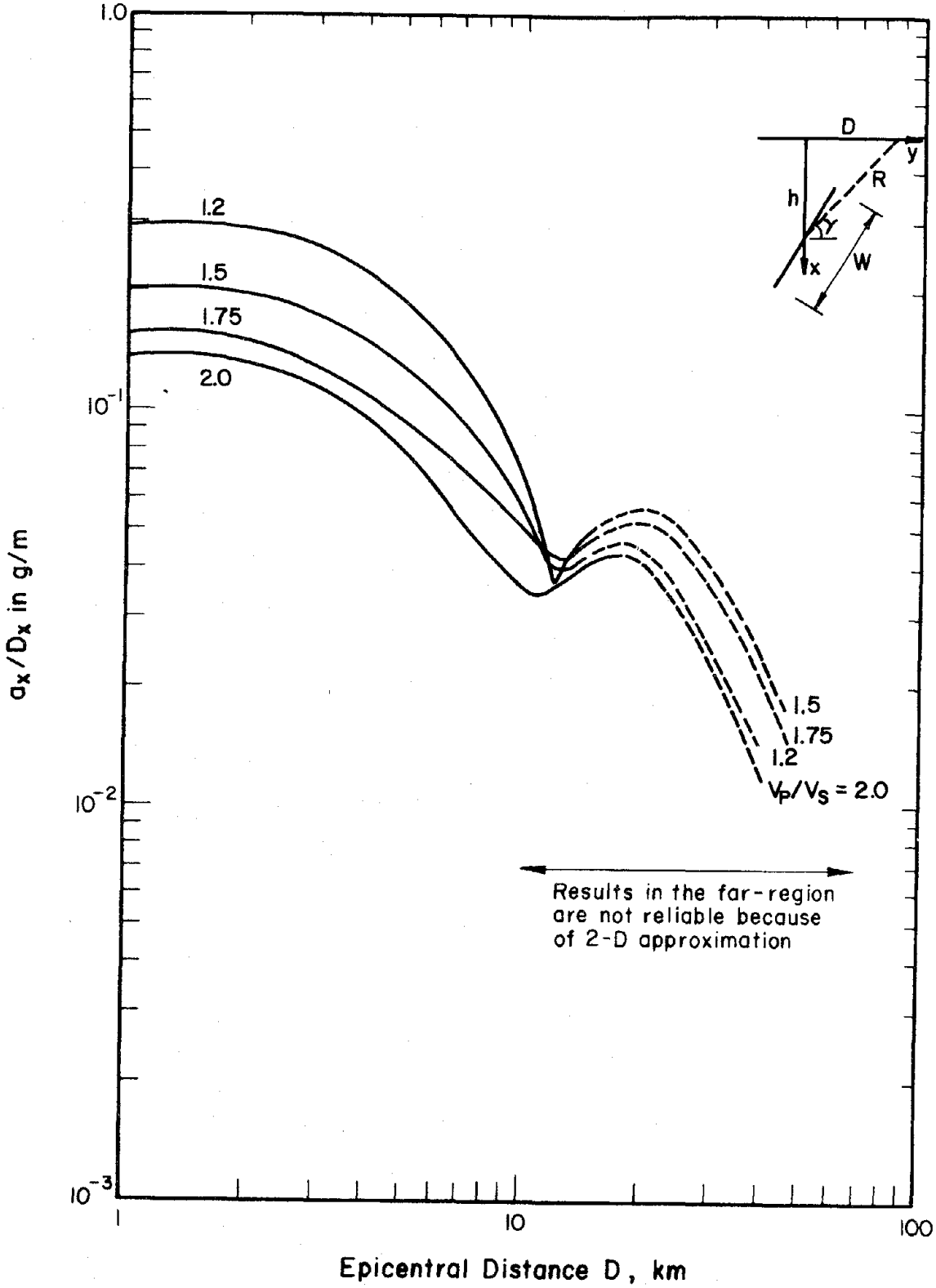

FIG. 2.17 VARIATION OF a_x/D_x WITH D FOR DIFFERENT v_p/v_s
(W = 4, h = 15 km, $\gamma = 90^o$)

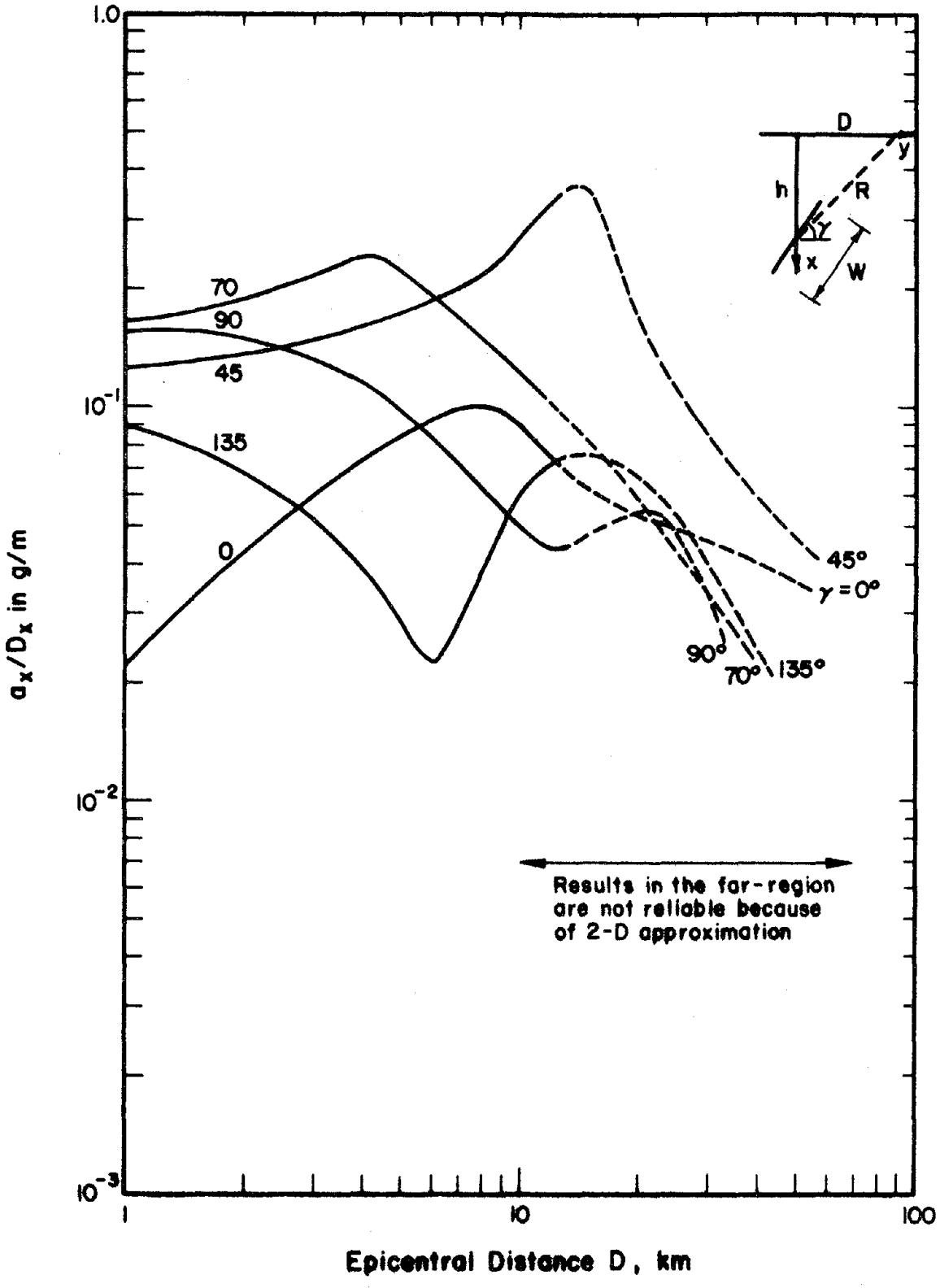

FIG. 2.18 VARIATION OF a_x/D_x WITH D FOR DIFFERENT γ
(W = 4, h = 15 km, v_p/v_s = 1.75)

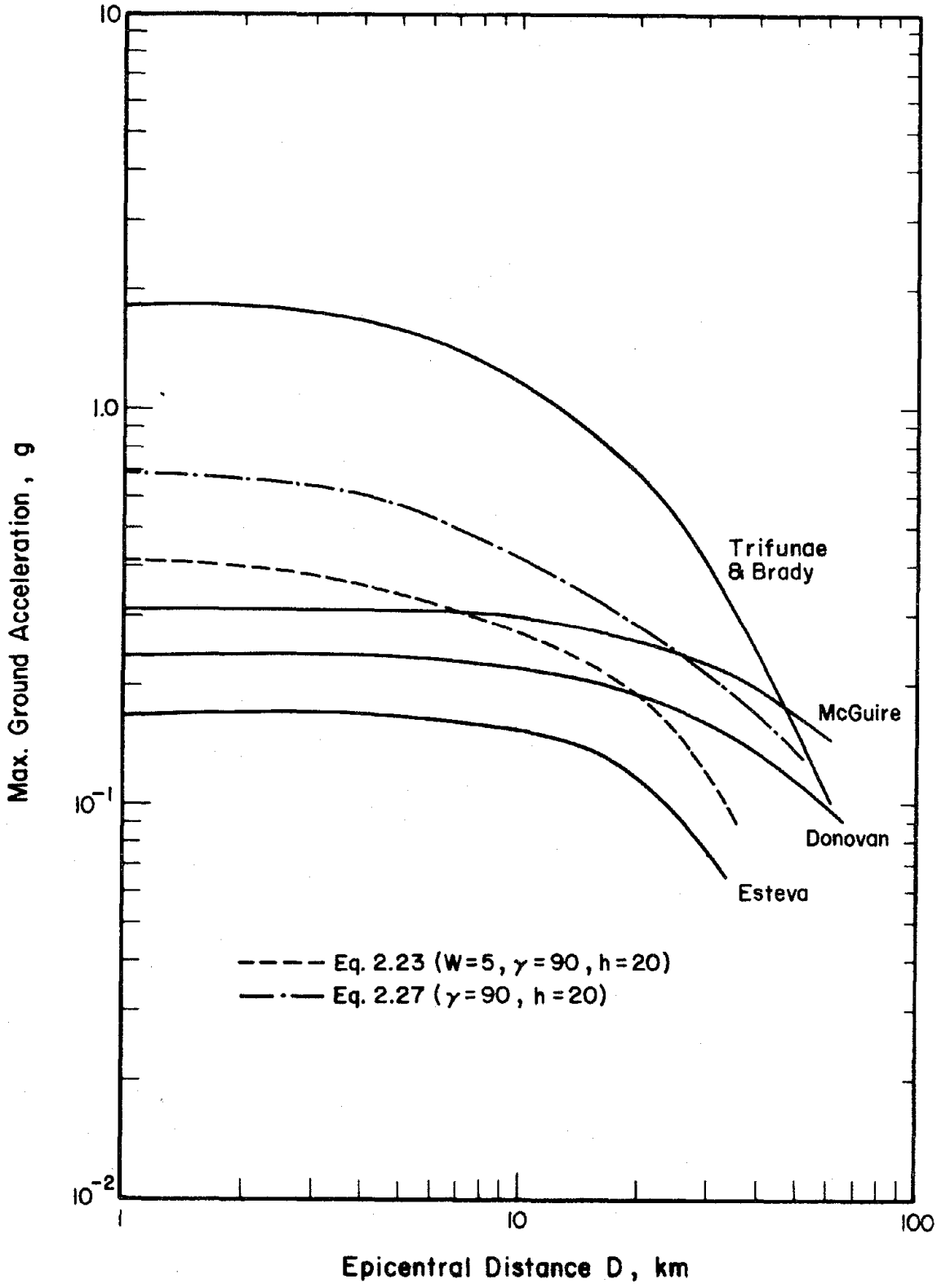

FIG. 2.19 ATTENUATION OF MAXIMUM GROUND ACCELERATION (m = 7.0)

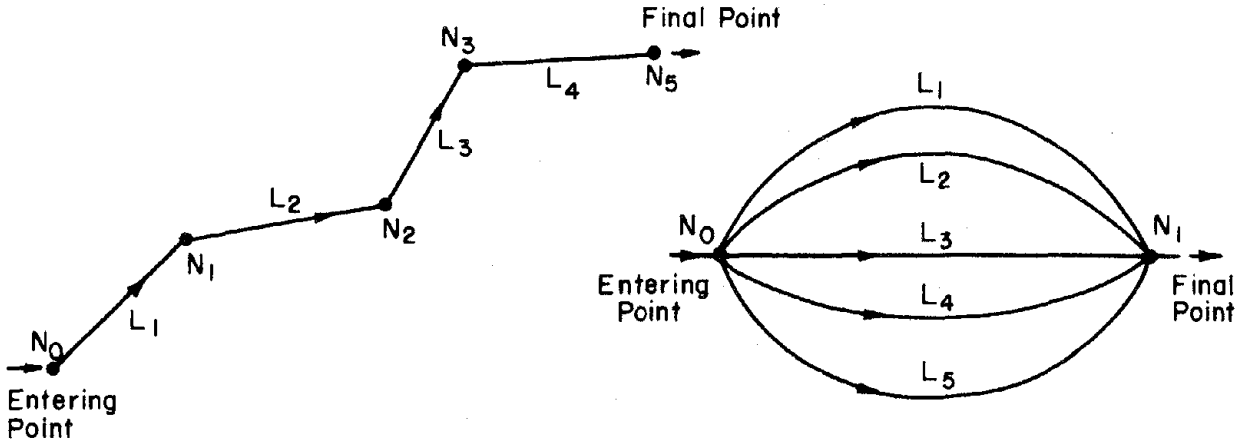

FIG. 4.1 SIMPLE LIFELINE NETWORKS

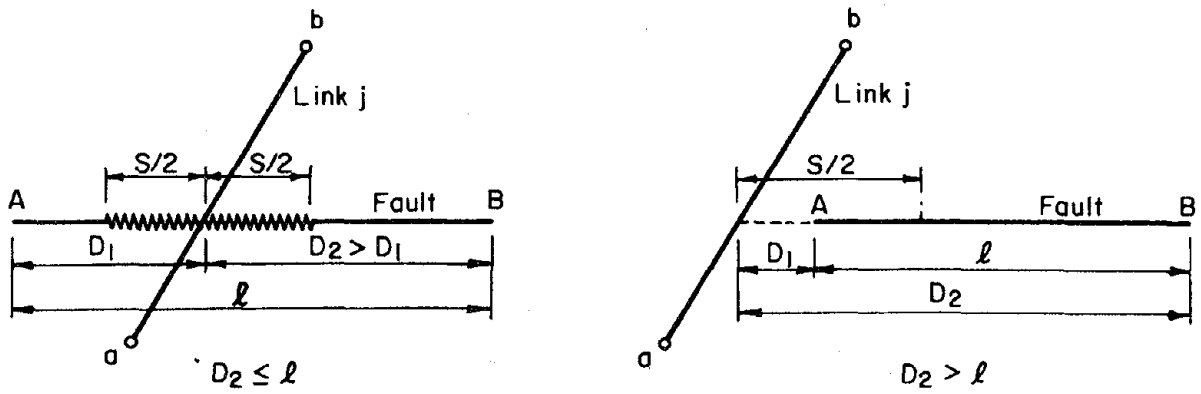

FIG. 4.2 TYPE 1 SOURCE

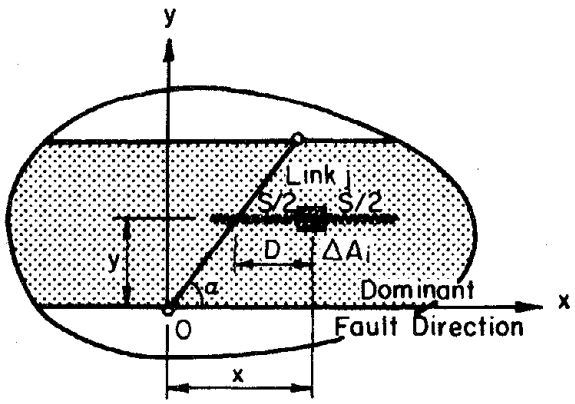

FIG. 4.3 TYPE 2 SOURCE

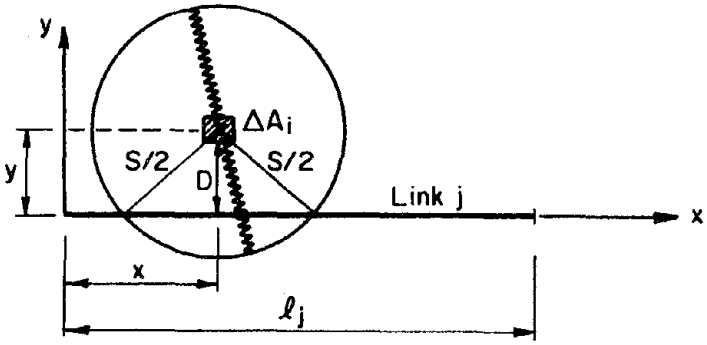

FIG. 4.4 TYPE 3 SOURCE

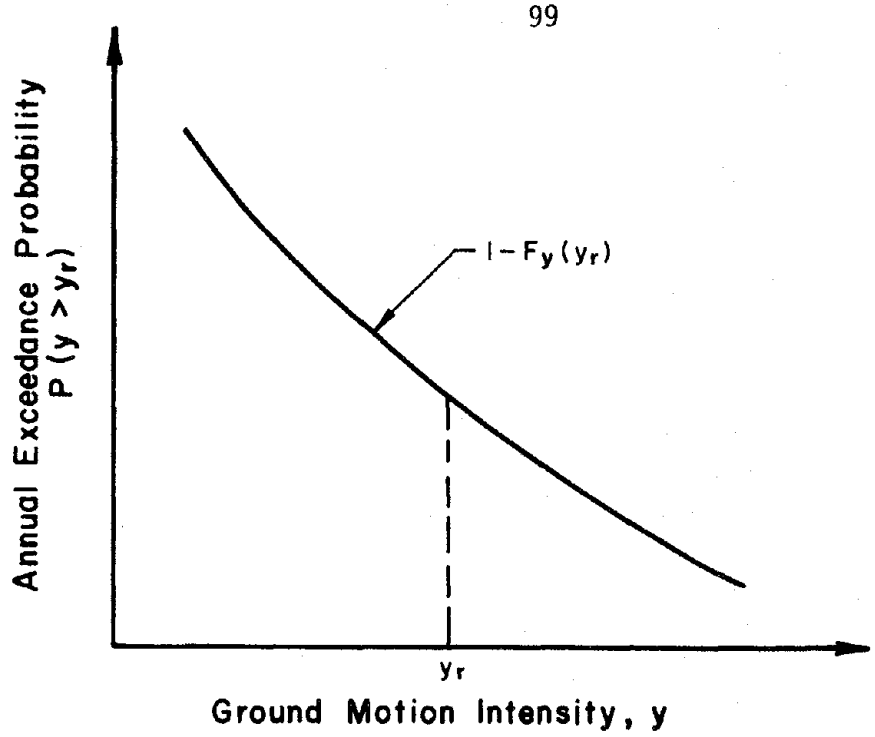

FIG. 5.1 ANNUAL PROBABILITY OF EXCEEDANCE

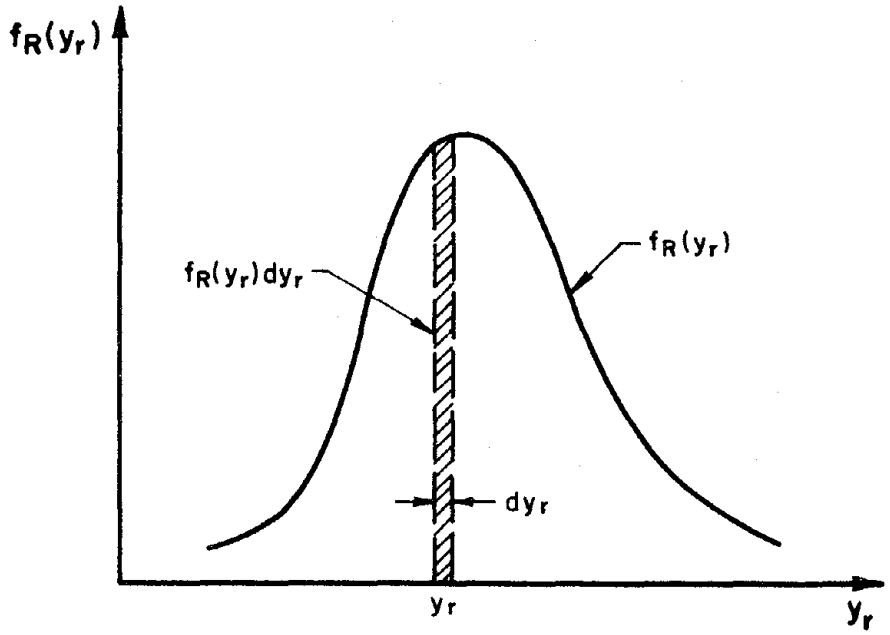

FIG. 5.2 PDF OF LINK RESISTANCE

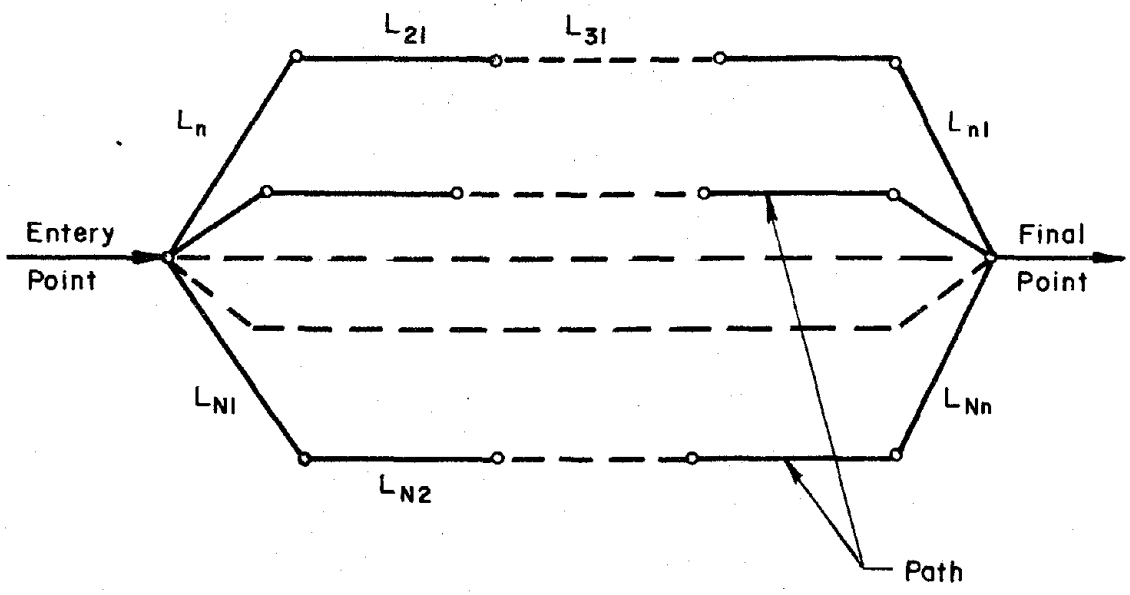

FIG. 5.3 A NETWORK OF PARALLEL PATHS

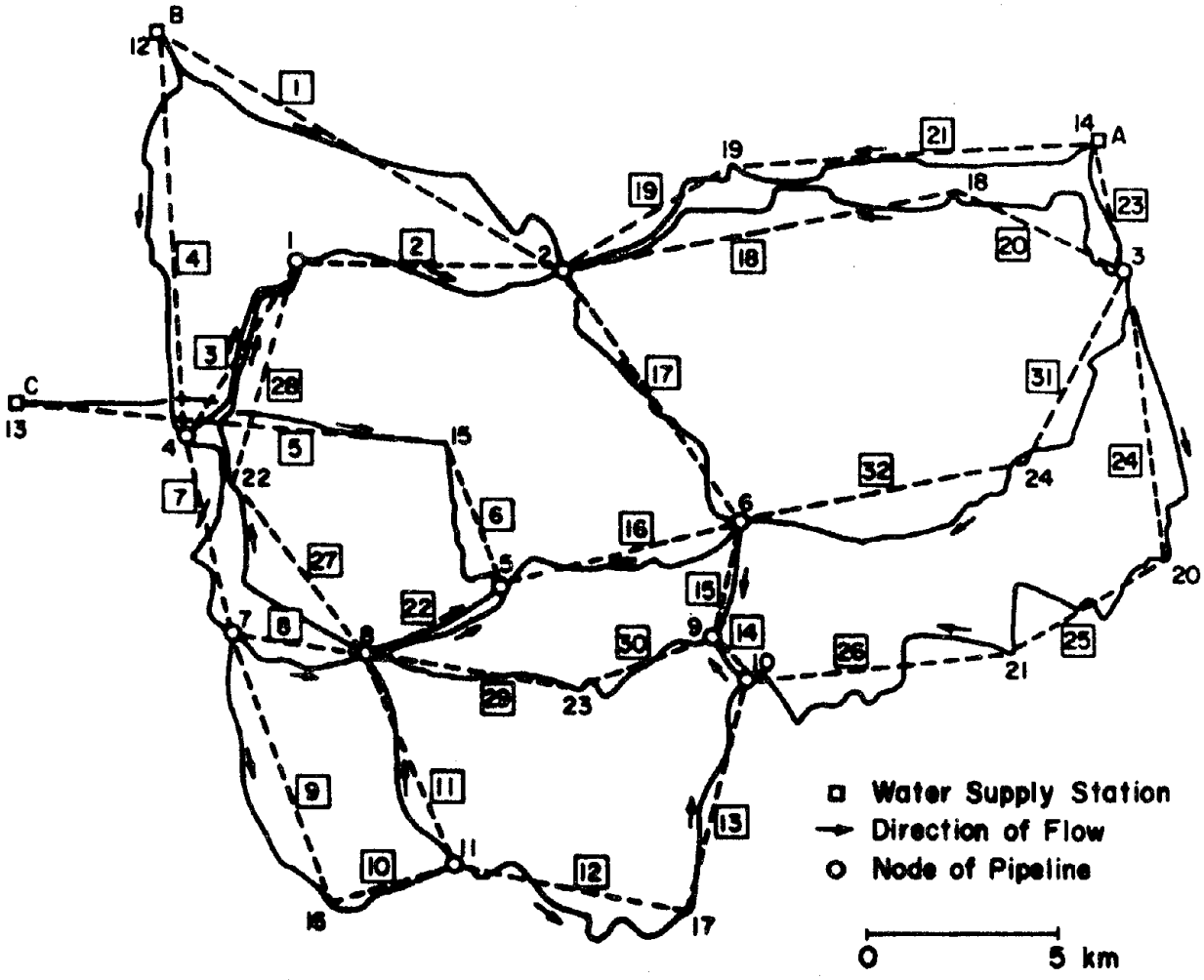

FIG. 6.1 WATER SUPPLY NETWORK FOR TOKYO

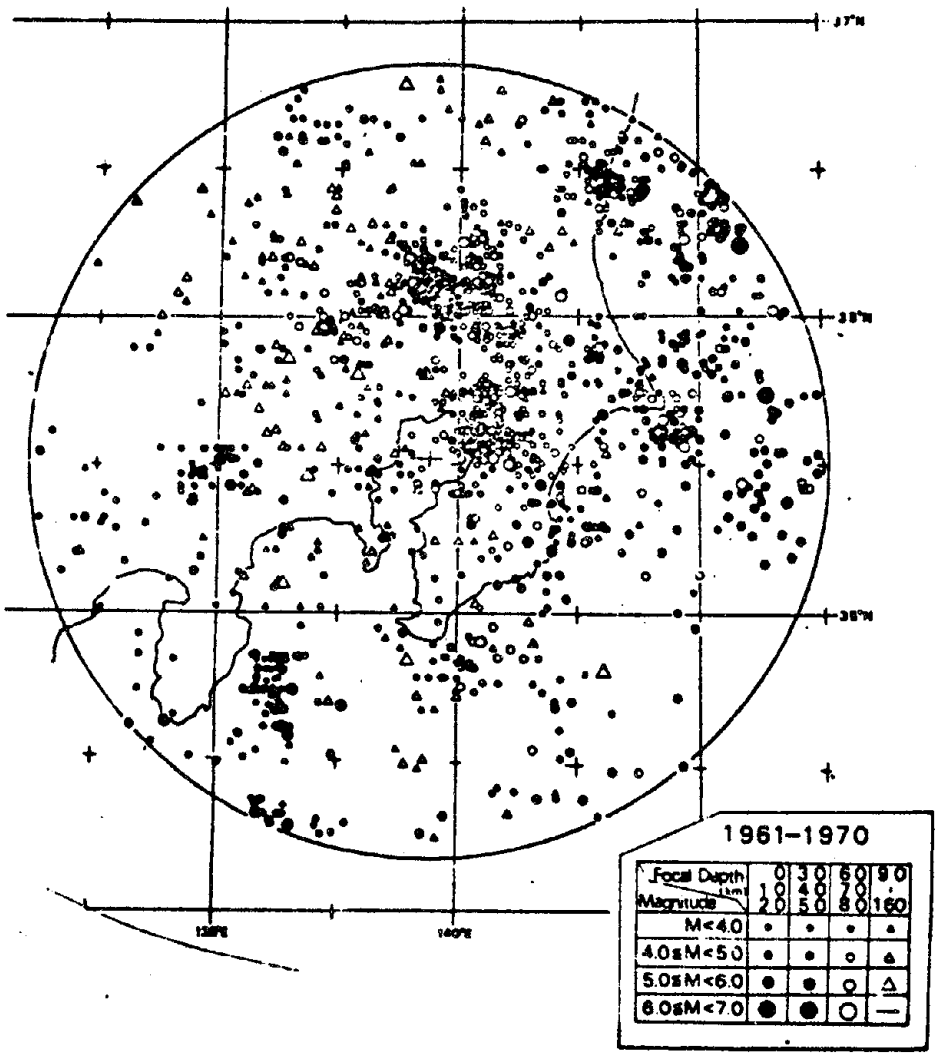

6.2 EPICENTER MAP OF TOKYO BAY AREA (1961-1970) -- FROM REF. 28

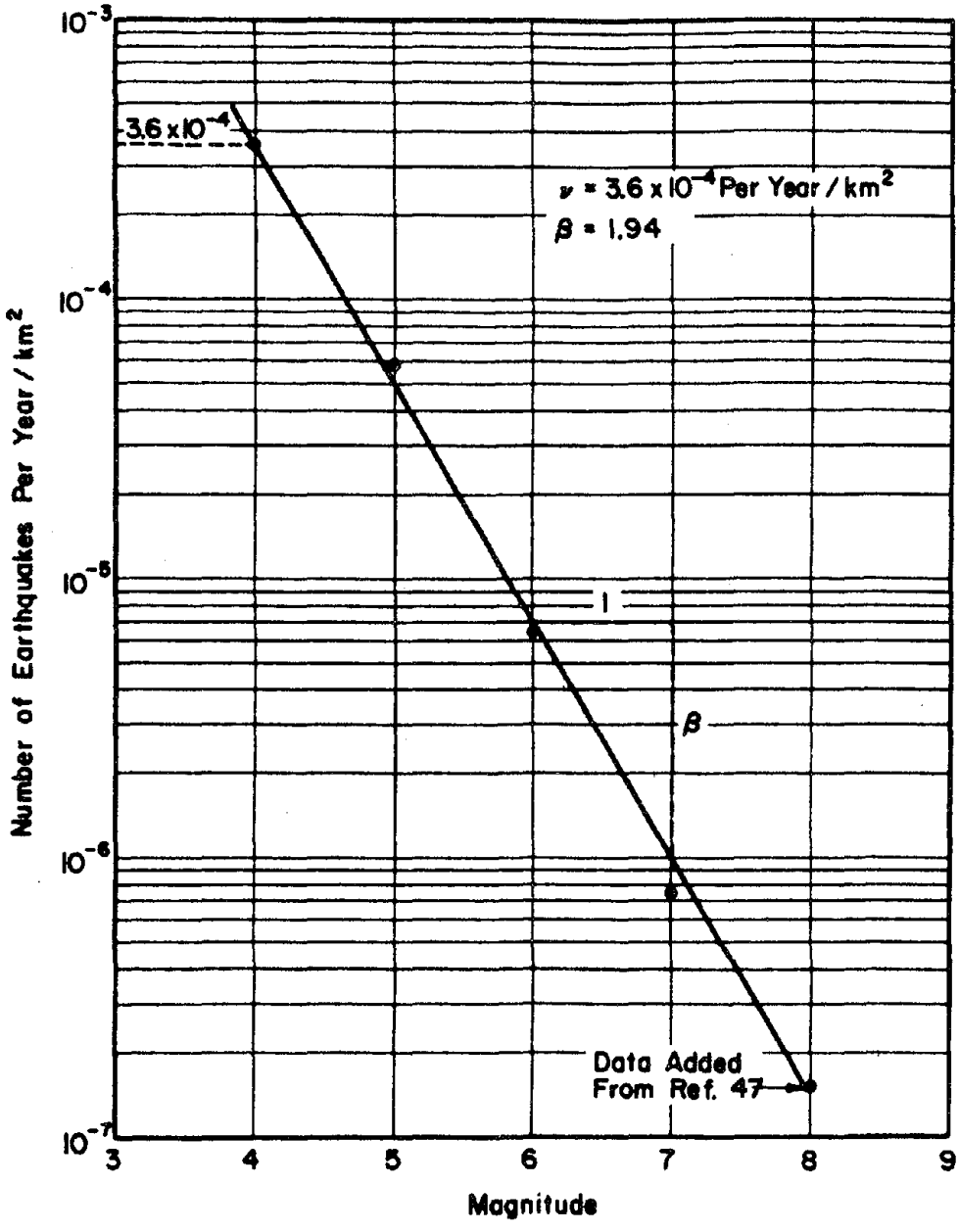

FIG. 6.3 MAGNITUDE RECURRENCE CURVE

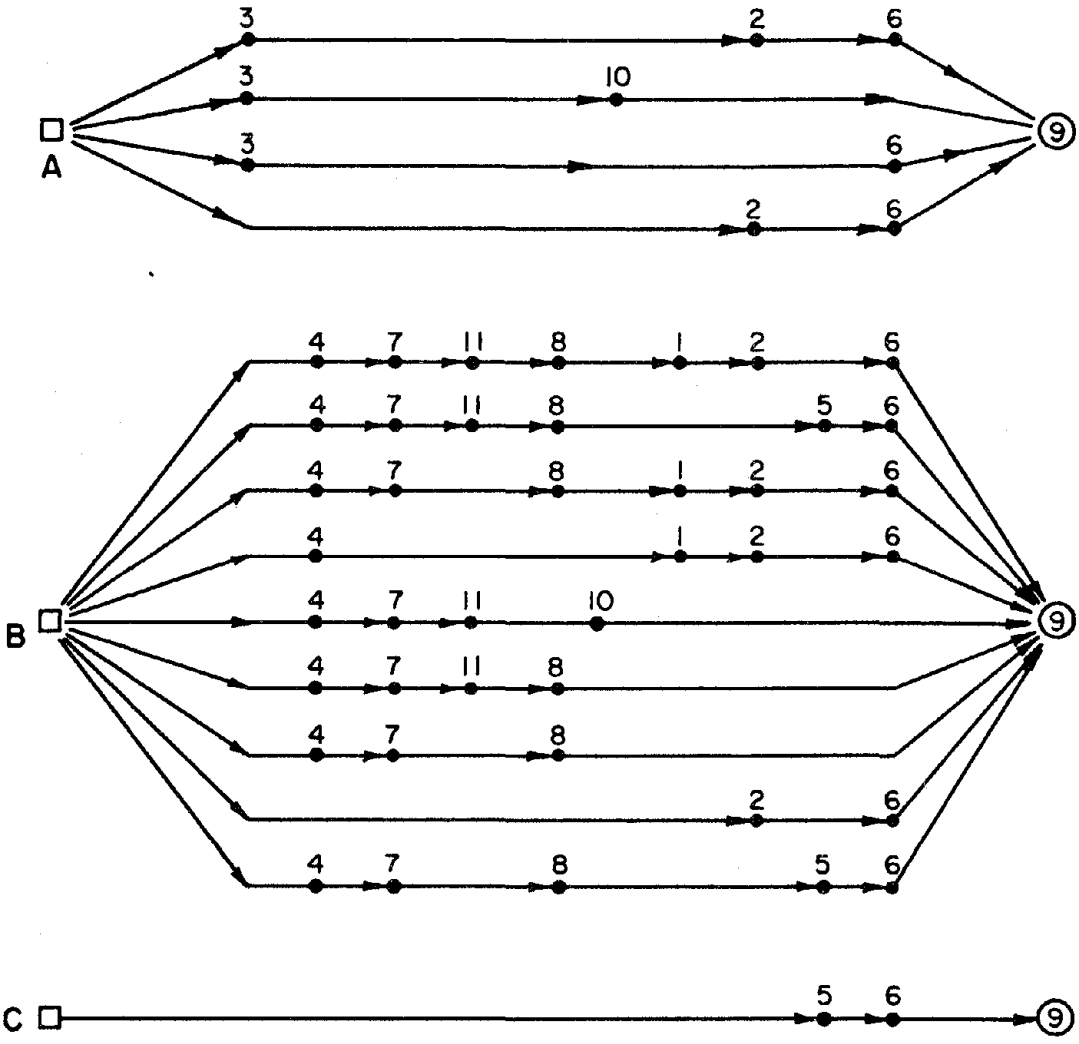

FIG. 6.4 EQUIVALENT PARALLEL NETWORKS FOR TOKYO

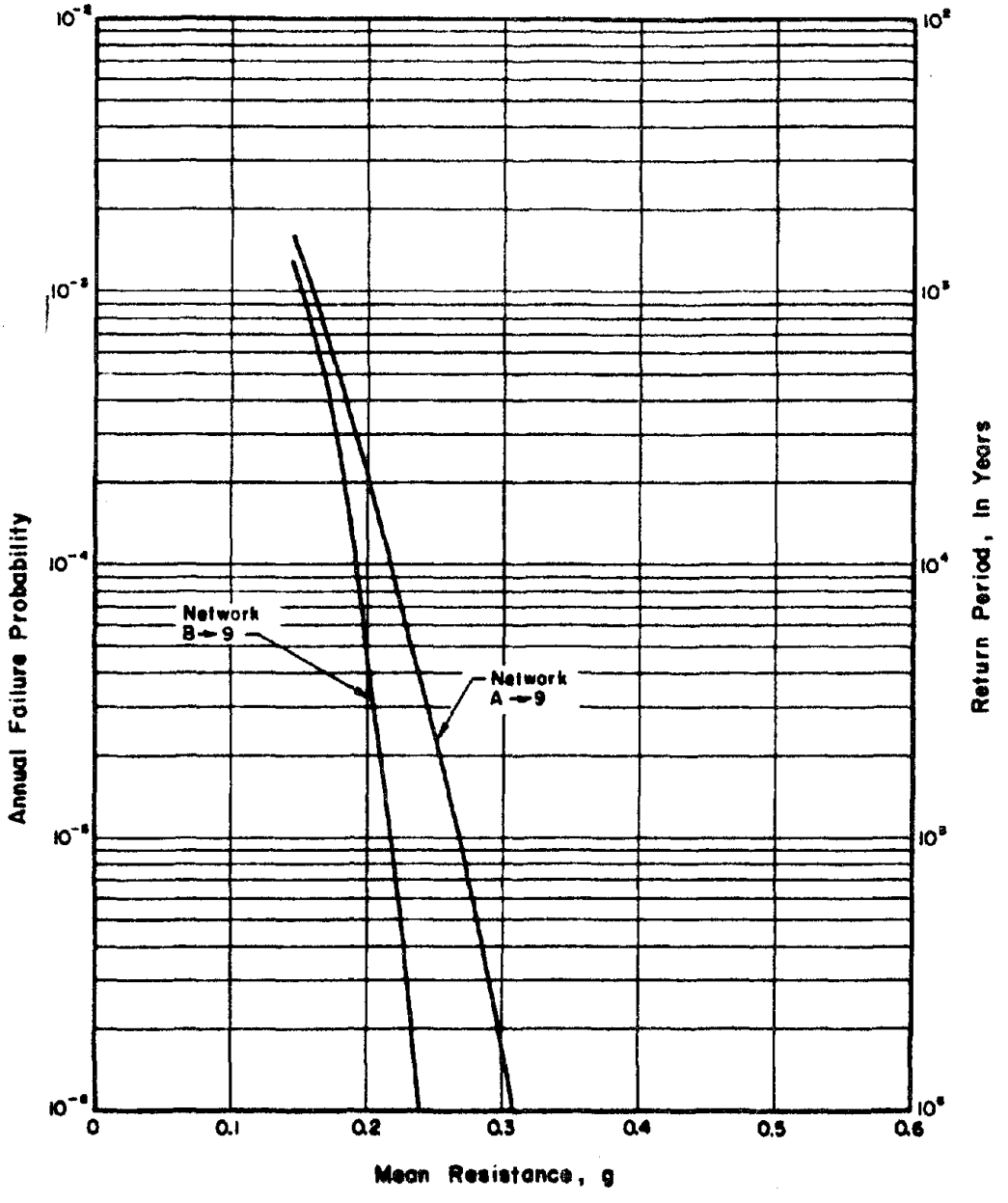

FIG. 6.5 FAILURE PROBABILITY, NETWORK A → 9 AND B → 9 (HAZARD OF GROUND SHAKING)

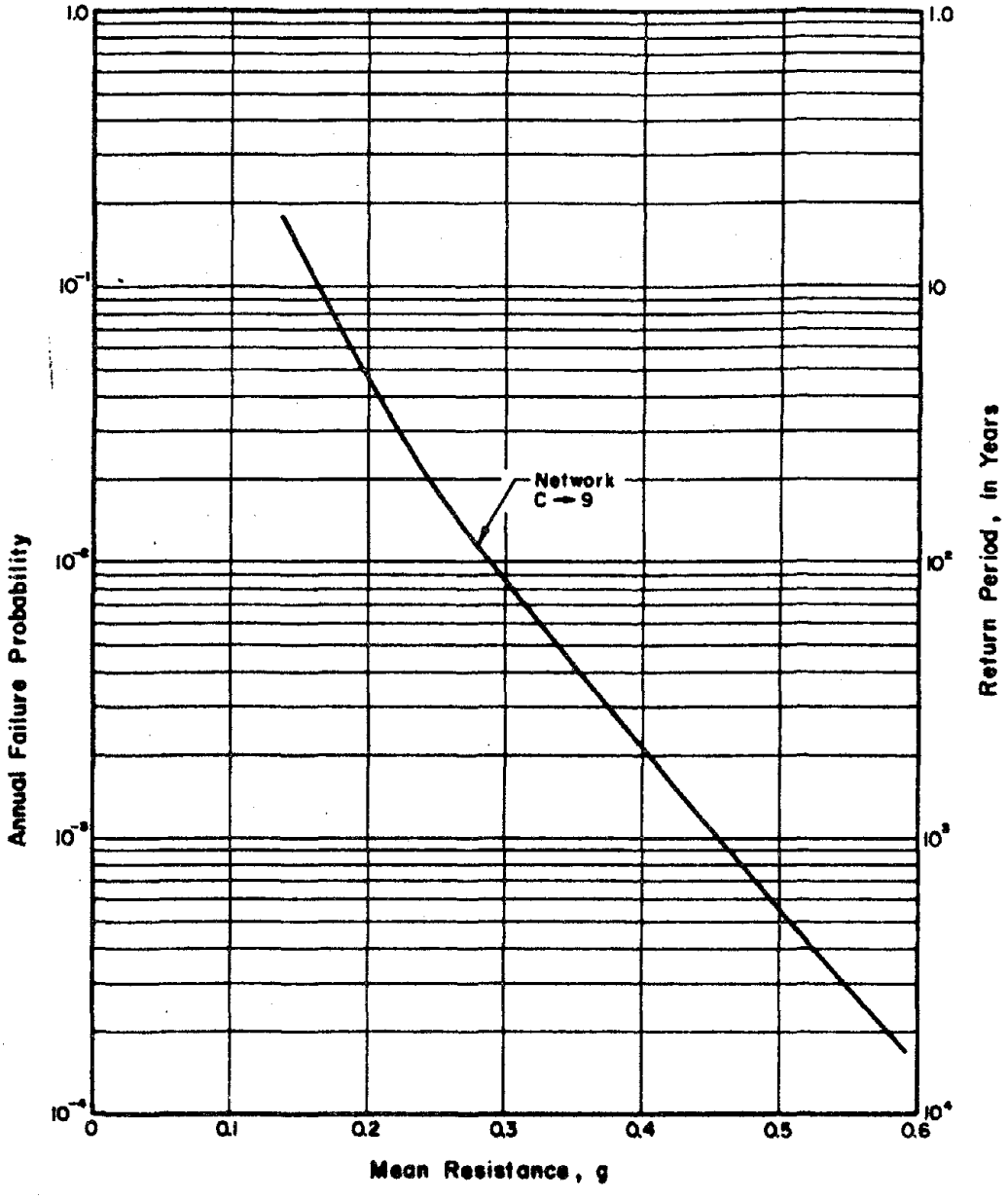

FIG. 6.6 FAILURE PROBABILITY, NETWORK C → 9
(HAZARD OF GROUND SHAKING)

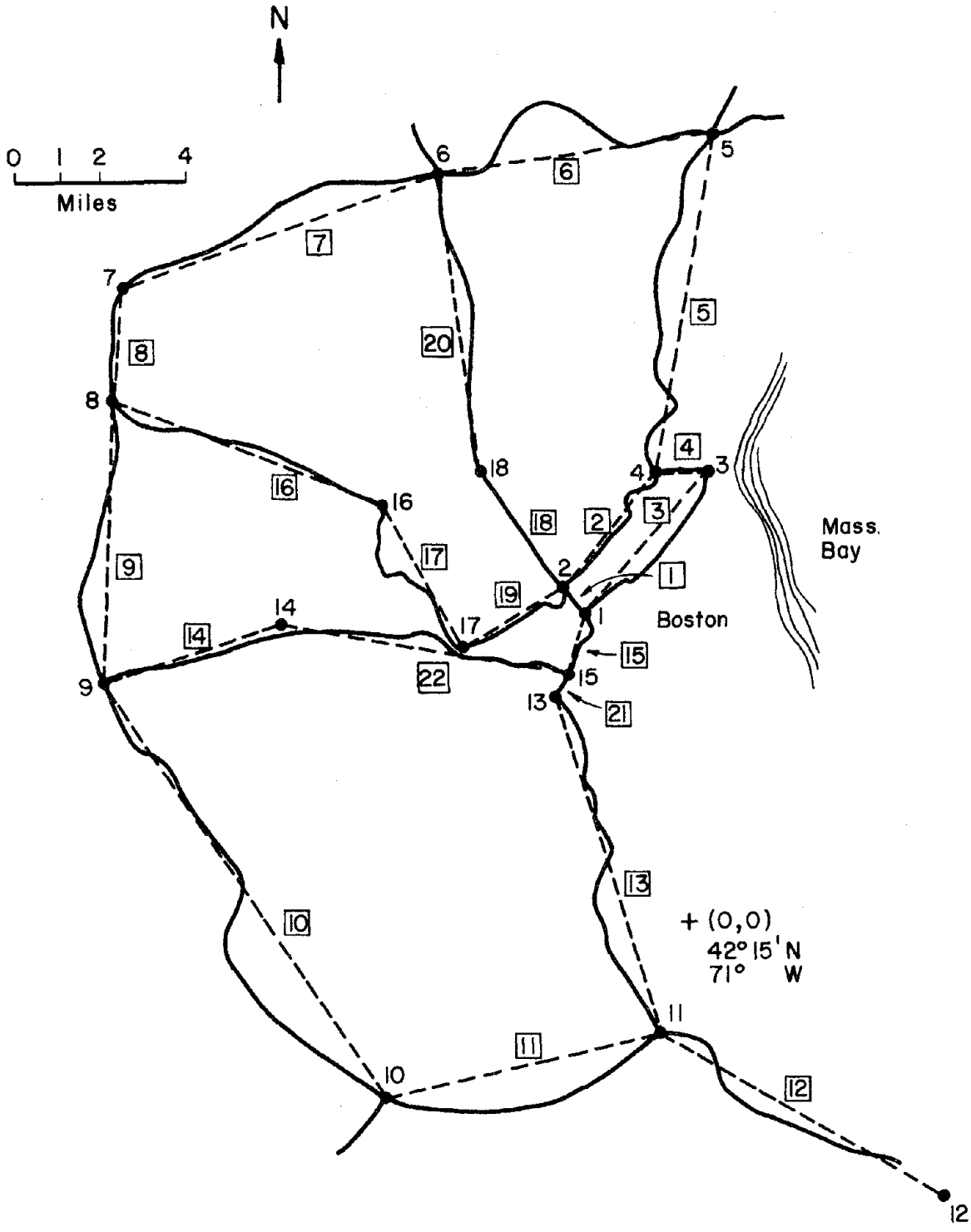

FIG. 6.7 BOSTON MAJOR HIGHWAYS

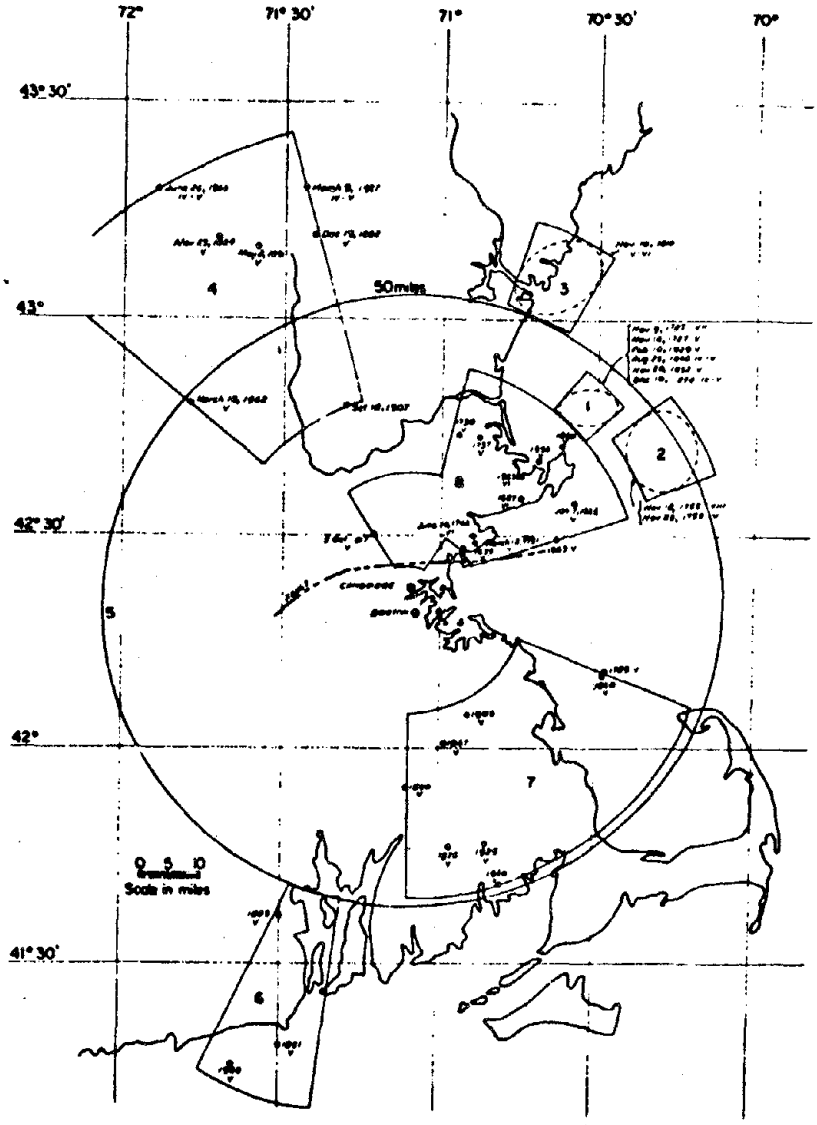

FIG. 6.8 IMPORTANT EARTHQUAKES IN BOSTON AREA (REF. 49)